Characterization of Suppressors of Fat-like Cadherin CDH-4 in Context of Axon Guidance during Embryonic Development

by

Zina Aburegeba

Bachelors of Science, Simon Fraser University, 2015

Thesis Submitted in Partial Fulfillment of the
Requirements for the Degree of
Master of Science

in the
Department of Biological Sciences
Faculty of Science

SIMON FRASER UNIVERSITY
Spring 2018

Approval

Name:	**Zina Aburegeba**
Degree:	**Masters of Science (Biological Sciences)**
Title:	**Characterization of Suppressors of Fat-like Cadherin CDH-4 in Context of Axon Guidance during Embryonic Development**
Examining Committee:	**Chair: Lynne Quarmby** Professor
	Harald Hutter Senior Supervisor Professor
	Nancy Hawkins Supervisor Professor
	Michael Silverman Supervisor Professor
	Sherryl Bisgrove Internal Examiner Associate Professor
Date Defended/Approved:	April 10, 2018

Abstract

Developing the nervous system requires axons to grow and connect to specific targets, forming neuronal circuits, through axon navigation. One of the genes controlling axon navigation is the fat-like cadherin CDH-4, a member of the cadherin superfamily. To identify genes acting together with *cdh-4,* mutants suppressing the axon guidance defects of *cdh-4* mutants were isolated previously. The goal of this thesis was to characterize and identify these suppressor genes. Five suppressors were studied in detail. They partially suppressed axon guidance and movement defects observed in the *cdh-4* mutants. Three suppressor genes were identified: *math-48,* a functionally uncharacterized gene, *prp-6* and *prp-8,* both encoding components of the spliceosome. A previous study documented changes in expression of several hundred genes when *prp-6* or *prp-8* are partially inactivated. This suggests that the suppression effect might be mediated by upregulation of one or more genes, compensating for the loss of CDH-4.

Keywords: *cdh-4; C. elegans*; Ventral nerve cord; Dorsal nerve cord; Suppressors; Axon Guidance; Nervous system development

To my Parents, my Brother, and my Sister

Acknowledgements

I first have to thank my parents for their constant support and encouragement throughout this process, and for their hard work and sacrifices that have secured a privileged and peaceful life and future for my siblings and myself.

My time in the Hutter lab has been one of the highlights of my life. It would have not been special and heart-"worming" without my co-workers in the lab. Dr. Jie (Jessie) Pan, thank you for all your help with my project and for all the good talks and laughter we shared. Jesse Taylor, thank you for always hearing me when I needed someone to talk to and for all the fun planning that we did, like Harald's surprise birthdays, designing the Hutter lab T-shirts, and together dressing up as Harald for Halloween (I'm sensing a Harald theme here). Rick Zapf, thank you for always being accommodating when I needed help with my lab work. Several times when I asked you a question, you just looked at me without saying anything and I suddenly got the answer in my head! Abigail Feresten, thank you for being your unique wonderful one of a kind self. I have never met someone who is opposite in personality to me but who I work with so well; thank you for your friendship as I am sure it will last beyond our times in the Hutter lab. Thank you to the past Hutter lab members, Dr. Jaffar Bhat and Sean Ritter for all the wonderful times we shared. Thank you to the undergraduate students Wendy, Shinelle, Vanessa, Saru, Kat, and Amanda, who all added their own special flavours to my time in the Hutter lab.

Thank you to my committee members Dr. Nancy Hawkins and Dr. Michael Silverman for sharing your knowledge and expertise in your fields. This project would have not been possible without your guidance, valuable feedback, and support. Thank you Dr. Sherryl Bisgrove for being my internal examiner and for all your super enjoyable conversations and discussions during class and out of class when I was TAing Developmental Biology with you. You helped me grow as a teacher just by watching your lectures. Thank you Dr. Lynne Quarmby for kindly agreeing to chair my defence. Thank you Marlene Nguyen for all your assistance and advice with regards to graduate studies and for always sharing your lovely sense of humour. I will miss it.

Thank you to the Moerman lab for performing whole genome sequencing of the *cdh-4* mutant suppressor strains, to Dr. Jie Pan for doing the suppressor screening of

cdh-4 mutants, and to Rick Zapf for generating the transgenic strains. Some strains were provided by the CGC, which is funded by NIH Office of Research Infrastructure Programs. This work is funded by CIHR. I am grateful for all the academic and financial support of these invaluable institutions.

I would like to thank Dr. Baillie for he was the first professor to introduce me to *C. elegans*; it was probably the only time I remember being enthusiastic about driving for two hours to attend an 8:30AM class. I would also like to thank Dr. Fredrick Pio for giving me my first experiences with *C. elegans*.

Thank you Dr. Howard Trottier for allowing me to be part of the SFU Trottier Observing group and for the privilege to do astrophotography using the SFU observatory. Being around the observatory and the observing group became my happy place at dark times (pun intended). When you look at the bright side, you will find the stars.

Leaving the best for last, thank you Dr. Harald Hutter for being the best supervisor I could ask for. Thank you for giving me the opportunity to do my master's project in your lab and work with *C. elegans*. Thank you for always being available to answer my many questions and guiding my project in the right direction. Your expertise in guidance extends beyond axon guidance. You are like a guidance cue, guiding your students as they grow towards their final destinations to peruse their goals in life.

Thank you everyone again, Harald and members of the Hutter lab. I will cherish my experiences with you and my time in the Hutter lab forever.

Table of Contents

List of Tables

List of Figures

List of Acronyms

ADF	Actin depolymerizing factor
Arp2/3	Actin related proteins 2/3
BMP	bone morphogenetic protein
Boc	biregional Cdon-binding protein
C. elegans	*Caenorhabditis elegans*
CAMs	cell surface adhesion molecules
CCC	cadherin-catenin complex
Cdc42	Cell division control protein 42 homolog
cdh	CaDHerin family
ced	CEll Death abnormality
cfz	Caenorhabditis FriZzled homolog
CNS	central nervous system
comm	commissureless
cwn	C. elegans WNT family
DCC	deleted in colorectal cancer
DNA	desoxy-ribonucleic acid
DNC	Dorsal nerve cord
EFN	Eph(F)riN
EGF	Epidermal growth factor
egl	EGg Laying defective
EMS	ethyl methanesulphonate
ena	Enabled
F1	first filial generation
F2	second filial generation
fmi-1	FlaMIngo (cadherin plus 7TM domain) homolog
GABA	γ-aminobutyric acid
GAP	GTPase activating protein
GEF	guanine nucleotide exchange factor
GFP	green fluorescent protein
grd	GRounDhog (hedgehog-like family)
glr	ground-like

GPI	Glycosyl phosphatidylinositol
GTPase	Guanosine triphosphatase
Hh	Hedgehog
Hh-r	hedgehog related
Hip	Hedgehog interacting protein
hmr	HaMmeRhead embryonic lethal
hmp	huMPack
Ig	immunoglobulin
kb	Kilobase
LAD	L1 CAM Adhesion molecule homolog
lin	abnormal cell LINeage
mab	Male ABnormal
MATH	meprin and TRAF homology
mig	abnormal cell MIGration
MLCK	myosin light chain kinase
mm	millimetre
mM	milliMolar
mom	More Of MS
MT	microtubule
PCCD	primitive classical cadherin domain
PCP	planar cell polarity
PCR	polymerase chain reaction
PLX	PLeXin
PNS	peripheral nervous system
Ptc	Patched
PTR	Patched related proteins
Rac	Ras-related C3 botulinum toxin substrate
Rho	Ras Homolog Family Member
RNAi	RNA interference
Robo	Roundabout
ROCK	Rho-associated, Coiled-Coil Containing protein kinase
RTK	receptor tyrosine kinases
sax	Sensory AXon guidance

Sema	Semaphorin
Shh	Sonic hedgehog
SLT	SLiT (Drosophila) homolog
SMART	Simple Modular Architecture Research Tool
Smo	Smoothened
SNP	single nucleotide polymorphism
snRNPs	small nuclear ribonucleoproteins
Stan	STArry Night
TGF-β	Transforming Growth factor-β
unc	uncoordinated
vab	Variable ABnormal morphology
VASP	VAsolidatorStimulated Phosphoprotein
VNC	ventral nerve cord
WGS	Whole Genome Sequencing
Wnt	wingless
ZIG	(Zwei) IG domain protein

Chapter 1.

Introduction

1.1. Neuronal circuit formation during nervous system development

The nervous system is the most complex system in the animal embryo. In mammals, the nervous system is divided into the central nervous system (CNS) that includes the brain and spinal cord, and the peripheral nervous system (PNS), which connects the whole body to the central nervous system. The brain has the ability to receive, process, and deliver information to different parts of the body in order to control it. Therefore, proper neuronal connections are important for establishing coordinated and controlled input and output signals. There are two main types of cells within the nervous system, the neurons, which are nerve cells that controls the processing of signals, and glial cells, which are non-neuronal cells that surround the neurons, providing support roles for their function. Signal transmission within nervous system is carried in the form of an electrical signal. Neurons receives inputs from other neurons through highly branched structures called dendrites, the signal is then processed in the cell body of the neuron, generating an electrical impulse to be carried along the axon that is connected to a target cell through a synapse (Wolpert 2011).

During development of nervous system in both vertebrate and invertebrates, the ectoderm layer gives rise to the epidermis, the non-neuronal tissue, and the neuronal tissue. In *Drosophila*, the neuroectoderm gives rise to neuroblasts. The neuroblasts undergo asymmetrical divisions, giving rise to neuronal precursor cells and neuroblasts. In vertebrates, the neural plate (neuroepithelium) gives rise to the neural tube, which in turn gives rise to cells forming the brain and to neural crest cells that contribute to the PNS. Neurons are generated within a region of the neural tube called the proliferative zone and then migrate towards different regions of the brain and spinal cord. The brain is divided into three regions, forebrain, midbrain, and hindbrain. During embryo development, after neuronal precursors differentiate into neurons, they extend neuronal processes, which include axons and dendrites, that travel distances to find their target cells. This process of axon guidance will be explained in further detail below. Once

axons arrive at their target field, they form synapses with their synaptic partners, target cells that could be either a muscle cell or another neuron. Once contacts are established, connections will be refined for axons that got associated with incorrect target cells (Squire 2008; Wolpert 2011). Overall, the process of nervous system development involves the following steps: specification and determination of neuronal cell identities, neuron formation and migration, axon outgrowth towards their targets, synapse formation with the target cells, and synapse refinement. How much we understand each of these steps for neuronal circuit formations is reflected in the order, in which the process is best understood at the neuronal specification and differentiation stage and then understanding ceases towards the synapse refinement.

Synaptogenesis includes formation of defined alignments between presynaptic neurons that function in docking synaptic vesicles that release neurotransmitters into the synaptic cleft, and postsynaptic neurons that harbor neurotransmitter receptors, voltage gated channels, and second-messenger signaling molecules (Cowan *et al*. 2001). It is thought that synapses are held in register through filamentous proteins that extend from presynaptic active zone and across synaptic cleft. Synapses can be categorized according to type, function, and synaptic efficacy. The type of a synapse refers to the specific neurotransmitter(s) that it releases. Function of a synapse is whether it is excitatory, inhibitory, or modulatory. Synaptic efficacy is whether the synaptic firing is done constitutively or irregularly, and whether it is consistently or inconsistently (Waites *et al.* 2005). Synaptogenesis occurs during embryogenesis and adulthood. During development, synaptogenesis occurs after neuronal differentiation and establishment of neuronal network. Genes encoding pre- and postsynaptic proteins are expressed and hence trafficked to their designated synaptic site. Specification of correct neuronal connections includes utilization of signaling molecules, secreted factors, receptors, and cell surface adhesion molecules (CAMs) in order to allow formation of synapse and cell-cell recognition. During development, synapses can either be stabilized or eliminated, but what determines the fate of a synapse remains unknown.

1.2. Axon guidance during development of the nervous system

Development of the nervous system requires proper assembly of neuronal circuits. During embryogenesis, axons must grow and navigate large distances before

they establish synapses with the correct target cell. Axon guidance requires responding to signals known as guidance cues that allow axons to reach their correct destination. Guidance cues are ligands that interact with receptors displayed on the tip of the axon, the “growth cone”. These cues can be in the form of chemoattractants that produce a gradient or in the form of cell-surface bound adhesion molecules (Figure 1.1). Some guidance cues function as an attractive signal, leading the axon towards a specific path and target, while some function as a repulsive signal, preventing the axon from going along the wrong trajectory. Guidance cues that have been identified so far include UNC-6/netrins (Hedgecock *et al.* 1990; Ishii *et al.* 1992; Hutter 2003), slits (Rothberg *et al.* 1988), ephrins (Gale *et al.* 1996), and semaphorins (Kolodkin 1996) (Figure 1.2). Some of them function both as an attractant and repellant and some work together in navigating an axon. The state of cues, whether being attractive or repulsive, is sometimes determined and facilitated by expression of receptors in neurons mediating either attraction or repulsion. Axon pathfinding involves interactions between the cues and the growth cone, which is located at the end of a growing axon. The process of axon navigation has been well studied in both vertebrate (zebrafish, *Xenopus*, chicken, mouse) and invertebrate (*C. elegans*, *Drosophila*, grasshopper) model organisms. In vertebrate, the navigation of the retinal axons to the optic tectum within the midbrain is the best understood system with regards to axon guidance (McLaughlin *et al.* 2003; Lemke and Reber 2005).

1.3. Intracellular signaling and cytoskeletal dynamics in growth cones

At the tip of axons exists a motile specialized structure known as the growth cone (Cajal 1890). This structure behaves as a sensor for guidance cues found in its environment. When the growth cone senses a cue, the interaction translates into directional signaling. The cues are either chemoattractants, guiding axons towards a path, or chemorepellents, guiding axons away from the wrong path. There are two types of protrusions that growth cones form, filopodia and lamellipodia (Figure 1.3) (Yamada *et al.* 1970; Gomez and Letourneau 2014). Guidance cues bind to their corresponding receptors on filopodia of growth cones, which sends an inward intracellular signal that controls cytoskeleton remodeling. The action of growth cones involves microtubules that stabilize the outgrowing axon and dynamic actin-filaments. When an attractive cue binds

to growth cone, the actin-filaments are stabilized in the direction of the cue, thus actin polymerization occurs. When a repulsive cue binds to growth cone, the actin-filaments are collapsed, and thus actin depolymerization occurs in direction of the cue, causing the growth cone to turn away and avoid that ligand (Dent and Gertler 2003; Quinn and Wadsworth 2008).

The axon guidance cues Netrin, Slit, Semaphorin and ephrins when interacting with their corresponding receptors on the growth cone, activate members of Rho family GTPases, which include RhoA, Rac, and Cdc42 (Figure 1.4) (Hall and Lalli 2010; Bashaw and Klein 2010). Rho GTPases are signaling proteins involved in coordinating cytoskeletal effectors controlling responses such as actin polymerization and depolymerization (Ridley and Hall 1992; Ridley *et al.* 1992; Lowery and Van Vactor 2009). Upstream regulators of Rho GTPases are the GEFs (guanine nucleotide exchange factors), which activate Rho GTPases, and the GAPs (GTPase activating protein), which are inactivators of these proteins (Koh 2006; Watabe-Uchida *et al.* 2006). For example, the ligand-receptor pair EphrinB3/EphA4 activates a Rac GAP that leads to inhibiting growth cone extension (Iwasato *et al.* 2007) and a Rho GEF protein that activates RhoA to induce growth cone collapse (Shamah *et al.* 2001). Both in *C. elegans* and *Drosophila*, the Rac-GEF (guanine nucleotide exchange factors) protein, UNC-73/Trio, activates Rac-like proteins during axon guidance (Steven *et al.* 1998; Newsome *et al.* 2000). In *C. elegans*, there are three redundant Rac-like proteins, CED-10, MIG-2, and RAC-2, involved in axon guidance (Lundquist *et al.* 2001). The Rho-family GTPases that involves GEF, GAP, and GTPase signalling network combinations are many and complicated.

While the Rho-family GTPase effectors regulate all aspects of cytoskeletal remodeling, actin dynamics at the leading edges are regulated by regulators that include the actin nucleators Arp2/3 complex and Formins, which are Actin-Related Proteins, and Ena/VASP (Enabled/vasolidatorstimulated phosphoprotein), which is an F-actin polymerization factor (Figure 1.4) (Goley and Welch 2006). The Arp2/3 complex affects protrusion dynamics (Korobova and Svitkina 2008) while Formin, a downstream regulator of Rho GTPases (Goode and Eck 2007), acts together with Rac GTPases to regulate filopodial formation during axonal growth (Matusek *et al.* 2008). The Ena/VASP proteins function in actin polymerization by recruiting actin subunits to the leading edges of growth cones and inhibiting proteins like Formins that inhibit actin elongation (Drees

and Gertler 2008). There are genetic interactions between the Ena/VASP proteins and the Rho-GTPases signaling (Liebl *et al.* 2000), suggesting that the two systems communicate with each other to regulate cytoskeleton dynamics. ROCK, the most studied cytoskeletal effector downstream of the Rho GTPases RhoA, is involved in actin depolymerization and actin retrograding (Lowery and Van Vactor 2009). Actin retrograde flow involves assembly and disassembly of actin filaments inside filopodia in order to generate force at the leading edge of a cell to move forward. ROCK phosphorylates MLCK (myosin light chain kinase) to promote myosin II activity, causing actomyosin contraction and hence actin retrograding (Zhang *et al.* 2003; Burnette *et al.* 2008), and phosphorylates LIMK (LIM domain kinase), which in turn phosphorylates ADF/Cofilin, inactivating the protein and thus leading to actin-disassembly (Figure 1.4) (Wen *et al.* 2007).

In addition to actin-dynamics, microtubule (MT) dynamics has to be coordinated as well in order to control growth cone steering. Controlling microtubule interactions with actin involves coupling and uncoupling of MTs with actin retrograde flow. Positive cues are likely to produce an uncoupling effect that allows MTs to enter filopodia with the cue/receptor signaling sites, while negative cues result in coupling of MT and actin. MAP proteins have been implicated in MT dynamics in which it functions in stabilizing the growing ends of MTs, MT plus-ends, and controlling MT cross-linkage to actin (Lowery and Van Vactor 2009).

1.4. *C. elegans* nervous system

The nervous system in humans is extremely intricate because it contains on average 100 billions of neurons that form trillions of highly organized patterns of connections, creating the neuronal circuit that produces a functioning nervous system (Squire 2008). This generates a highly complex nervous system, which makes investigation of neuronal circuit development in human challenging. However, a complete neuronal wiring diagram had been established in *Caenorhabditis elegans*. This simple model organism is a free-living roundworm that contains 302 neurons (Brenner 1974; White *et al.* 1986). Achieving the neuronal circuit map was made possible by manual reconstruction using electron microscopic sections in a project that lasted for two decades. This study identified around 7000 synapses in the *C. elegans* nervous system (White *et al.* 1986).

Most of the neurons are found in the head region where axons form a structure known as the nerve ring. There are two different longitudinal nerve bundles, the dorsal nerve cord (DNC) on the dorsal side and ventral nerve cord (VNC) on the ventral side (Figure 1.5). These tracts run parallel to each other along the anterior and posterior axis. The VNC of *C. elegans* consists of four axons in the left tract and 50 axons in the right tract in an adult animal, creating an asymmetric distribution of axons. The motor neuron cell bodies within the VNC extend their axons along the VNC tract and commissures towards the DNC. The right tract includes interneuron and motor neuron axons. The dorsal nerve cord consists mainly of motor neuron axons coming from the ventral nerve cord. In the tail region, there are two pairs of interneurons with cell bodies known as PVP and PVQ. These extend towards the head. Another pair of motor neurons with cell bodies close to the vulva includes HSN, which extend anteriorly in both VNC tracts. AVK neurons extend from the head and towards the posterior of the animal (Figure 1.6) (White *et al.* 1976, 1986). Overall, the nervous system of *C. elegans* is well described and hence makes investigation of nervous system development possible.

C. elegans movement behavior comprises of crawling on solid surfaces and swimming in liquids. Their motility repertory consists of alternating ventral and dorsal contractions of the body. Muscles associated with dorsal and ventral cords are controlled by distinct motor neurons. Generating a sinusoidal pattern of movement relies on producing alternating contractions between dorsal and ventral body wall muscles. There are eight classes of motor neurons that control this process. Type A and B (VA, VB, DB, AS) are excitatory classes of neurons, using the neurotransmitter acetylcholine, while type D (VD, DD) is an inhibitory class of neurons, using GABA. The dorsal muscles are innervated by DA, DB, DD, and AS, while ventral muscles are by VA, VB, VC, and VD (Figure 1.7). The locomotory production occurs via interactions between the stimulatory and inhibitory motor neurons, causing muscle contraction and relaxation, respectively. Therefore, this interaction is necessary for preventing dorsal and ventral muscle contraction simultaneously. The forward and backward movements in *C. elegans* are controlled through interactions between specific interneuron pairs and motor neurons. The interneuron pairs include AVA, AVB, AVD, and PVC, which run along the length of VNC, providing input into the ventral motor neurons. The circuit for executing forward movement includes the AVB and PVC interneurons and the B type motor neurons. For

the reverse movement, the circuit includes the interneurons AVA and AVD and type A motor neurons (Figure 1.7) (Riddle *et al.* 1997).

Genetic screens have been done in *C. elegans* to identify genes controlling axon guidance. For example, *unc-6* mutant animals exhibit an obvious movement defect, in which the worm lacks that sinusoidal movement pattern, and UNC-6 is a protein with a role in axonal navigation (Hedgecock *et al.* 1990), which will be described in the following section.

1.5. Guidance cues for outgrowing axons

1.5.1. UNC-6/Netrin

UNC-6/Netrin is a secreted extracellular matrix protein with structural similarities to laminin (Hedgecock *et al.* 1990; Ishii *et al.* 1992) and is also highly conserved between vertebrate and invertebrates. UNC-6 homologs in *Drosophila* and vertebrate are called Netrins. UNC-6/Netrin was first discovered and implicated in neuronal circuit formation in *C. elegans* (Hedgecock *et al.* 1990). This guidance cue was identified in screens for animals with movement defects (Brenner 1974), hence the gene being named *unc,* short for uncoordinated movement. UNC-6/Netrin has a bifunctional role because it can promote both attraction and repulsion depending on the repertoire of receptors displayed on the surface of growth cone (Chisholm *et al.* 2016). Attraction is mediated by binding to the UNC-40/DDC (Deleted in colorectal cancer) transmembrane receptor, while repulsion is mediated by binding to UNC-5 or the heterodimer UNC-5/UNC-40 transmembrane receptors (Hedgecock *et al.* 1990).

In *C. elegans*, UNC-6 is involved in dorsal-ventral navigation of axons known as commissures. UNC-6 is produced by the ventral cells, forming a gradient from ventral to dorsal (Figure 1.8)(Wadsworth *et al.* 1996; Wadsworth and Hedgecock 1996). Axons expressing *unc-40* receive an attractive signal by UNC-6 and hence grow towards the ventral side, while axons expressing the UNC-5 receptor alone or together with UNC-40 are repelled by UNC-6 and thus grow towards the dorsal side (Chisholm *et al.* 2016). UNC-6 is thought to localize to the basement membrane of the epidermis, which is a substrate for neurons to grow their axons. UNC-6 also has a role in guiding a subset of neurons along the VNC that include motor neurons and the interneurons PVQ and PVP

(Hutter 2003). In addition to axon guidance, UNC-6 has roles in localization of presynaptic components to subcellular compartments of specific neurites, such as VNC neurites, in order to connect with the appropriate partner cell (Park *et al.* 2011).

In *Drosophila*, Netrin is involved in navigation of commissural axons towards the ventral midline within the CNS, by acting as an attractive guidance cue located ventrally (Harris *et al.* 1996). For trochlear motor neurons in vertebrates, Netrin acts as a repellent to guide axons dorsally and away from floor plate (Colamarino and Tessier-Lavigne 1995). Similar to *Drosophila*, commissural neurons in vertebrates differentiate in the dorsal regions and then extend their axons towards the floor plate at the ventral midline guided by Netrin and then towards the midbrain region.

1.5.2. SLT-1/Slit

Slit is a repulsive guidance cue that was first discovered in *Drosophila* (Rothberg *et al.* 1988, 1990). It is secreted at the ventral midline to prevent axons from crossing the midline. Roundabout (Robo) is the receptor for Slit producing the repulsive signaling (Rothberg *et al.* 1990; Kidd *et al.* 1998; Brose *et al.* 1999; Battye *et al.* 2001; Howitt *et al.* 2004; Morlot *et al.* 2007). Slit interacts with three different Robo receptors, Robo, Robo2, and Robo3, displayed on the growth cones of axons. Commissural axons are able to cross the ventral midline bypassing the Slit repulsion, due to the presence of the Commissureless (COMM) protein, an endosomal sorting receptor protein (Keleman *et al.* 2002, 2005). COMM functions in regulating Robo trafficking, sorting the receptors for degradation preventing them from being displayed on the growth cone. When Robo is not at the growth cone, the axon is not sensitive to Slit and thus not repelled. Instead, the axon is attracted towards the midline due to the presence of the attractive guidance cue, Netrin. In *C. elegans*, Slit (SLT-1) in the form of a gradient, being higher on the dorsal side, functions in repelling axons to navigate towards the ventral cord (Zallen *et al.* 1998; Hao *et al.* 2001). There is one type of Robo receptor, SAX-3. In mice, there are three different Slits and three different Robos (Dickson and Gilestro 2006). Slits, the repulsive cue, and Netrin, the attractive cue, are found in a gradient at the midline of the floor plate, equivalent to the ventral midline in *Drosophila*. These guidance cues guide the commissarial axons towards the midline. ROBO3 exist in two isoforms, 3.1 and 3.2. ROBO3.1 inhibits the ROBO1 receptor to prevent interaction with Slit, thus allowing commissarial axons to cross the midline. ROBO3.2 interacts with ROBO1 receptor,

allowing interaction with Slit, and hence mediating repulsion from the midline (Chen *et al.* 2008; Evans and Bashaw 2010). Overall, the navigation process through the Slit/Robo signaling is conserved between vertebrate and invertebrates.

1.5.3. Semphorins

Semaphorins are a large family of signaling molecules that could be either in a secreted form for long-range influence or in a membrane-bound form for short-range influence (Kolodkin 1996; Raper 2000; Chilton 2006). Semaphorins are defined by having the highly conserved sema domain, comprised of about 500 amino acids (Kolodkin *et al.* 1997). These proteins are grouped into eight classes. From these classes, the class III secreted semaphorins (Sema III) in vertevrates and class I and II (Sema I and II) in invertebrates are studied in detail with regards to axon guidance (Luo *et al.* 1993; Kruger *et al.* 2005). Sema III was first identified as a repulsive cue in adult chick brain tissue (Luo *et al.* 1993) and grasshopper (Kolodkin *et al.* 1997). Neuropilins, in vertebrates (Kolodkin *et al.* 1997), and plexins (Winberg *et al.* 1998) are the receptors for semaphorins. Activation of semaphorin-plexin signaling leads to regulation of GTPases that are involved in actin-filament and microtubule dynamics (Kruger *et al.* 2005). In *C. elegans*, there are three semaphorin and two plexin proteins, with MAB-20/Sema-2 (Roy *et al.* 2000) and its receptor PLX-2 and co-receptor LAD-2 (Wang *et al.* 2008) being involved in axon guidance and cell migration. Semaphorins have roles outside development of the nervous system (Raper 2000), such as in the immune system in vertebrates (Kruger *et al.* 2005) and embryonic morphogenesis in *C. elegans* (Roy *et al.* 2000).

1.5.4. Ephrins

Ephrins are cell surface-bound proteins that cause growth cone collapse when bound to Eph receptors (EphR). Both Ephrins and their Eph receptors are divided into families A and B. The Eprhrin A group has a glycosylphosphatidylinositol (GPI) anchor, while the Ephrin B group has a transmembrane domain (Gale *et al.* 1996; Chilton 2006). EphA and EphB are receptor tyrosine kinases (Pasquale 2005). The Ephrin/Eph system has been well studied in vertebrates for their role in establishing a topographic map in the optic tectum within the midbrain (Lemke and Reber 2005; Chilton 2006; Cang and Feldheim 2013). Opposing gradients of the Ephrin ligands and their Eph receptors sets

up these topographic maps. EphrinA/EphA signling controls the topographic mapping along the anterior-posterior axis of the tectum, while EphrinB/EhpB signaling controls patterning along the dorsal-ventral axis (Hindges *et al.* 2002; Mann *et al.* 2002). Ephrins and Eph receptors are evolutionary conserved proteins among phyla, with nine Ephrins and 16 Eph receptors in vertebrates (Lackmann and Boyd 2008), a single Ephrin/Eph receptor pair in *Drosophila* (Boyle *et al.* 2006), and four Ephrins and one Eph receptor in *C. elegans* (George *et al.* 1998; Chin-Sang *et al.* 1999). In *C. elegans*, the four Ephrin ligands are VAB-2/EFN-1, EFN-2, EFN-4, and EFN-4, and the Eph receptor is VAB-1. These proteins have pleiotropic functions (Chisholm *et al.* 2016) that include axon guidance, neuroblast migration, axon extension, muscle cell migration (Tucker and Han 2008; Viveiros *et al.* 2011), and epidermal morphogenesis. Activation of VAB-1 via EFN-1, EFN-2, and EFN-3 contributes to preventing axonal midline crossing at the VNC (Boulin *et al.* 2006). EFN-2, EFN-3, EFN-4, and VAB-1 act in extension and stopping point termination of certain axons (Mohamed and Chin-Sang 2006). EFN-4 is involved in axonal outgrowth of AIY and D-type motor neurons (Schwieterman *et al.* 2016). EFN-4 is also involved in migration of SDQ axons (Dong *et al.* 2016) by interacting with LAD-2 instead of VAB-1(Chin-Sang *et al.* 2002).

1.6. Role of Wingless/WNT, Hh/Shh, and BMP/TGF-β families in axon guidance

Members of Wingless/Wnt, Hh/Shh and BMP/ TGF-β families have been implicated in axon guidance. In mammals, WNT4 acts as an attractive cue for commissural axons along the anterior-posterior axis of the spinal cord (Lyuksyutova *et al.* 2003). A WNT4 gradient attracts axons towards the anterior side of the spinal cord after midline crossing. The Frizzled co-receptor RYK mediates repulsion of posterior-directed axons by WNTs (Lu *et al.* 2004; Liu *et al.* 2005). In *Drosophila*, during navigation of commissural axons along the ventral midline in the CNS, WNT5, being expressed at the posterior commissures, functions as a repulsive cue via the Derailed/RYK receptor, which is expressed at the anterior commissures (Yoshikawa *et al.* 2003). In *C. elegans*, there are five WNTs (*lin-44, egl-20, mom-2, cwn-1, cwn-2*), four Frizzled receptors (*lin-17, mom-5, mig-1, cfz-2*), and one Derailed/RTK homolog (*lin-18*), which is an atypical tyrosine kinase (Goldstein *et al.* 2006; Green *et al.* 2008; Song *et al.* 2010; Gleason and Eisenmann 2010; Harterink *et al.* 2011), that are involved in axon

extension along the anterior-posterior axis (Hilliard and Bargmann 2006; Pan *et al.* 2006; Zinovyeva *et al.* 2008). In mammals BMP/TGF-β proteins are expressed at the roof plate of the neural tube, functioning as a chemorepllent for dorsal commisural axons to direct them towards the floor plate where netrin, the attracive cue, is expressed (Augsburger *et al.* 1999; Butler and Dodd 2003). In *C. elegans*, UNC-129, a member of the BMP/TGF-β family, is expressed in the dorsal body wall muscles, creating a gradient along the dorsal-ventral direction opposite to the UNC-6/Nertin gradient to attract motor neuron axons towards the dorsal side. In addition to responding to UNC-129, these motor axons express UNC-40/DCC and UNC-5 receptors in order to be repelled by UNC-6/Netrin away from ventral region (Colavita *et al.* 1998; MacNeil *et al.* 2009).

In mice, Sonic hedgehog (Shh) is expressed at the floor plate of the neural tube, acting as attractive cue together with Netrin to guide commissural axons towards the floor plate/ventral midline (Charron *et al.* 2003). The receptor in these axons is Boc and its co-receptor. After midline crossing, axons of dorsolateral commissural neurons turn dorsally into the longitudinal axis of the spinal cord. In mouse, the graded distribution of Wnt4 attracts post-crossing axons dorsally. In contrast, in the chicken embryo, the graded distribution of Sonic hedgehog (Shh) guides post-crossing axons by a repulsive mechanism mediated by hedgehog-interacting protein. Based on these observations, we tested for a possible cooperation between the two types of morphogens. Indeed, we found that Wnts also act as axon guidance cues in the chicken spinal cord. However, in contrast to the mouse, Wnt transcription did not differ along the anteroposterior axis of the spinal cord. Rather, Wnt function was regulated by a gradient of the Wnt antagonist Sfrp1 (Secreted frizzled-related protein 1) that in turn was shaped by the Shh gradient. Thus, Shh affects post-crossing axon guidance both directly and indirectly by regulating Wnt function (Domanitskaya *et al.* 2010). Smoothened (Smo). In chick, Shh also acts as a repulsive cue for commissural axons via the Hip receptor to allow axons crossing the ventral midline before navigating anteriorly towards the floor plate (Domanitskaya et al. 2010). In retinal ganglion cell axons, Shh signaling occurs through the receptors Patched (Ptc) and and co-receptor Smo (Trousse *et al.* 2001). In *C. elegans*, hedgehog (Hh) and Smo are absent. However, the *C. elegans* genome encodes around 60 Hedgehog-related (Hh-r), 3 Patched (Ptc), and 24 Patched-related (PTR) genes (Bürglin and Kuwabara 2006). So far, none of these genes have been implicated in nervous system development.

1.7. Cadherins

Cadherins are adhesion molecules that mediate adhesion between cells through homophilic and/or heterophilic interactions. They are named cadherins for having cadherin repeats in their extracellular domains that facilitate the proper cell-cell contacts. The cadherin family is divided into subfamilies. These include the classical cadherins, desmosomal, protocadherins, Flamingo/STAN, Dachsous, and the Fat cadherins (Figure 1.9; Figure 1.10) (Tanoue and Takeichi 2005). The best-studied subfamily of cadherins is the Ca^{2+}-dependent and homophilically interacting classical cadherin (Patel *et al.* 2003). Classical cadherins are divided into three subgroups with respect to the organization of their extracellular domain. Types I and II classical cadherins have five repeats of cadherin that are specific to chordates. Type III on the other hand consist of a variable number of cadherin repeats that are found in both invertebrates and vertebrates, except for mammals. Type III also includes a variable number of EGF-like and Laminin A globular repeats and a PCCD (primitive classical cadherin domain), a conserved domain that have been implicated in proteolyic cleavage (Oda and Tsukita 1999; Tanabe *et al.* 2004). Adhesion is facilitated though interactions of the cadherin intracellular domain with actin cytoskeleton through the proteins β-catenin, α-catenin, and p120-catenin. This complex of cadherin with the three catenins forms the cadherin-catenin complex (CCC) and is found at adherens junctions of epithelial cells. *C. elegans* has a single classical cadherin gene, *hmr-1,* that encodes two isoforms of the protein, HMR-1A, expressed in all epithelial cells and a set of neurons, and HMR-1B, expressed only in neurons (Broadbent and Pettitt 2002). The genes encoding for the three catenins are *α-catenin/hmp-1, β-catenin/hmp-2 and p120/jac-1* and they are predicted to form the cadherin-catenin complex according to sequence similarities and the mutant phenotypes which include embryonic elongation and embryonic morphogenesis defects (Costa *et al.* 1998; Pettitt *et al.* 2003), indicating the importance of the catenin proteins for cadherin function in cell-cell adhesion. HMR-1B has a role in axon guidance, more specifically in the fasciculation of subset of motor neurons within DNC and VNC, during embryogenesis. It is thought that these proteins function in maintaining cell-cell contacts between the growth cone and the substrate for axon development (Broadbent and Pettitt 2002).

The desmosomal cadherins, having five repeats of cadherin, are named as such for being specific to desmosomes. They mediate cell-cell adhesion through the protein plakoglobin/desmoplakin that connects the cadherin with intermediate filaments (Garrod *et al.* 2002; Tanoue and Takeichi 2005). Protocadherins can have a number of cadherin repeats that range from five to 27 repeats and with divergent sequences for their cytoplasmic domain, suggesting that they may have different functions compared to classical and desmosomal cadherins (Tanoue and Takeichi 2005). They are mainly expressed in neurons and found in vertebrates. No homologs are found in *Drosophila* and *C. elegans* (Halbleib and Nelson 2006). Dachsous is a cadherin with 24 cadherin repeats that has been implicated in development of wing, leg, and bithorax morphology and in PCP in *Drosophila* (Tanoue and Takeichi 2005).

Flamingo (FMI-1)/Starry night (Stan) is a seven-transmembrane cadherin, with nine cadherin repeats, that was initially implicated in planar cell polarity (PCP) including pattering of wing bristle and ommatidial rotation in *Drosophila* (Chae *et al.* 1999; Tanoue and Takeichi 2005) and polarity of ear sensory hairs in mice (Curtin *et al.* 2003). Flamingo/FMI-1 is also involved in axon guidance and synaptic development in *Drosophila* (Sweeney *et al.* 2002; Lee *et al.* 2003; Bao *et al.* 2007) and *C. elegans* (Steimel *et al.* 2010; Najarro *et al.* 2012). In the development of visual system of *Drosophila*, Flamingo mediates target selection of photoreceptor axons within their target field (Lee *et al.* 2003) and axonal outgrowth within peripheral nervous system (PNS) (Sweeney et al. 2002). It appears that it is involved in homophilic and heterophilic interactions depending on the signal. In *C. elegans*, FMI-1 is required for navigation of both PVPR and PVPL axons and their follower axons through cell-cell adhesion (Steimel *et al.* 2010), suggesting homophilic interactions. FMI-1 interacts with CDH-4 for synapse development in inhibitory (GABAregic) motorneurons (Najarro *et al.* 2012), implying heterophilic interactions.

The Fat cadherins are characterized by an extracellular domain with 34 cadherin repeats that are highly conserved between vertebrates and invertebrates (Figure 1.10) (Schmitz *et al.* 2008). Fat cadherin was first described in *Drosophila* and implicated in PCP (Mahoney *et al.* 1991). The gene got its name “Fat” from the initial observation of the phenotype in *Drosophila,* where a knockout causes an enlargement of tissues within the imaginal disc. Fat cadherins in *Drosophila* function in controlling cell proliferation and planar cell polarity (PCP) within the imaginal disc (Cho and Irvine 2004). PCP was

implicated in proximal-distal orientations of hairs in wing (Cho and Irvine 2004) and dorsal-ventral orientation of ommatidia in eyes (Yang *et al.* 2002). The Fat signaling pathway with respect to PCP involves the proteins Frizzled, Four-jointed, and Dachsous. Fat is suggested to be downstream of four-jointed and dachsous and upstream of Frizzled (Strutt 2002; Matakatsu and Blair 2004; Cho and Irvine 2004). Dachsous is proposed to regulate Fat though its cadherin domain (Matakatsu and Blair 2004). How Fat regulates Frizzled is currently unknown.

In vertebrates, there are four Fat cadherins: Fat1, Fat2, Fat3, and Fat-J (Tanoue and Takeichi 2005). Fat1 knockout in mice causes perinatal lethality with phenotypes that include defects in kidney, forebrain, and eye development (Ciani *et al.* 2003). The kidney phenotype is due to the loss of renal glomerular slit junctions, indicating that Fat1 is acting as an adhesion molecule in this case. Fat1 and Fat3 are involved in the regulation of actin-cytoskeleton though association with Ena/VASP proteins (Tanoue and Takeichi 2004; Krol *et al.* 2016). In mice, Fat1, Fat3, and Fat4 have been implicated in regulating PCP (Tanoue and Takeichi 2004; Saburi *et al.* 2008; Krol *et al.* 2016). Fat1 and Fat3 polarize placement of actin-cytoskeleton within cells during kidney and retinal development, respectively (Tanoue and Takeichi 2004; Krol *et al.* 2016).

In *C. elegans*, there are two Fat-like cadherins: CDH-3 and CDH-4. The fat-like cadherins consist of three major domains: a conserved large number of cadherin repeats in the extracellular domain, an EGF and laminin A G repeats, and an intracellular domain (Figure 1.10) (Schmitz *et al.* 2008). *cdh-3* appears to be expressed in both the vulva and neurons that are associated with egg-laying, and the mutants show morphological defects in the tail (Pettitt *et al.* 1996). CDH-4 has diverse functions during embryonic development (Schmitz *et al.* 2008). *cdh-4* is a well-characterized gene with respect to axon guidance during nervous system development and since it is the key gene for this thesis, it will be described separately in the following section.

1.8. Role of the fat-like cadherin CDH-4 in axon guidance

The fat-like cadherin *cdh-4* was identified in a genetic screen for axon navigation defects (Schmitz *et al.* 2008) and also in a large-scale RNAi screen for genes involved in axon guidance of the motor circuit (Schmitz *et al.* 2007). *cdh-4* is conserved between vertebrates and invertebrates (Figure 1.10). During embryonic development of *C.*

elegans, *cdh-4* was shown to have multiple functions with pleiotropic effects. These functions include axonal navigation in the VNC, fasciculation of the DNC, migration of Q neuroblasts, and development of hypodermis and pharynx (Figure 1.11; Figure 1.12; Figure 1.13). Three different alleles (*hd40, rh310,* and *hd13*) were isolated in genetic screens (Figure 1.10). All of them resulted in defects in the major longitudinal axon tracts, VNC and DNC (Table 1.1). The *hd40* allele is a deletion of the first exon including the start codon, thus suggesting a complete loss of function, while the other alleles bear nonsense mutations generating stop codons within the cadherin domain, thus resulting in a truncated CDH-4 protein. The defasciculation in the DNC, improper elongation during embryonic development, and loss of attachment between pharynx and mouth during larval development, all indicate an adhesive function for CDH-4, mediating proper cell-cell contacts (Schmitz *et al.* 2008).

1.9. Thesis Objective

How *cdh-4* functions in axon guidance is unknown. Dr. Jie Pan performed a suppressor screen on *cdh-4(hd40)* mutants to identity genes within the *cdh-4* pathway or genes interacting with components of the pathway itself. Selecting suppressors from the screen after mutagenesis was initially based on producing a higher number of viable progeny in comparison to that of the *cdh-4(hd40)* mutants. F4 animals were subcloned, grown at 20^{o}C, and then allowed to starve the plate. Lines that starved in 14 days or less were checked for dorsal cord defasciculation defects. In the pilot screen, fifteen suppressors have been isolated, showing partial suppression of DNC defects of *cdh-4(hd40)* mutants. When I started this project, none of these suppressors was characterized.

The goal of this thesis was to phenotypically characterize the suppressors and to identify the suppressor genes. I phenotypically characterized thirteen suppressors for suppression of DNC and VNC defects and suppression of total lethality. From this subgroup, six were characterized for suppression of migration defects in the Q neuroblasts (*math-48(hd158), hd160, prp-8(hd161), hd162, hd163, prp-7(hd170)*) and five were assessed for suppression of movement defects (*math-48(hd158), hd160, prp-8(hd161), hd163, prp-7(hd170)*). Three suppressor genes were identified as *math-48*, *prp-6*, and *prp-8*. *math-48* is currently a functionally uncharacterized gene. Both *prp-6* and *prp-8* genes encode for components of the spliceosome machinery.

1.10. Figures

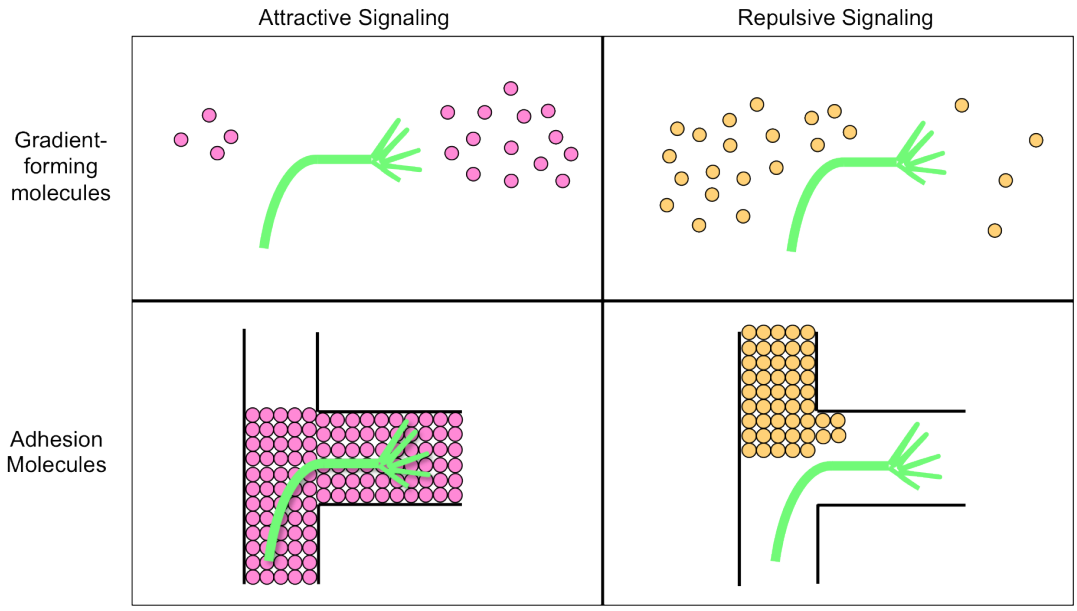

Figure 1.1 Growth cone and axon guidance cues.

Growth cone responds to guidance cues that are either positive cues (pink circles), attracting the axon towards a certain path, or to a negative cue (yellow circles), repelling the axon away from the wrong path. Guidance cues can be either in the form of diffusible molecules that create a gradient (long-range) or in the form of adhesion molecules (short-range) that require cell-cell contact between the growth cone and substrate.

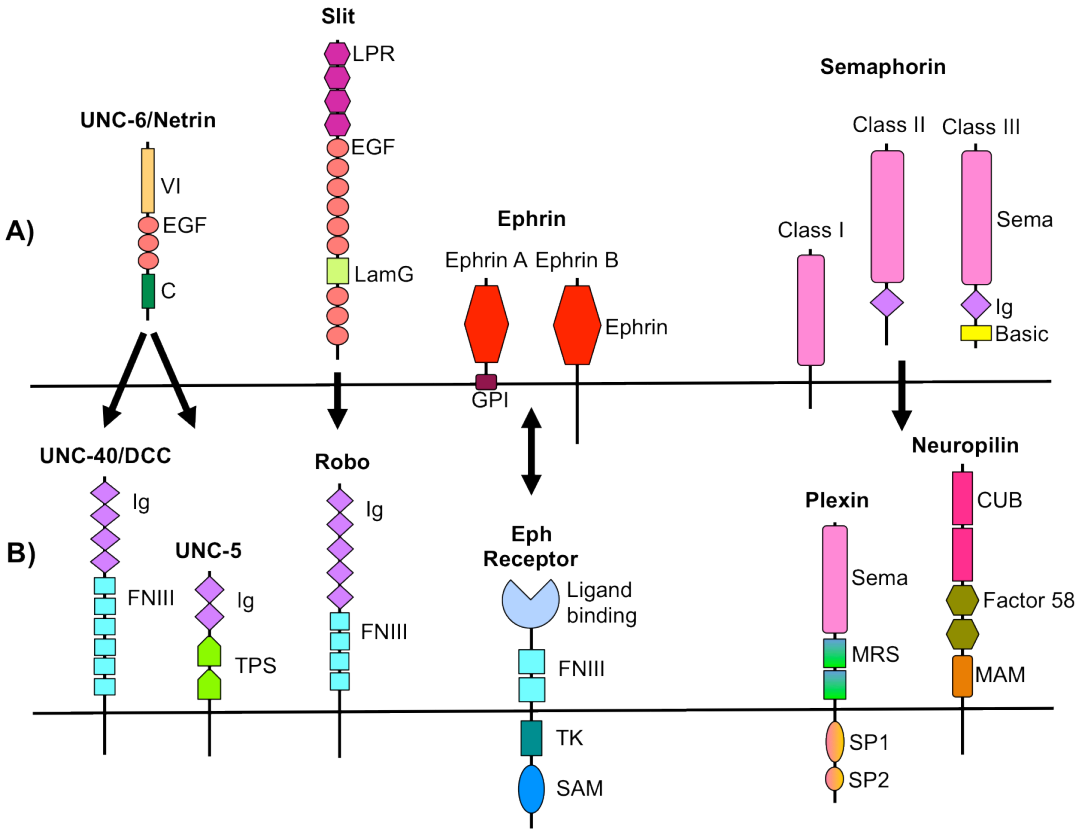

Figure 1.2 Conserved families of guidance molecules (A) and their receptors (B).

Domain names are from SMART (http://smart.embl-heidelberg.de). C (netrin C terminus), CUB (C1/Uegf/BMP-1 domain), DCC (deleted in colorectal cancer), EGF (epidermal growth factor), FNIII (fibronectin type III domain), GPI (glycosylphosphatidyl–inositol anchor), Ig (immunoglobulin domain), MAM (meprin/A5 antigen motif), MRS (Mettyrosine kinase–related sequence), SAM (sterile alpha motif), SP ('sex and plexins' domain), TK (tyrosine kinase domain), TSP (thrombospondin domain), VI (homology to laminin domain VI). (Figure creation inspired from Dickson 2002 and Timothy W. Yu and Cornelia I. Bargmann 2001).

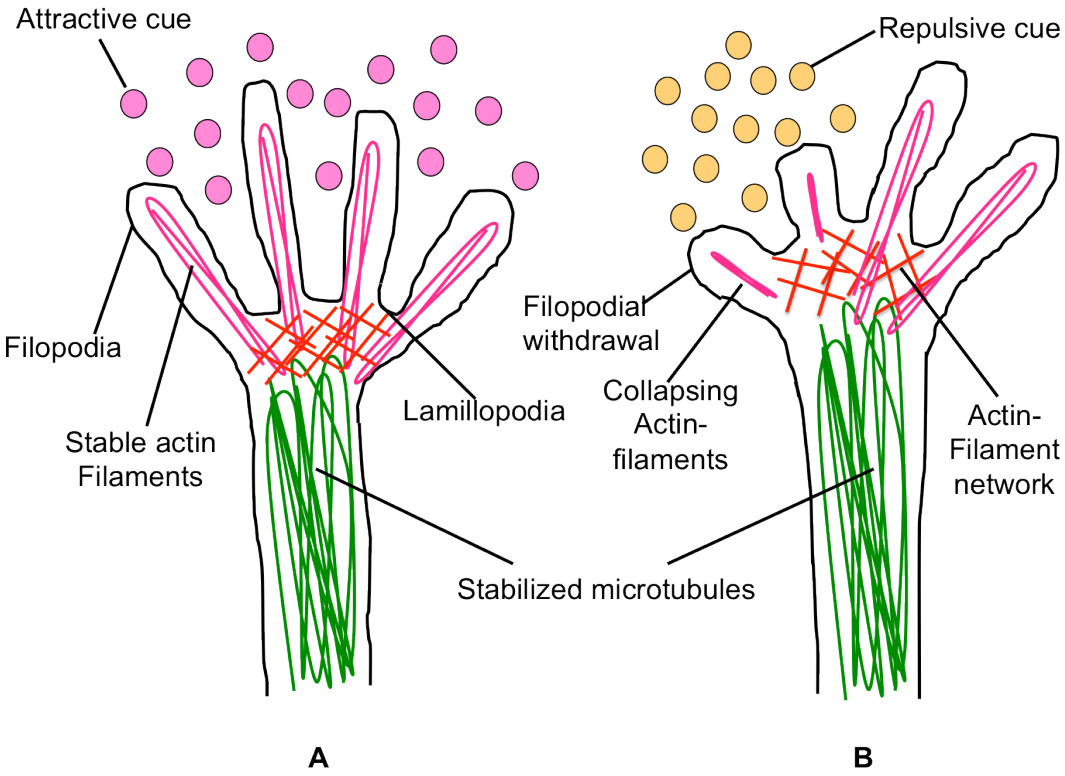

Figure 1.3 Growth cone dynamics.

Filopodia protrusions are dynamic structures with an actin core. A) Positive guidance signals lead to stabilization of actin-filaments within filopodia, promoting actin-polymerization. B) Actin-filament collapse occurs when growth cone encounters negative guidance signals, leading to depolymerisation and filopodial-withdrawal in the filopodia that are facing the negative cue. When changing directions, whether to extend towards a positive cue or to turn away from a negative cue, actin-filaments collapse, causing depolymerisation and filopodial-withdrawal in the filopodia that are in the unwanted direction. (Figure creation inspired from Dickson 2002).

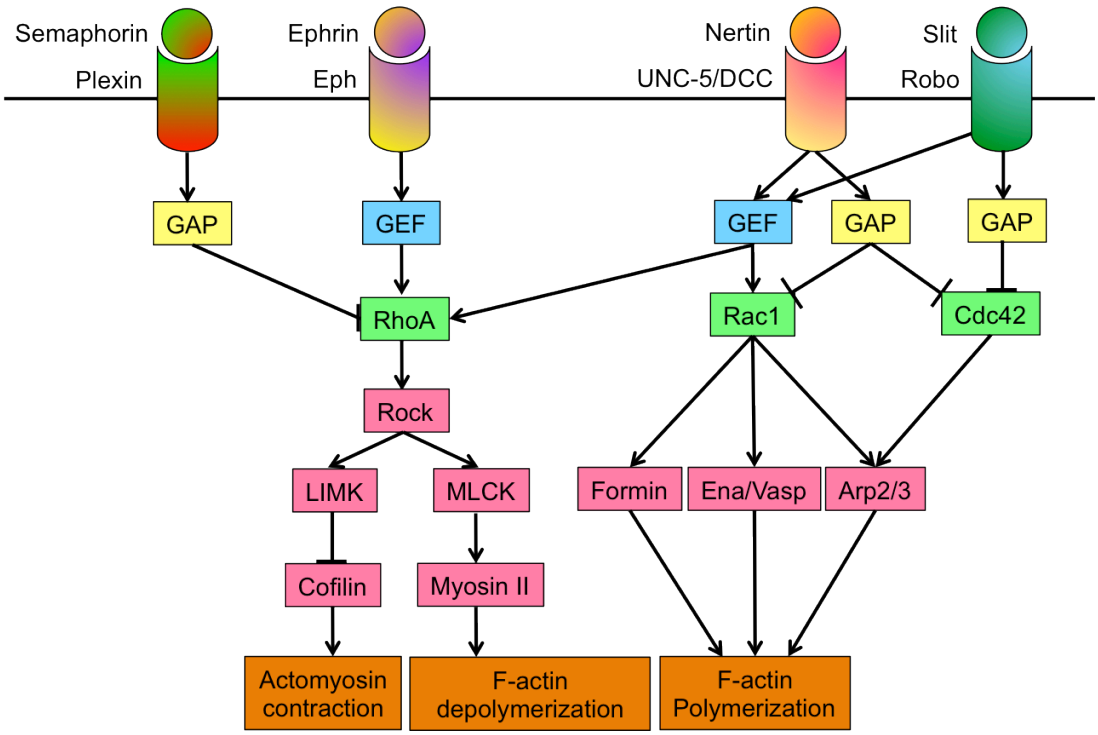

Figure 1.4 Growth cone signaling.

When guidance cue bind to their corresponding receptors in filopodia of growth cones, signaling leads to activating the Rho-GTPase regulators that include the Rho-GTPase activators GEFs (guanine nucleotide exchange factors) or Rho-GTPase inhibitors GAPs (GTPase activating proteins). Activation of Rho-GTPase regulators leads to regulation of cytoskeletal effectors resulting in effects that include actomyosin contraction, F-actin depolymerization, and F-actin polymerization. The type of cytoskeletal effect depends on the type of axon guidance signaling. Boxed inset shows the Rho-GTPase activation/inactivation cycle, in which GAPs lead to the hydrolysis of GTP to GDP, whereas GEFs catalyze the exchange of GDP for GTP. Actin-Related Protein (Arp)2/3, Enabled/vasolidator-stimulated (Ena/VASP), LIM domain kinase (LIMK), myosin light chain kinase (MLCK), and Rho kinase (ROCK) (Figure creation inspired from Lowery and Van Vactor 2009).

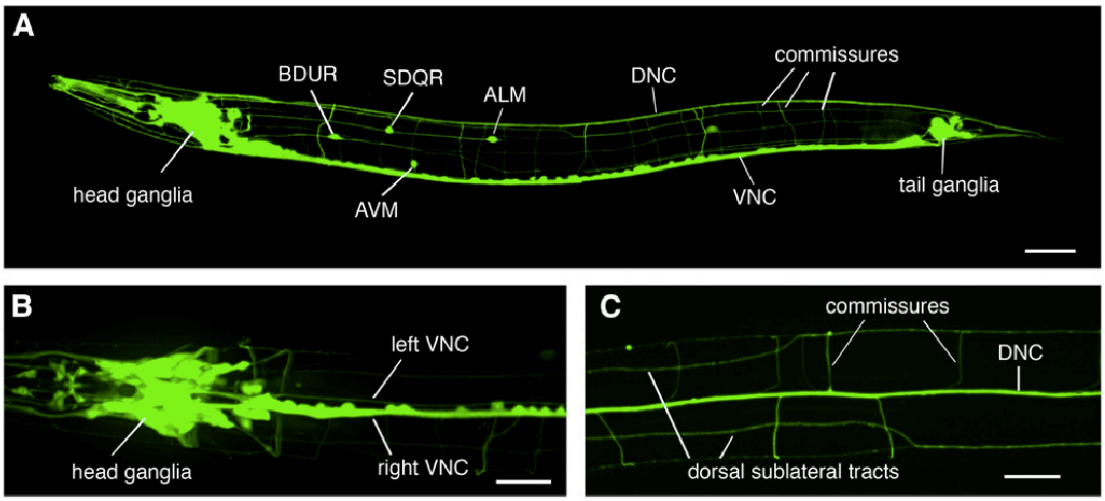

Figure 1.5 Overall architecture of axon tracts in *C. elegans*.

(A) Adult animal, side view, showing major ganglia, process bundles (dorsal and ventral nerve cords, DNC and VNC), and lateral neurons ALM, AVM, BDU, and SDQ. (B) Head region, ventral view, showing the left and right bundles of the VNC. (C) Midbody region, dorsal view, showing motor commissures, the DNC and dorsal sublateral tracts. Images are of the panneural marker Prgef-1-GFP(*evIs111*); Bars, 50 mm (A), 20 mm (B, C) (Chisholm *et al.* 2016)

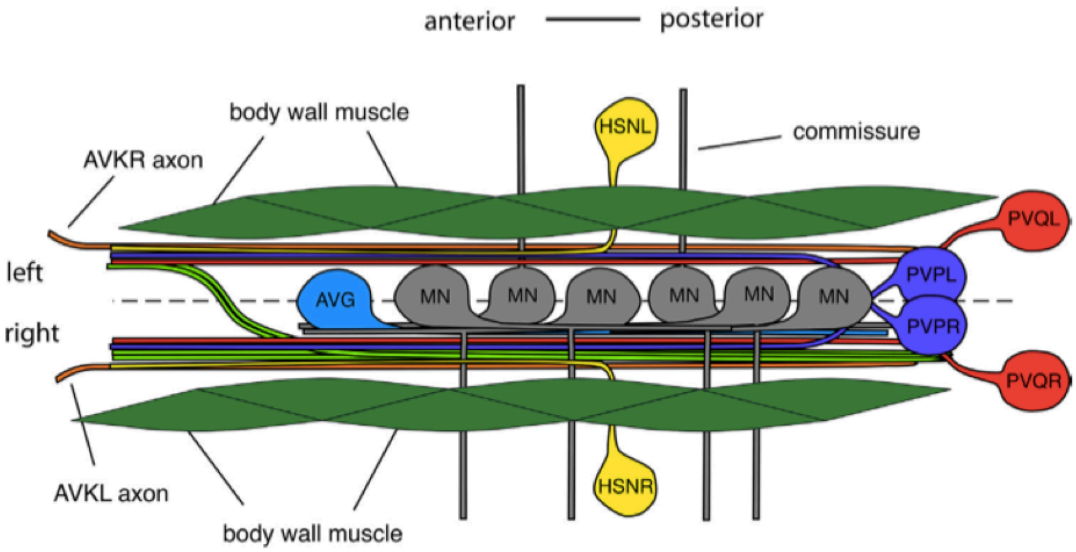

Figure 1.6 Schematic drawing of the ventral nerve cord in *C. elegans*.

MN: motor neurons (Review Hutter 2017).

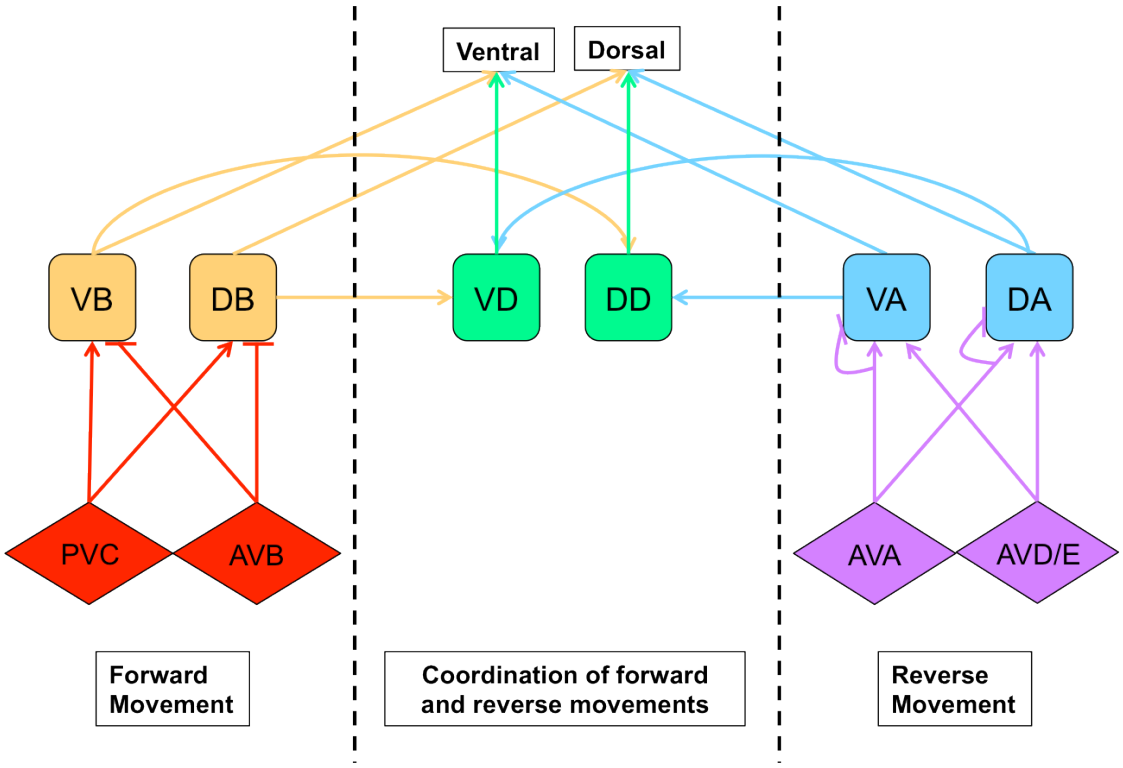

Figure 1.7 Neuronal circuits within ventral cord for locomotion in *C. elegans*.

There are six classes of motor neurons (square) that innervate body muscles of the animal. DB, DD, and DA innervate the dorsal muscles, while VB, VD, and VA innervate the ventral muscles. Forward movement is coordinated by activating DB and VB and their association with AVB and PVC interneurons (diamond), while the backward movement by DA and VA and their association with AVA, AVD, and AVE interneurons. DA, VA, DB, and VB act as excitatory motor neurons using acetylcholine as the neurotransmitter. DD and VD act as inhibitory motor neurons using the neurotransmitter GABA (Figure creation inspired from Wood 1988).

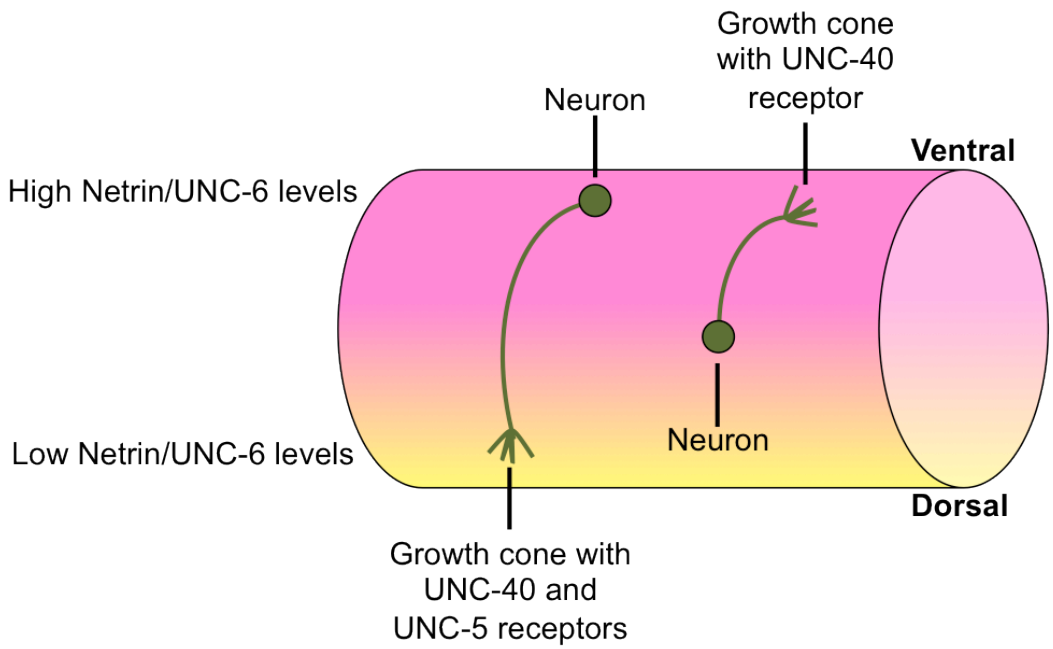

Figure 1.8 Axon guidance along dorsal ventral axis by UNC-6 in *C. elegans*.

UNC-6/Netrin (Pink) is secreted by epidermal cells on the ventral side and forms a gradient along the ventral-dorsal axis. Axons (green) grow on basement membrane on the epidermal side. Growth cones expressing UNC-40/DCC are attracted ventrally towards the high concentration of UNC-6/Netrin while growth cones expressing UNC-5 together with UNC-40/DCC are repelled by UNC-6/Netrin and hence axons grows dorsally towards the low UNC-6/Netrin gradient (Figure creation inspired from William G.Wadsworth 2002).

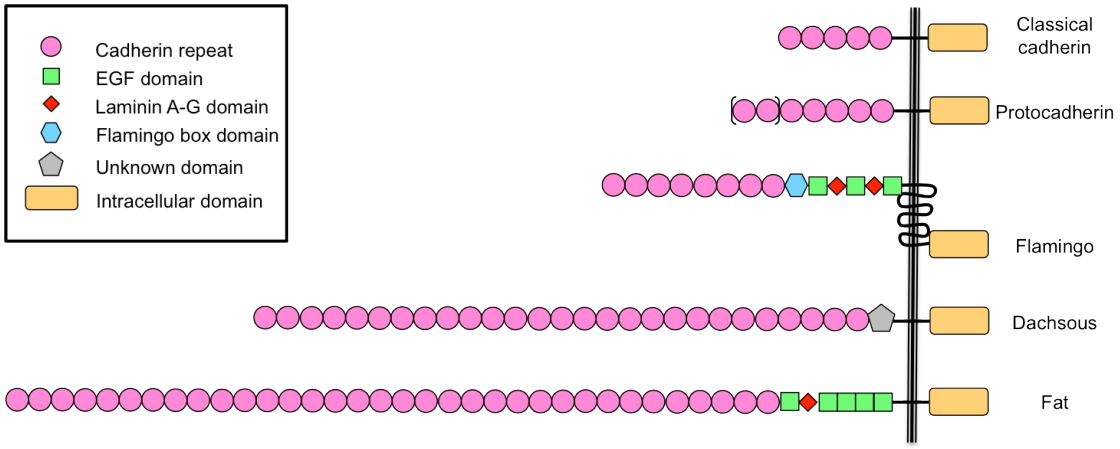

Figure 1.9 Cadherin structure.

All cadherins possess calcium-binding cadherin repeats that vary in number depending on the subfamily. Non-classical cadherins also have additional extracellular motifs including laminin A-G and EGF domains and flamingo boxes. Cadherins are transmembrane proteins, with flamingo being a seven-pass membrane protein. The cytoplasmic domain of classical cadherins is

conserved. Brackets indicate that protocadherins could have either six or seven cadherin repeats. Note that this is not a molecular scale representation of the cadherin sizes (Figure creation inspired from Halbleib and Nelson W. 2015).

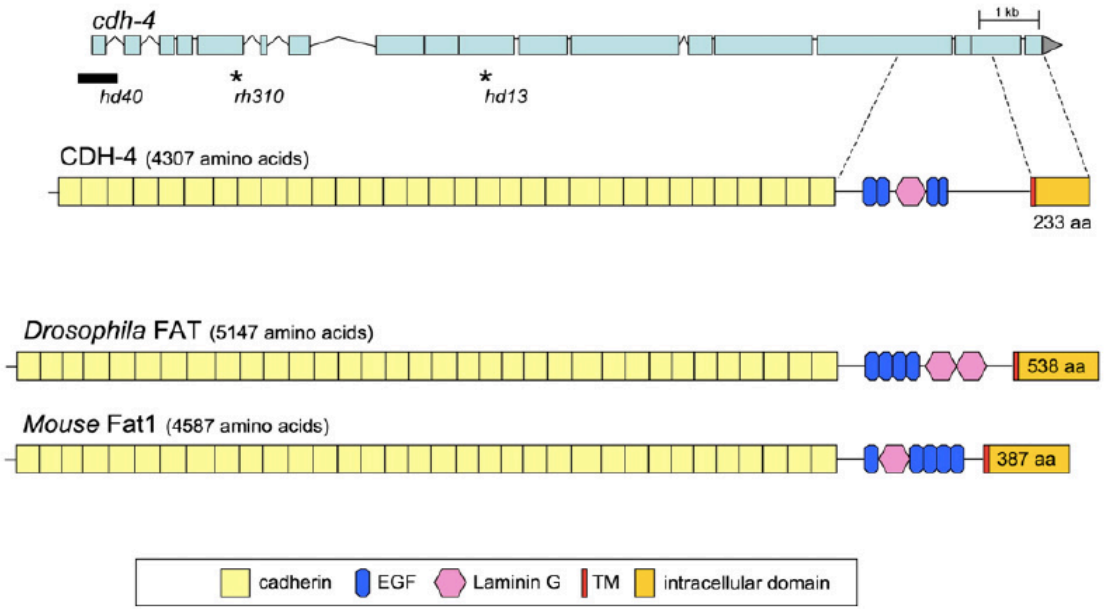

Figure 1.10 Structure of *cdh-4*.

C. elegans gene structure, including both exons and introns, and location of the *cdh-4* mutations. The bar refers to a deletion mutation while the asterisks to point mutations. Domain organization of CDH-4 protein in *C. elegans* is compared to the FAT in *Drosophila* and Fat1 in mice. The extracellular is comprised of a highly conserved large number of cadherins, and a non-conserved number of both EGF and Laminin G domains (Schmitz et al. 2008).

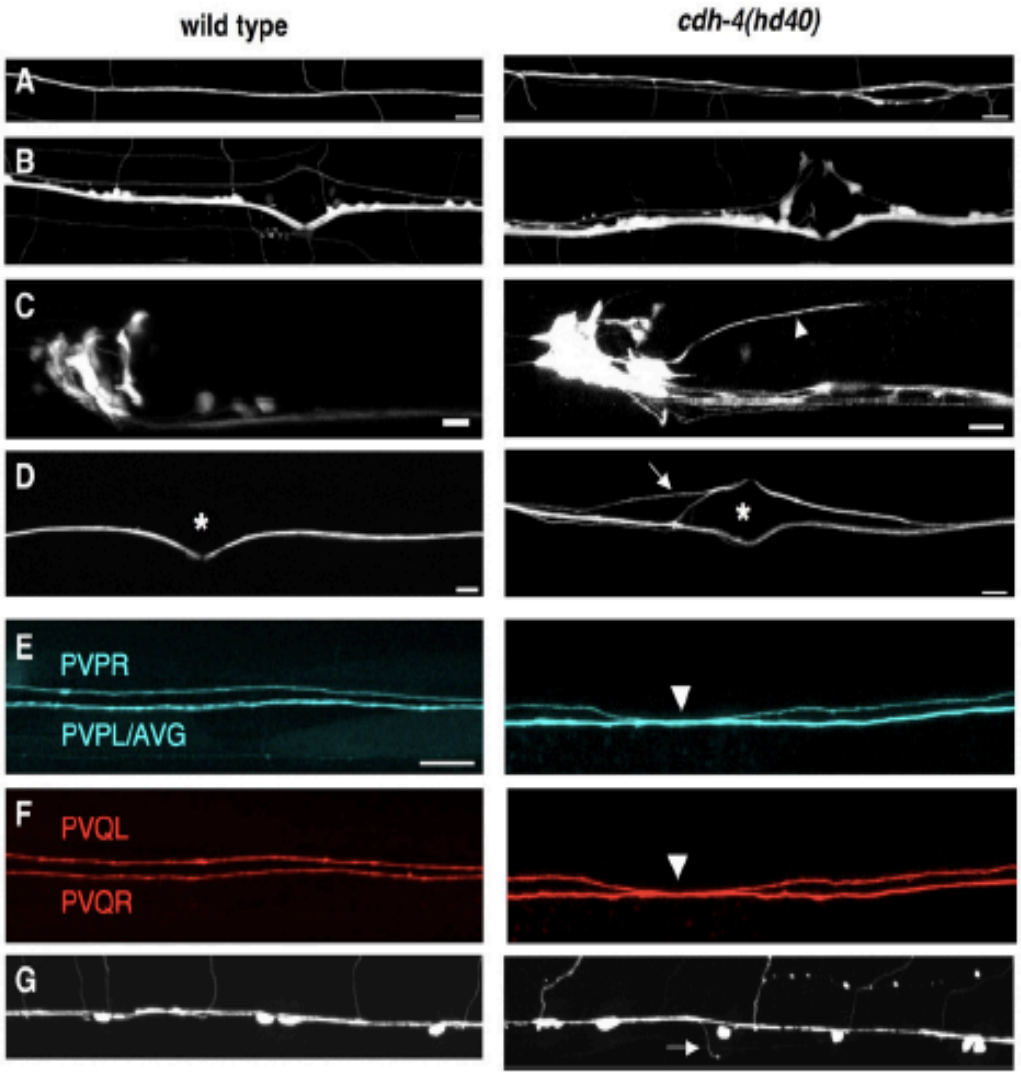

Figure 1.11 Axonal defects in *cdh-4* mutants.

(A) The dorsal nerve cord labeled with *F25B3.3::GFP*. The DNC in wild type is a tight bundle, which is frequently defasciculated in *cdh-4* mutants. (B) In the ventral nerve cord, axons frequently cross the midline in *cdh-4* mutants. (C, D) Interneurons are labeled using *glr-1::GFP* marker. Axons enter nerve ring and exit on the ventral side in wild type. Some axons exit laterally in *cdh-4* mutants (C, arrowhead) or cross into the left tract (D, arrow) as seen near the vulva region (asterisk). (E) AVG and PVP labeled with *odr-2::CFP* marker show crossover defects of PVPR in mutants (arrowhead). (F) PVQ labeled with *sra-6::DsRed* show PVQL defects that correlate with that of PVPR. (G) DD/VD motor neurons labeled with *unc-47::DsRed2*. In wild type, all commissures branch off from VNC on the right side, while in mutants, some commissures leave from the left side. (A): dorsal view, B, D–G): ventral view, (C): lateral view, scale bar: 10 μm (Schmitz et al. 2008).

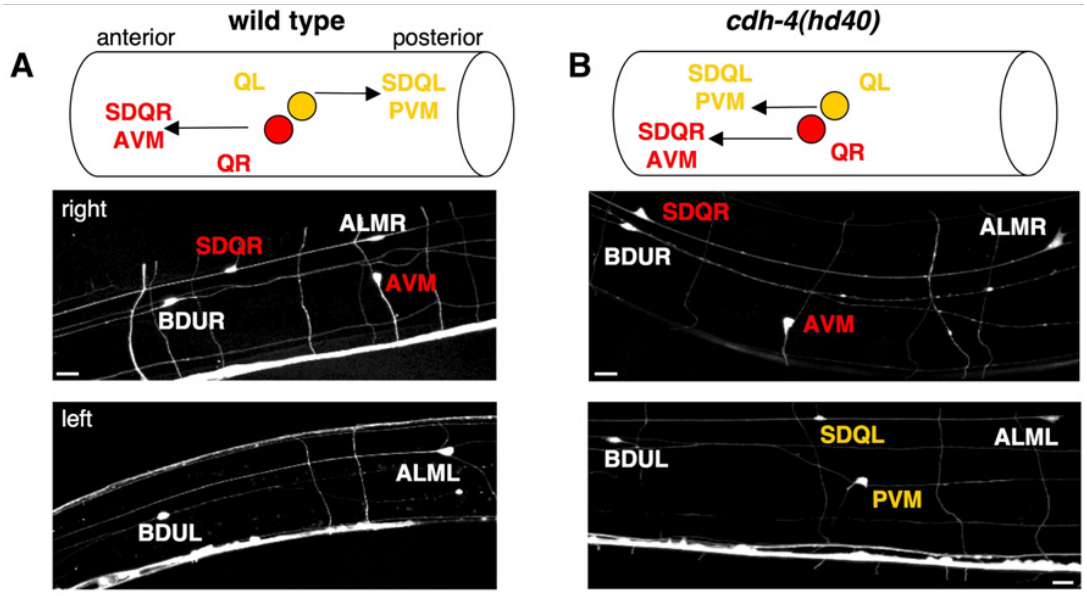

Figure 1.12 Neuroblast migration defects in *cdh-4* mutants.

(A) In wild type animals the Q neuroblasts migrate postembryonically in opposite directions. QR descendents (SDQR and AVM) are eventually located in the anterior part, whereas QL descendents (SDQL and PVM) end up in the posterior part of the animal. Pictures show only the anterior region. (B) In *cdh-4(hd40)* mutants descendents of both Q cells are found in the anterior part of the animal, revealing a migration defect of QL and its descendents. Marker used: evIs111; Scale bar: 10 µm (Schmitz et al 2008).

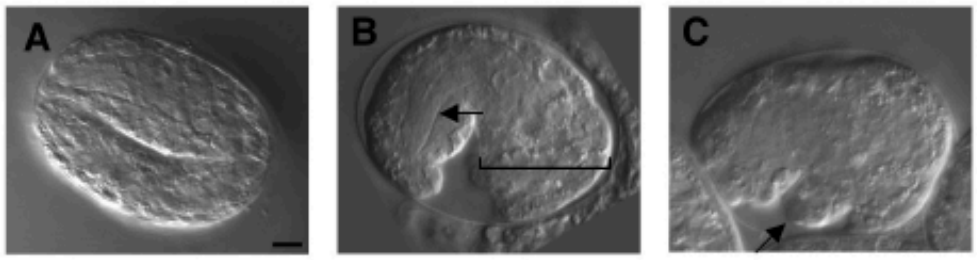

D

	% dead eggs	% surviving adults
wild type	0 ± 0	106 ± 7
cdh-4(hd40)	22 ± 6	22 ± 6
cdh-4(rh310)	11 ± 5	62 ± 8
cdh-4(hd13)	27 ± 4	14 ± 5

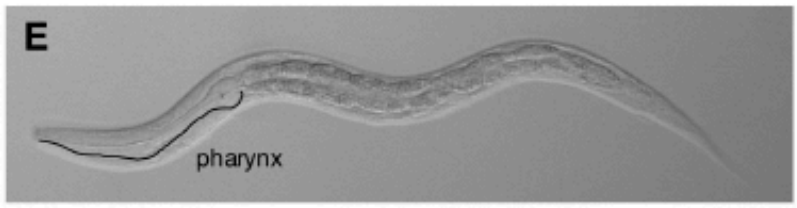

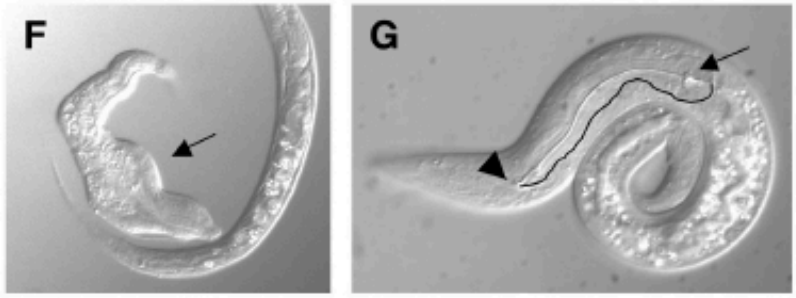

H

	% variable abnormal morphology	% pharynx unattached
wild type	0	0
cdh-4(hd40)	12	30
cdh-4(rh310)	15	24
cdh-4(hd13)	22	37

Figure 1.13 Embryonic lethality (A-D) and larval lethality (E-H) in *cdh-4* mutants.

(A) Wild type 2-fold embryo. (B) *cdh-4(hd40)* mutant embryos fail to elongate properly (bracket), but show differentiated structures like the pharynx (arrow). (C) Protrusions appear at various sites in the embryo (arrow). Scale bar: 10 µm. (D) All cdh-4 alleles show embryonic lethality and a decreased number of animals growing to adulthood. Progeny of 8 to 10 hermaphrodites was counted. Average number of progeny ranged from 131 for *cdh-4(hd40)* to 220 for *cdh-4(hd13).* (E) The pharynx in L1 wild type larvae is connected to the anterior hypodermis to form the mouth. (F) Some *cdh-4(hd40)* larvae have a variable abnormal morphology (arrow) and (G) the pharynx is not properly connected to the mouth (arrowhead). The overall morphology of the pharynx is normal (arrow points at the posterior bulb with grinder). (H) Penetrance for both phenotypes in the three *cdh-4* alleles is comparable. n=100. All phenotypes are statistically significant with $p < 0.01$ (χ2-test) (Schmitz et al. 2008).

1.11. Tables

Table 1.1 VNC and DNC defasciculation defects in *cdh-4* mutants (% animals with midline crossing defects in the ventral nerve cord or defasciculation defects in the dorsal nerve cord) (Schmitz et al. 2008)

			CIN			
allele	VNC	DNC	VNC	lateral axon	PVPR	PVQL
wild type	4	5	3	2	11	11
cdh-4(hd40)$^{+}$	51**	54**	39**	58**	33**	34**
cdh-4(hd13)	56**	63**	29**	41**	28**	33**
cdh-4(rh310)	37**	68**	20**	23**	75**	61**

n >= 100 for all data points; markers used: *evIs111*(VNC, DNC), *rhIs4* (command interneurons CIN), *hdIs26* (PVP, PVQ); ** $p<0.01$ (χ^2 test); modified from Schmitz et al., 2008

1.12. References

Augsburger, A., A. Schuchardt, S. Hoskins, J. Dodd, and S. Butler, 1999 BMPs as mediators of roof plate repulsion of commissural neurons. Neuron 24: 127–141.

Bao, H., M. L. Berlanga, M. Xue, S. M. Hapip, R. W. Daniels *et al.*, 2007 The atypical cadherin flamingo regulates synaptogenesis and helps prevent axonal and synaptic degeneration in Drosophila. Mol Cell Neurosci 34: 662–78.

Bashaw, G. J., and R. Klein, 2010 Signaling from axon guidance receptors. Cold Spring Harb Perspect Biol 2: a001941.

Battye, R., A. Stevens, R. L. Perry, and J. R. Jacobs, 2001 Repellent signaling by Slit requires the leucine-rich repeats. J. Neurosci. Off. J. Soc. Neurosci. 21: 4290–4298.

Boulin, T., R. Pocock, and O. Hobert, 2006 A novel Eph receptor-interacting IgSF protein provides C. elegans motoneurons with midline guidepost function. Curr Biol 16: 1871–83.

Boyle, M., A. Nighorn, and J. B. Thomas, 2006 Drosophila Eph receptor guides specific axon branches of mushroom body neurons. Dev. Camb. Engl. 133: 1845–1854.

Brenner, S., 1974 The genetics of Caenorhabditis elegans. Genetics 77: 71–94.

Broadbent, I. D., and J. Pettitt, 2002 The C. elegans hmr-1 gene can encode a neuronal classic cadherin involved in the regulation of axon fasciculation. Curr Biol 12: 59–63.

Brose, K., K. S. Bland, K. H. Wang, D. Arnott, W. Henzel *et al.*, 1999 Slit proteins bind Robo receptors and have an evolutionarily conserved role in repulsive axon guidance. Cell 96: 795–806.

Bürglin, T. R., and P. E. Kuwabara, 2006 Homologs of the Hh signalling network in C. elegans (The C. elegans Research Community, Ed.). WormBook.

Burnette, D. T., L. Ji, A. W. Schaefer, N. A. Medeiros, G. Danuser *et al.*, 2008 Myosin II activity facilitates microtubule bundling in the neuronal growth cone neck. Dev. Cell 15: 163–169.

Butler, S. J., and J. Dodd, 2003 A role for BMP heterodimers in roof plate-mediated repulsion of commissural axons. Neuron 38: 389–401.

Cajal S. R. Y., 1890 A quelle epoque apparaissent les expansions des cellules nerveuses de la moelle epiniere du poulet. Anat Anz 5: 609-613,631-639.

Cang, J., and D. A. Feldheim, 2013 Developmental mechanisms of topographic map formation and alignment. Annu. Rev. Neurosci. 36: 51–77.

Chae, J., M. J. Kim, J. H. Goo, S. Collier, D. Gubb *et al.*, 1999 The Drosophila tissue polarity gene starry night encodes a member of the protocadherin family. Development 126: 5421–9.

Charron, F., E. Stein, J. Jeong, A. P. McMahon, and M. Tessier-Lavigne, 2003 The Morphogen Sonic Hedgehog Is an Axonal Chemoattractant that Collaborates with Netrin-1 in Midline Axon Guidance. Cell 113: 11–23.

Chen, Z., B. B. Gore, H. Long, L. Ma, and M. Tessier-Lavigne, 2008 Alternative splicing of the Robo3 axon guidance receptor governs the midline switch from attraction to repulsion. Neuron 58: 325–332.

Chilton, J. K., 2006 Molecular mechanisms of axon guidance. Dev. Biol. 292: 13–24.

Chin-Sang, I. D., S. E. George, M. Ding, S. L. Moseley, A. S. Lynch *et al.*, 1999 The ephrin VAB-2/EFN-1 functions in neuronal signaling to regulate epidermal morphogenesis in C. elegans. Cell 99: 781–90.

Chin-Sang, I. D., S. L. Moseley, M. Ding, R. J. Harrington, S. E. George *et al.*, 2002 The divergent C. elegans ephrin EFN-4 functions inembryonic morphogenesis in a pathway independent of the VAB-1 Eph receptor. Development 129: 5499–510.

Chisholm, A. D., H. Hutter, Y. Jin, and W. G. Wadsworth, 2016 The Genetics of Axon Guidance and Axon Regeneration in Caenorhabditis elegans. Genetics 204: 849–882.

Cho, E., and K. D. Irvine, 2004 Action of fat, four-jointed, dachsous and dachs in distal-to-proximal wing signaling. Dev. Camb. Engl. 131: 4489–4500.

Ciani, L., A. Patel, N. D. Allen, and C. ffrench-Constant, 2003 Mice lacking the giant protocadherin mFAT1 exhibit renal slit junction abnormalities and a partially penetrant cyclopia and anophthalmia phenotype. Mol Cell Biol 23: 3575–82.

Colamarino, S. A., and M. Tessier-Lavigne, 1995 The role of the floor plate in axon guidance. Annu Rev Neurosci 18: 497–529.

Colavita, A., S. Krishna, H. Zheng, R. W. Padgett, and J. G. Culotti, 1998 Pioneer axon guidance by UNC-129, a *C. elegans* TGF-beta. Science 281: 706–9.

Costa, M., W. Raich, C. Agbunag, B. Leung, J. Hardin *et al.*, 1998 A putative catenin-cadherin system mediates morphogenesis of the Caenorhabditis elegans embryo. J Cell Biol 141: 297–308.

Cowan, W. M., T.C. Sudhof, and C.F. Stevens, 2001 Synapses. The Johns Hopkins University Press, Baltimore, Maryland.

Curtin, J. A., E. Quint, V. Tsipouri, R. M. Arkell, B. Cattanach *et al.*, 2003 Mutation of Celsr1 disrupts planar polarity of inner ear hair cells and causes severe neural tube defects in the mouse. Curr Biol 13: 1129–33.

Dent, E. W., and F. B. Gertler, 2003 Cytoskeletal dynamics and transport in growth cone motility and axon guidance. Neuron 40: 209–227.

Dickson, B. J., and G. F. Gilestro, 2006 Regulation of commissural axon pathfinding by slit and its Robo receptors. Annu. Rev. Cell Dev. Biol. 22: 651–675.

Domanitskaya, E., A. Wacker, O. Mauti, T. Baeriswyl, P. Esteve *et al.*, 2010 Sonic Hedgehog Guides Post-Crossing Commissural Axons Both Directly and Indirectly by Regulating Wnt Activity. J. Neurosci. 30: 11167–11176.

Dong, B., M. Moseley-Alldredge, A. A. Schwieterman, C. J. Donelson, J. L. McMurry *et al.*, 2016 EFN-4 functions in LAD-2-mediated axon guidance in Caenorhabditis elegans. Dev. Camb. Engl. 143: 1182–1191.

Drees, F., and F. B. Gertler, 2008 Ena/VASP: proteins at the tip of the nervous system. Curr. Opin. Neurobiol. 18: 53–59.

Evans, T. A., and G. J. Bashaw, 2010 Functional diversity of Robo receptor immunoglobulin domains promotes distinct axon guidance decisions. Curr. Biol. CB 20: 567–572.

Gale, N. W., S. J. Holland, D. M. Valenzuela, A. Flenniken, L. Pan *et al.*, 1996 Eph receptors and ligands comprise two major specificity subclasses and are reciprocally compartmentalized during embryogenesis. Neuron 17: 9–19.

Garrod, D. R., A. J. Merritt, and Z. Nie, 2002 Desmosomal cadherins. Curr. Opin. Cell Biol. 14: 537–545.

George, S. E., K. Simokat, J. Hardin, and A. D. Chisholm, 1998 The VAB-1 Eph receptor tyrosine kinase functions in neural and epithelial morphogenesis in C. elegans. Cell 92: 633–43.

Gleason, J. E., and D. M. Eisenmann, 2010 Wnt signaling controls the stem cell-like asymmetric division of the epithelial seam cells during C. elegans larval development. Dev Biol 348: 58–66.

Goldstein, B., H. Takeshita, K. Mizumoto, and H. Sawa, 2006 Wnt signals can function as positional cues in establishing cell polarity. Dev Cell 10: 391–6.

Goley, E. D., and M. D. Welch, 2006 The ARP2/3 complex: an actin nucleator comes of age. Nat. Rev. Mol. Cell Biol. 7: 713–726.

Gomez, T. M., and P. C. Letourneau, 2014 Actin dynamics in growth cone motility and navigation. J. Neurochem. 129: 221–234.

Goode, B. L., and M. J. Eck, 2007 Mechanism and function of formins in the control of actin assembly. Annu. Rev. Biochem. 76: 593–627.

Green, R. A., A. Audhya, A. Pozniakovsky, A. Dammermann, H. Pemble *et al.*, 2008 Expression and imaging of fluorescent proteins in the C. elegans gonad and early embryo, pp. 179–218 in *Fluorescent proteins*, edited by Sullivan KF. Elsevier, Amsterdam.

Halbleib, J. M., and W. J. Nelson, 2006 Cadherins in development: cell adhesion, sorting, and tissue morphogenesis. Genes Dev 20: 3199–214.

Hall, A., and G. Lalli, 2010 Rho and Ras GTPases in axon growth, guidance, and branching. Cold Spring Harb. Perspect. Biol. 2: a001818.

Hao, J. C., T. W. Yu, K. Fujisawa, J. G. Culotti, K. Gengyo-Ando *et al.*, 2001 C. elegans slit acts in midline, dorsal-ventral, and anterior-posterior guidance via the SAX-3/Robo receptor. Neuron 32: 25–38.

Harris, J., L. Honigberg, N. Robinson, and C. Kenyon, 1996 Neuronal cell migration in C. elegans: regulation of Hox gene expression and cell position. Development 122: 3117–31.

Harterink, M., D. H. Kim, T. C. Middelkoop, T. D. Doan, A. van Oudenaarden *et al.*, 2011 Neuroblast migration along the anteroposterior axis of C. elegans is controlled by opposing gradients of Wnts and a secreted Frizzled-related protein. Development 138: 2915–24.

Hedgecock, E. M., J. G. Culotti, and D. H. Hall, 1990 The unc-5, unc-6, and unc-40 genes guide circumferential migrations of pioneer axons and mesodermal cells on the epidermis in C. elegans. Neuron 4: 61–85.

Hilliard, M. A., and C. I. Bargmann, 2006 Wnt signals and frizzled activity orient anterior-posterior axon outgrowth in C. elegans. Dev Cell 10: 379–90.

Hindges, R., T. McLaughlin, N. Genoud, M. Henkemeyer, and D. D. M. O'Leary, 2002 EphB forward signaling controls directional branch extension and arborization required for dorsal-ventral retinotopic mapping. Neuron 35: 475–487.

Howitt, J. A., N. J. Clout, and E. Hohenester, 2004 Binding site for Robo receptors revealed by dissection of the leucine-rich repeat region of Slit. EMBO J 23: 4406–12.

Hutter, H., 2003 Extracellular cues and pioneers act together to guide axons in the ventral cord of C. elegans. Development 130: 5307–18.

Ishii, N., W. G. Wadsworth, B. D. Stern, J. G. Culotti, and E. M. Hedgecock, 1992 UNC-6, a laminin-related protein, guides cell and pioneer axon migrations in C. elegans. Neuron 9: 873–81.

Iwasato, T., H. Katoh, H. Nishimaru, Y. Ishikawa, H. Inoue *et al.*, 2007 Rac-GAP α-Chimerin Regulates Motor-Circuit Formation as a Key Mediator of EphrinB3/EphA4 Forward Signaling. Cell 130: 742–753.

Keleman, K., S. Rajagopalan, D. Cleppien, D. Teis, K. Paiha *et al.*, 2002 Comm sorts robo to control axon guidance at the Drosophila midline. Cell 110: 415–427.

Keleman, K., C. Ribeiro, and B. J. Dickson, 2005 Comm function in commissural axon guidance: cell-autonomous sorting of Robo in vivo. Nat. Neurosci. 8: 156–163.

Kidd, T., C. Russell, C. S. Goodman, and G. Tear, 1998 Dosage-sensitive and complementary functions of roundabout and commissureless control axon crossing of the CNS midline. Neuron 20: 25–33.

Koh, C.-G., 2006 Rho GTPases and their regulators in neuronal functions and development. Neurosignals 15: 228–237.

Kolodkin, A. L., 1996 Semaphorins: mediators of repulsive growth cone guidance. Trends Cell Biol 6: 15–22.

Kolodkin, A. L., D. V. Levengood, E. G. Rowe, Y.-T. Tai, R. J. Giger *et al.*, 1997 Neuropilin Is a Semaphorin III Receptor. Cell 90: 753–762.

Korobova, F., and T. Svitkina, 2008 Arp2/3 complex is important for filopodia formation, growth cone motility, and neuritogenesis in neuronal cells. Mol. Biol. Cell 19: 1561–1574.

Krol, A., S. J. Henle, and L. V. Goodrich, 2016 Fat3 and Ena/VASP proteins influence the emergence of asymmetric cell morphology in the developing retina. Development 143: 2172–2182.

Kruger, R. P., J. Aurandt, and K.-L. Guan, 2005 Semaphorins command cells to move. Nat. Rev. Mol. Cell Biol. 6: 789–800.

Lackmann, M., and A. W. Boyd, 2008 Eph, a protein family coming of age: more confusion, insight, or complexity? Sci. Signal. 1: re2.

Lee, R. C., T. R. Clandinin, C. H. Lee, P. L. Chen, I. A. Meinertzhagen *et al.*, 2003 The protocadherin Flamingo is required for axon target selection in the Drosophila visual system. Nat Neurosci 6: 557–63.

Lemke, G., and M. Reber, 2005 Retinotectal mapping: new insights from molecular genetics. Annu. Rev. Cell Dev. Biol. 21: 551–580.

Liebl, E. C., D. J. Forsthoefel, L. S. Franco, S. H. Sample, J. E. Hess *et al.*, 2000 Dosage-sensitive, reciprocal genetic interactions between the Abl tyrosine kinase and the putative GEF trio reveal trio's role in axon pathfinding. Neuron 26: 107–118.

Liu, Y., J. Shi, C.-C. Lu, Z.-B. Wang, A. I. Lyuksyutova *et al.*, 2005 Ryk-mediated Wnt repulsion regulates posterior-directed growth of corticospinal tract. Nat. Neurosci. 8: 1151–1159.

Lowery, L. A., and D. Van Vactor, 2009 The trip of the tip: understanding the growth cone machinery. Nat. Rev. Mol. Cell Biol. 10: 332–343.

Lu, W., V. Yamamoto, B. Ortega, and D. Baltimore, 2004 Mammalian Ryk Is a Wnt Coreceptor Required for Stimulation of Neurite Outgrowth. Cell 119: 97–108.

Lundquist, E. A., P. W. Reddien, E. Hartwieg, H. R. Horvitz, and C. I. Bargmann, 2001 Three C. elegans Rac proteins and several alternative Rac regulators control axon guidance, cell migration and apoptotic cell phagocytosis. Development 128: 4475–88.

Luo, Y., D. Raible, and J. A. Raper, 1993 Collapsin: a protein in brain that induces the collapse and paralysis of neuronal growth cones. Cell 75: 217–27.

Lyuksyutova, A. I., C. C. Lu, N. Milanesio, L. A. King, N. Guo *et al.*, 2003 Anterior-posterior guidance of commissural axons by Wnt-frizzled signaling. Science 302: 1984–8.

MacNeil, L. T., W. R. Hardy, T. Pawson, J. L. Wrana, and J. G. Culotti, 2009 UNC-129 regulates the balance between UNC-40 dependent and independent UNC-5 signaling pathways. Nat Neurosci 12: 150–5.

Mahoney, P. A., U. Weber, P. Onofrechuk, H. Biessmann, P. J. Bryant *et al.*, 1991 The fat tumor suppressor gene in Drosophila encodes a novel member of the cadherin gene superfamily. Cell 67: 853–868.

Mann, F., S. Ray, W. Harris, and C. Holt, 2002 Topographic mapping in dorsoventral axis of the Xenopus retinotectal system depends on signaling through ephrin-B ligands. Neuron 35: 461–473.

Matakatsu, H., and S. S. Blair, 2004 Interactions between Fat and Dachsous and the regulation of planar cell polarity in the Drosophila wing. Development 131: 3785–94.

Matusek, T., R. Gombos, A. Szécsényi, N. Sánchez-Soriano, A. Czibula *et al.*, 2008 Formin proteins of the DAAM subfamily play a role during axon growth. J. Neurosci. Off. J. Soc. Neurosci. 28: 13310–13319.

McLaughlin, T., R. Hindges, and D. D. M. O'Leary, 2003 Regulation of axial patterning of the retina and its topographic mapping in the brain. Curr. Opin. Neurobiol. 13: 57–69.

Mohamed, A. M., and I. D. Chin-Sang, 2006 Characterization of loss-of-function and gain-of-function Eph receptor tyrosine kinase signaling in C. elegans axon targeting and cell migration. Dev. Biol. 290: 164–176.

Morlot, C., N. M. Thielens, R. B. G. Ravelli, W. Hemrika, R. A. Romijn *et al.*, 2007 Structural insights into the Slit-Robo complex. Proc. Natl. Acad. Sci. U. S. A. 104: 14923–14928.

Najarro, E. H., L. Wong, M. Zhen, E. P. Carpio, A. Goncharov *et al.*, 2012 Caenorhabditis elegans flamingo cadherin fmi-1 regulates GABAergic neuronal development. J Neurosci 32: 4196–211.

Newsome, T. P., S. Schmidt, G. Dietzl, K. Keleman, B. Asling *et al.*, 2000 Trio combines with dock to regulate Pak activity during photoreceptor axon pathfinding in Drosophila. Cell 101: 283–294.

Oda, H., and S. Tsukita, 1999 Nonchordate Classic Cadherins Have a Structurally and Functionally Unique Domain That Is Absent from Chordate Classic Cadherins. Dev. Biol. 216: 406–422.

Pan, C. L., J. E. Howell, S. G. Clark, M. Hilliard, S. Cordes *et al.*, 2006 Multiple Wnts and frizzled receptors regulate anteriorly directed cell and growth cone migrations in Caenorhabditis elegans. Dev Cell 10: 367–77.

Park, J., P. L. Knezevich, W. Wung, S. N. O'Hanlon, A. Goyal *et al.*, 2011 A conserved juxtacrine signal regulates synaptic partner recognition in Caenorhabditis elegans. Neural Develop. 6: 28.

Pasquale, E. B., 2005 Eph receptor signalling casts a wide net on cell behaviour. Nat. Rev. Mol. Cell Biol. 6: 462–475.

Patel, S. D., C. P. Chen, F. Bahna, B. Honig, and L. Shapiro, 2003 Cadherin-mediated cell-cell adhesion: sticking together as a family. Curr Opin Struct Biol 13: 690–8.

Pettitt, J., E. A. Cox, I. D. Broadbent, A. Flett, and J. Hardin, 2003 The Caenorhabditis elegans p120 catenin homologue, JAC-1, modulates cadherin-catenin function during epidermal morphogenesis. J Cell Biol 162: 15–22.

Pettitt, J., W. B. Wood, and R. H. Plasterk, 1996 cdh-3, a gene encoding a member of the cadherin superfamily, functions in epithelial cell morphogenesis in Caenorhabditis elegans. Development 122: 4149–57.

Quinn, C. C., and W. G. Wadsworth, 2008 Axon guidance: asymmetric signaling orients polarized outgrowth. Trends Cell Biol. 18: 597–603.

Raper, J. A., 2000 Semaphorins and their receptors in vertebrates and invertebrates. Curr. Opin. Neurobiol. 10: 88–94.

Riddle, D. L., T. Blumenthal, B. J. Meyer, and J. R. Priess (Eds.), 1997 *C. elegans II*. Cold Spring Harbor Laboratory Press, Cold Spring Harbor (NY).

Ridley, A. J., and A. Hall, 1992 The small GTP-binding protein rho regulates the assembly of focal adhesions and actin stress fibers in response to growth factors. Cell 70: 389–399.

Ridley, A. J., H. F. Paterson, C. L. Johnston, D. Diekmann, and A. Hall, 1992 The small GTP-binding protein rac regulates growth factor-induced membrane ruffling. Cell 70: 401–410.

Rothberg, J. M., D. A. Hartley, Z. Walther, and S. Artavanis-Tsakonas, 1988 slit: an EGF-homologous locus of D. melanogaster involved in the development of the embryonic central nervous system. Cell 55: 1047–59.

Rothberg, J. M., J. R. Jacobs, C. S. Goodman, and S. Artavanis-Tsakonas, 1990 slit: an extracellular protein necessary for development of midline glia and commissural axon pathways contains both EGF and LRR domains. Genes Dev. 4: 2169–2187.

Roy, P. J., H. Zheng, C. E. Warren, and J. G. Culotti, 2000 mab-20 encodes Semaphorin-2a and is required to prevent ectopic cell contacts during epidermal morphogenesis in Caenorhabditis elegans. Development 127: 755–67.

Saburi, S., I. Hester, E. Fischer, M. Pontoglio, V. Eremina *et al.*, 2008 Loss of Fat4 disrupts PCP signaling and oriented cell division and leads to cystic kidney disease. Nat. Genet. 40: 1010–1015.

Schmitz, C., P. Kinge, and H. Hutter, 2007 Axon guidance genes identified in a large-scale RNAi screen using the RNAi-hypersensitive Caenorhabditis elegans strain nre-1(hd20) lin-15b(hd126). Proc Natl Acad Sci U A 104: 834–9.

Schmitz, C., I. Wacker, and H. Hutter, 2008 The Fat-like cadherin CDH-4 controls axon fasciculation, cell migration and hypodermis and pharynx development in Caenorhabditis elegans. Dev Biol 316: 249–59.

Schwieterman, A. A., A. N. Steves, V. Yee, C. J. Donelson, M. R. Bentley *et al.*, 2016 The Caenorhabditis elegans Ephrin EFN-4 Functions Non-cell Autonomously with Heparan Sulfate Proteoglycans to Promote Axon Outgrowth and Branching. Genetics 202: 639–660.

Shamah, S. M., M. Z. Lin, J. L. Goldberg, S. Estrach, M. Sahin *et al.*, 2001 EphA Receptors Regulate Growth Cone Dynamics through the Novel Guanine Nucleotide Exchange Factor Ephexin. Cell 105: 233–244.

Song, S., B. Zhang, H. Sun, X. Li, Y. Xiang *et al.*, 2010 A Wnt-Frz/Ror-Dsh pathway regulates neurite outgrowth in Caenorhabditis elegans. PLoS Genet 6:.

Squire, L. R., 2008 *Fundamental neuroscience*. Elsevier/Academic Press, Amsterdam; Boston.

Steimel, A., L. Wong, E. H. Najarro, B. D. Ackley, G. Garriga *et al.*, 2010 The Flamingo ortholog FMI-1 controls pioneer-dependent navigation of follower axons in C. elegans. Development 137: 3663–73.

Steven, R., T. J. Kubiseski, H. Zheng, S. Kulkarni, J. Mancillas *et al.*, 1998 UNC-73 activates the Rac GTPase and is required for cell and growth cone migrations in C. elegans. Cell 92: 785–95.

Strutt, D. I., 2002 The asymmetric subcellular localisation of components of the planar polarity pathway. Semin Cell Dev Biol 13: 225–31.

Sweeney, N. T., W. Li, and F. B. Gao, 2002 Genetic manipulation of single neurons in vivo reveals specific roles of flamingo in neuronal morphogenesis. Dev Biol 247: 76–88.

Tanabe, K., M. Takeichi, and S. Nakagawa, 2004 Identification of a nonchordate-type classic cadherin in vertebrates: Chicken Hz-cadherin is expressed in horizontal cells of the neural retina and contains a nonchordate-specific domain complex. Dev. Dyn. 229: 899–906.

Tanoue, T., and M. Takeichi, 2004 Mammalian Fat1 cadherin regulates actin dynamics and cell-cell contact. J Cell Biol 165: 517–28.

Tanoue, T., and M. Takeichi, 2005 New insights into Fat cadherins. J Cell Sci 118: 2347–53.

Trousse, F., E. Martí, P. Gruss, M. Torres, and P. Bovolenta, 2001 Control of retinal ganglion cell axon growth: a new role for Sonic hedgehog. Dev. Camb. Engl. 128: 3927–3936.

Tucker, M., and M. Han, 2008 Muscle cell migrations of C. elegans are mediated by the α-integrin INA-1, Eph receptor VAB-1, and a novel peptidase homologue MNP-1. Dev. Biol. 318: 215–223.

Viveiros, R., H. Hutter, and D. G. Moerman, 2011 Membrane extensions are associated with proper anterior migration of muscle cells during Caenorhabditis elegans embryogenesis. Dev. Biol. 358: 189–200.

Wadsworth, W. G., H. Bhatt, and E. M. Hedgecock, 1996 Neuroglia and pioneer neurons express UNC-6 to provide global and local netrin cues for guiding migrations in C. elegans. Neuron 16: 35–46.

Wadsworth, W. G., and E. M. Hedgecock, 1996 Hierarchical guidance cues in the developing nervous system of C. elegans. BioEssays News Rev. Mol. Cell. Dev. Biol. 18: 355–362.

Waites, C. L., A. M. Craig, and C. C. Garner, 2005 Mechanisms of vertebrate synaptogenesis. Annu. Rev. Neurosci. 28: 251–274.

Wang, X., W. Zhang, T. Cheever, V. Schwarz, K. Opperman *et al.*, 2008 The C. elegans L1CAM homologue LAD-2 functions as a coreceptor in MAB-20/Sema2 mediated axon guidance. J Cell Biol 180: 233–46.

Watabe-Uchida, M., E.-E. Govek, and L. V. Aelst, 2006 Regulators of Rho GTPases in Neuronal Development. J. Neurosci. 26: 10633–10635.

Wen, Z., L. Han, J. R. Bamburg, S. Shim, G. Ming *et al.*, 2007 BMP gradients steer nerve growth cones by a balancing act of LIM kinase and Slingshot phosphatase on ADF/cofilin. J. Cell Biol. 178: 107–119.

White, J. G., E. Southgate, J. N. Thomson, and S. Brenner, 1986 The structure of the nervous system of the nematode Caenorhabditis elegans. Phil Trans R. Soc Lond. B 314: 1–340.

White, J. G., E. Southgate, J. N. Thomson, and S. Brenner, 1976 The structure of the ventral nerve cord of Caenorhabditis elegans. Philos Trans R Soc Lond B Biol Sci 275: 327–48.

Winberg, M. L., J. N. Noordermeer, L. Tamagnone, P. M. Comoglio, M. K. Spriggs *et al.*, 1998 Plexin A is a neuronal semaphorin receptor that controls axon guidance. Cell 95: 903–916.

Wolpert, L., 2011 *Principles of development*. Oxford University Press, Oxford; New York.

Yamada, K. M., B. S. Spooner, and N. K. Wessells, 1970 AXON GROWTH: ROLES OF MICROFILAMENTS AND MICROTUBULES*. Proc. Natl. Acad. Sci. U. S. A. 66: 1206–1212.

Yang, C. H., J. D. Axelrod, and M. A. Simon, 2002 Regulation of Frizzled by fat-like cadherins during planar polarity signaling in the Drosophila compound eye. Cell 108: 675–88.

Yoshikawa, S., R. D McKinnon, M. Kokel, and J. B Thomas, 2003 Wnt-mediated axon guidance via the Drosophila Derailed receptor. Nature 422: 583–8.

Zallen, J. A., B. A. Yi, and C. I. Bargmann, 1998 The conserved immunoglobulin superfamily member SAX-3/Robo directs multiple aspects of axon guidance in C. elegans. Cell 92: 217–27.

Zhang, X.-F., A. W. Schaefer, D. T. Burnette, V. T. Schoonderwoert, and P. Forscher, 2003 Rho-dependent contractile responses in the neuronal growth cone are independent of classical peripheral retrograde actin flow. Neuron 40: 931–944.

Zinovyeva, A. Y., Y. Yamamoto, H. Sawa, and W. C. Forrester, 2008 Complex network of Wnt signaling regulates neuronal migrations during Caenorhabditis elegans development. Genetics 179: 1357–71.

Chapter 2.

Materials and Methods

2.1. Maintenance and strains

Worms were grown on easiest worm media (EWM) plates with OP50 *Escherichia coli*. EWM is a mix of 55g Tris-HCl, 24g Tris-OH, 310g Bacto Peptone, 800mg Cholesterol, and 200g NACl. The EWM plates included a mix of 5.9g EWM, 18g agar, and 1L volume of H2O. Worms were grown at 20^{o}C for experimental purposes (Brenner 1974), unless mentioned otherwise.

Fluorescent markers used either for examining phenotypes within nervous system or for selection strategies in genetic schemes: *hdIs26[odr-2::DsRed2]III, cdk-12(tm3846)/qC1 [dpy-19(e1259) glp-1(q339)] nIs281 III* (Courtesy of Dr. Kelly), *evIs111[rgef-1::DFP]V* (Courtesy of Dr. Culotti), *hdIs36 [F25B3.3::DsRed2].*

Suppressor strains used for phenotypic characterization:

cdh-4(hd40)III; evIs111 V (Schmitz *et al.* 2008)

cdh-4(hd40)III; evIs111 V; hd158

cdh-4(hd40)III; evIs111 V; hd160

cdh-4(hd40)III; evIs111 V; hd161

cdh-4(hd40)III; evIs111 V; hd162

cdh-4(hd40)III; evIs111 V; *hd163*

cdh-4(hd40)III; evIs111 V; *hd164*

cdh-4(hd40)III; evIs111 V; hd165

cdh-4(hd40)III; evIs111 V; hd167

cdh-4(hd40)III; evIs111 V; hd168

cdh-4(hd40)III; evIs111 V; hd169

cdh-4(hd40)III; evIs111 V; hd170

cdh-4(hd40)III; evIs111 V; hd171

cdh-4(hd40)III; evIs111 V; hd172

cdh-4(hd40)III; evIs111 V; hd173

cdh-4(hd40)III; evIs111 V; hd174

Strains used in confirmation of suppressor gene in *cdh-4(hd40)* mutant suppressors:

cdh-4(hd40)III; evIs111 V; hd161

math-48 (gk553779)

prp-6 (gk527875)

hdIs36 [F25B3.3::DsRed2]

evIs111[F25B3.3::GFP]V

Strains used in SNP mapping:

Hawaiian *CB4856* (Wicks *et al.* 2001)

hdIs26[odr-2::DsRed2]III

cdh-4(hd40)III; evIs111 V; hd158

cdh-4(hd40)III; evIs111 V; hd160

cdh-4(hd40)III; evIs111 V; hd161

cdh-4(hd40)III; evIs111 V; hd162

cdh-4(hd40)III; evIs111 V; *hd163*

cdh-4(hd40)III; evIs111 V; hd170

2.2. Outcrossing suppressor candidates

Suppressor candidates that were mapped and sent for sequencing were first outcrossed three to four times in order to eliminate background mutations that do not correspond to the suppressor gene. *cdh-4(hd40)* animals were crossed with *hdIs26* males in order to create heterozygous males that have both *hd40* and *hdIs26*. Both are on chromosome III. *hdIs26* is a dominant visible marker. Selecting against *hdIs26* allows the identification of animals homozygous for *hd40* in the F2 stage (Genetic scheme 2.1).

The *cdh-4(hd40)* mutants grow slowly when compared to the *cdh-4(hd40)* suppressors. When screening for F2 lines with suppressor gene, a starvation assay was done. Starvation assay is the time it takes for progeny of one P0 worm to consume the food on a plate. The Suppressor candidates reach starvation time ranging from ten to fifteen days. As for the *cdh-4(hd40)* mutants, it takes about at least three weeks to consume food on a plate. Therefore, selecting for F2 lines that could possibly have the suppressor gene was initially based on whether the F2 line starved more similarly to the suppressor strain and not to the *cdh-4(hd40)* mutants. These F2 lines would be then scored for suppression of DNC defects in order to confirm presence of the suppressor gene. In the genetic scheme 2.1 at the F1 stage, the animals, which were heterozygous for the suppressor, produced a low number of progeny similar to the *cdh-4(hd40)* mutants, suggesting that the suppressor is recessive.

2.3. Worm lysis

Worms were harvested using 50.0 µl of M9 buffer [3 g KH_2PO_4, 6 g Na_2HPO_4, 5 g NaCl, 1 ml 1 M $MgSO_4$, H_2O to 1 litre. Sterilize by autoclaving] and then added to 50.0 µl of 2X lysis buffer (provided with 100ug/ml Proteinase K). Samples were frozen at -80^{o}C for at least fifteen minutes. The temperatures used to perform lysis, using a PCR machine, were done in the following order: 1) 65^{o}C for 90 minutes. 2) 95^{o}C for 30 minutes. 3) 4^{o}C at infinite time. Lysis product was stored in -20^{o}C when not used for preparing PCR reactions.

2.4. Agarose gel electrophoresis

Agarose gel electrophoresis was done using either 1.0% or 2.5% agarose gel, depending on size of DNA band to be displayed on gel. For band sizes between 3.0kb and 0.5kb, 1% gel was used. For band sizes between 0.5kb and 0.1kb, then 2.5% gel was used. Gel was prepared by adding agarose to TBE buffer (89mM Tris-Borate and 2mM EDTA) with 0.5ug/ml of ethidium bromide. The gel prep was heated and then cooled down in cold water for two minutes, and then poured on a gel box. Once the gel solidified, samples were added in the wells and run.

2.5. Polymerase Chain Reaction (PCR), digestion, and DNA sequencing

PCR was executed either for SNP mapping of *cdh-4(hd40)* mutant suppressors or to confirm presence of *cdh-4* deletion region in the *cdh-4(hd40)* allele in suppressor candidates after being outcrossed. The wild type *cdh-4* shows 2.118kb band size, while the *cdh-4(hd40)* shows 1.227kb.

For confirming presence of *cdh-4(hd40)* band, PCR reactions were prepared on ice by mixing 14.9 µl water, 2.5ul TBA buffer (10X), 2.5µl dNTPs (2mM), 2.0µl $MgCl_2$ (25mM), 0.1µl self made-Taq, 1.0µl for each of the forward primer (10mM) and reverse primer (10mM), and 1.0 µl of template DNA. The total volume of the PCR product comes to 25µl.

For PCR reaction temperatures, it was in the following order: 1) 95^{o}C for 5 minutes. 2) 95^{o}C for 40 seconds. 3) 58^{o}C for 40 seconds. 4) 72^{o}C for 1kb/min (depends on product size). Steps 2,3, and 4 are repeated 34X. 5) 72^{o}C for 10 minutes. 6) 4^{o}C for infinite time. PCR product was kept in 4^{o}C fridge.

For SNP mapping, PCR reactions were prepared on ice by mixing 13.28µl of water, 2.0µl TBA buffer (10X), 2.0µl of dNTPs (2mM), 1.6µl of $MgCl_2$ (25mM), 0.12µl of self made-Taq, 0.8µl of primer mix of both forward and reverse primers (10mM each), and 0.2µl of Template DNA. The total volume of the PCR product comes to 20.0µl. For SNP mapping reaction temperatures, the order of steps was as follows: 1) 94^{o}C for 2 minutes. 2) 94^{o}C for 15 seconds. 3) 60^{o}C for 45 seconds. 4) 72^{o}C for 1 minute. Steps 2, 3, and 4 were repeated 35X. 5) 72^{o}C for 5 minutes. 6) 4^{o}C forever. PCR product was

kept in 4^{o}C fridge. For digestion of the PCR products, the digestion mix was prepared as followed: 8.3µl of water, 3.2µl of 10X NEB buffer, and 0.5µl of NEB digestion enzyme (Most commonly used enzyme was the Dra1). Digestion mix comes to total volume of 12.0 µl and is added to the PCR product and incubated at 37^{o}C for seven to sixteen hours before running the sample on gel.

As for sequencing of the PCR products, the products are sent to and done through Eurofins Operon with sample concentrations between 15.0-30.0ng/µl.

2.6. Whole Genome Sequencing

Whole Genome Sequencing (WGS) was performed in the Moerman lab at UBC with protocol adapted from the "The million mutation project" paper (Thompson *et al.* 2013). Briefly, sequencing was performed on a MiSeq with approximately 20-fold sequence coverage. The reference genome (WS230) was compared to the sequences of the tested *cdh-4(hd40)* suppressor strains in order to eliminate the common SNPs and background mutations and to maintain only the unique mutations in both the coding and non-coding regions.

cdh-4(hd40) suppressor candidates were outcrossed three or four times before sequencing. These suppressor candidates were: *cdh-4(hd40)III; evIs111 V; hd158, cdh-4(hd40)III; evIs111 V; hd160, cdh-4(hd40)III; evIs111 V; hd161, cdh-4(hd40)III; evIs111 V; hd162, cdh-4(hd40)III; evIs111 V*; *hd163,* and *cdh-4(hd40)III; evIs111 V; hd170*

2.7. Phenotypic characterization of *cdh-4(hd40)* mutant suppressors

2.7.1. Scoring for suppression of axon guidance defects in the *cdh-4(hd40)* mutant suppressors

Axon guidance defects were assessed with Zeiss Axiscope using a 40X objective lens. Worms were paralyzed with 10mM of sodium azide in M9 for one hour. Then, worms were mounted on either 3% or 4% agar pads. Axons were visualized with a pan-neuronal GFP marker (*evIs111*). Assessing axon guidance defects was based on scoring the dorsal nerve cord (DNC) and ventral nerve cord (VNC). In wild type the DNC appears as a tightly fasciculated bundle of axons. In wild type the VNC consists of two

tracts with the right side having more axons than the left side with no axons crossing between left and right tracts (Figure 1.11). Adult worms were scored for VNC defects, and either young or adult worms were used for scoring DNC defects. The *cdh-4(hd40)* mutant strain has animals that show defasciculated regions of axons within DNC and crossover(s) from right to left tract within the VNC. The *cdh-4(hd40)* mutants exhibit about 50% defects each within the VNC and DNC. To identify strains having the suppressor mutation 100 worms were scored and penetrant defects that scored below 40% in either DNC or VNC was considered a suppressed phenotype, indicating the presence of the suppressor.

2.7.2. Lethality assay of *cdh-4(hd40)* mutant suppressors

Measuring total lethality was based on comparing the total number of eggs produced by adults over two days to the total number of F1 animals that reached the adult stage. Starting with day zero, five to twelve L4 stage worms were placed on a plate marked “day 0”. These worms were transferred to a new plate everyday until day three (Figure 2.1). Therefore, total number of eggs and F1’s were counted on plates: day 0, day 1, and day 2. To measure embryonic lethality, the number of dead eggs was counted and then compared to the total number of eggs produced by P0. To measure larval lethality, the number of adult F1 worms was subtracted from the total number of surviving eggs.

2.7.3. Thrashing assay of *cdh-4(hd40)* mutant suppressors

A thrashing assay was performed to evaluate suppression of movement defects. An L4 stage animal was placed in an eyeglass filled with 1.0mL of M9 and observed for thrashing. The assay involved two aspects: average speed of thrashing and nature of thrashing. The speed was measured by counting the number of movements in 30 seconds. The nature of thrashing was whether the worm thrashed (or contracted) dorsally or/and ventrally. In a wild type strain, a worm would exhibit contraction in an alternating fashion between the dorsal and ventral directions. The number of worms counted ranged from 30-100 worms per experiment.

2.8. SNP mapping of *cdh-4(hd40)* mutant suppressors

After *cdh-4(hd40)* suppressor candidates were outcrossed three to four times, they were sent for whole genome sequencing in order to reveal mutations within coding regions. They were then crossed either with a Hawaiian (CB4856) strain, or a Bristol strain in order to create recombinants that would map to a specific region within a chromosome or to a specific mutation in a gene.

2.8.1. Gene mapping of genes that are not located on chromosome III

Suppressor candidates that were not expected to be located on chromosome III were mapped using a Hawaiian strain. The Hawaiian strain, *CB4856,* has SNPs of known genetic locations that are different from that in the Bristol strain (Davis *et al.* 2005). The *cdh-4(hd40)* mutants and the suppressor candidates are both in the Bristol background. Therefore, hawaiian strain was used to create recombinants with suppressor candidates. We can test for presence of those hawaiian SNPs to indicate a recombination event had occurred using PCR and digestions as described above in section 2.3.

2.8.2. Gene mapping of genes that are located on chromosome III

The *cdh-4(hd40)* allele is located on chromosome III in the Bristol background. Therefore, to map the mutations on chromosome III, the mutations that were already present in the suppressors were used as SNPs to identify recombinants. In this case, *hdIs26*, instead of a Hawaiian strain, was crossed into *cdh-4(hd40)* suppressors to create recombinants on chromosome III (Genetic Scheme 2.3). *hdIs26* was chosen for mapping because it is located on chromosome III and it tags the PVQ neurons with a red marker that is visible under the low-resolution microscope. Using *hdIs26* allowed for selecting against the red marker and hence for the homozygous *cdh-4(hd40)* individuals. For this case, the produced F2 lines were sent for sequencing in order to check for recombinants on chromosome III. Testing for recombinants was done by sequencing 0.4-0.7 kb region that included the mutation within the gene. If a mutation was lost, then that was an indication that a recombination event had occurred. If a mutation was still

present, a recombination event had not occurred. Suppressor candidates of *cdh-4(hd40)* that were mapped for chromosome III were *hd160, hd161, hd162,* and *hd163.*

2.9. Generating transgenic animals with *prp-8(+)* transgene and then crossing into *hd161* suppressor candidate for rescue

Rescue experiment was done by injecting WRM0625aG04 fosmid, containing a wild type version of *prp-8* (*prp-8(+)*), into wild type N2 animals. The transgenic wild type F2 lines with the *prp-8(+)* transgene were crossed into the suppressor strain *hd161* in the *cdh-4(hd40)* and *evIs111* backgrounds to test for loss of suppression of axon guidance defects (Genetic scheme 2.4). A green pharyngeal co-injection marker (*myo-2::GFP*) was injected along with the *prp-8(+)* fosmid to allow easy identification of individuals carrying the transgene. The fosmid was 39869 bp in size. The DNA injection mixes included 2ng/µl of WRM0625aG04 fosmid, 5ng/µl *myo-2::GFP*, and 93ng/µl of *pBluescript*. Transgenic strains were generated by Rick Zapf, using a standard DNA injection protocol (Mello *et al.* 1991).

2.10. Genetic Schemes

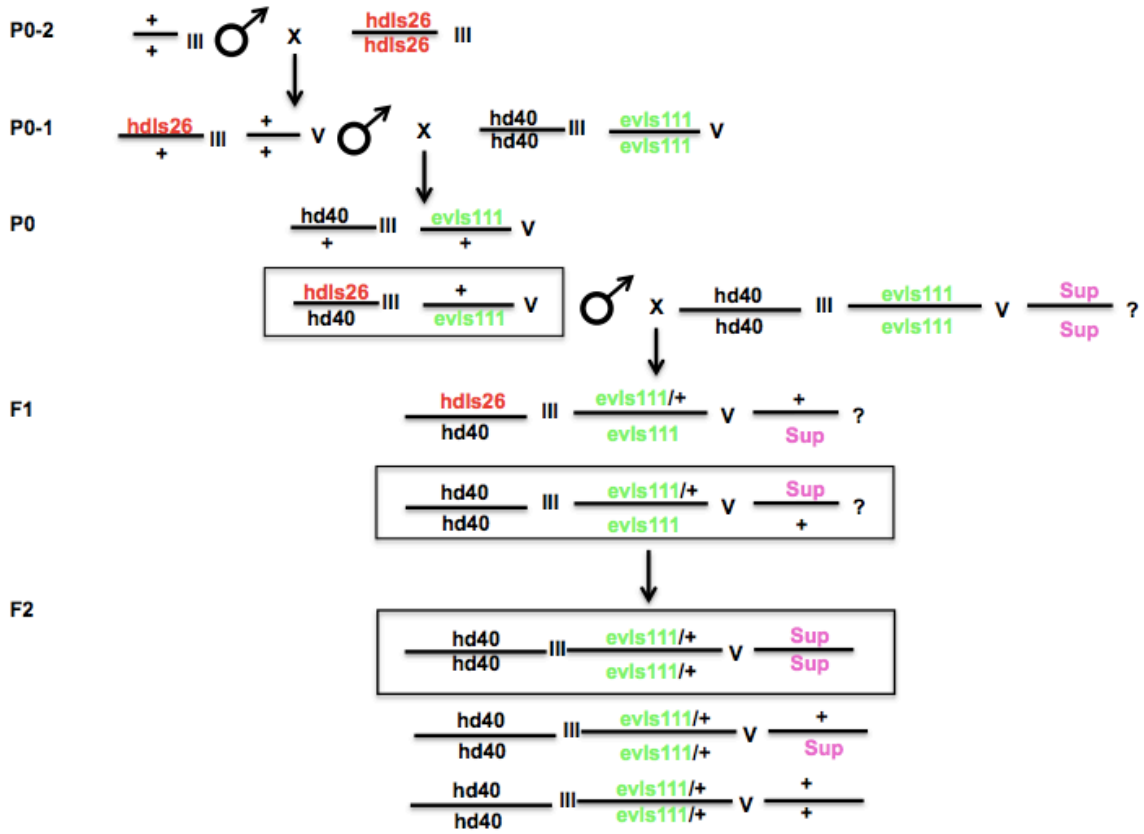

Genetic scheme 2.1 **Outcrossing *cdh-4(hd40)* suppressors to eliminate background mutations in the suppressor strains.**

The alleles used in this scheme: *hdIs26* is a transgene that marks PVQ neurons with a red fluorescent protein, *hd40* is an allele of *cdh-4*, *evIs111* is a transgene that marks the nervous system with GFP, and Sup refers to the suppressor mutation. P0=Parent generation, F1=First filial generation, F2=second filial generation. At the P0 stage, males with *hdIs26* were selected to mate with the suppressor candidate. At the F1 stage, hermaphrodites were selected for *evIs111* and against *hdIs26*. At the F2 stage, animals that starved in a time similar to starvation time of the suppressor candidate were checked for DNC suppression defects.

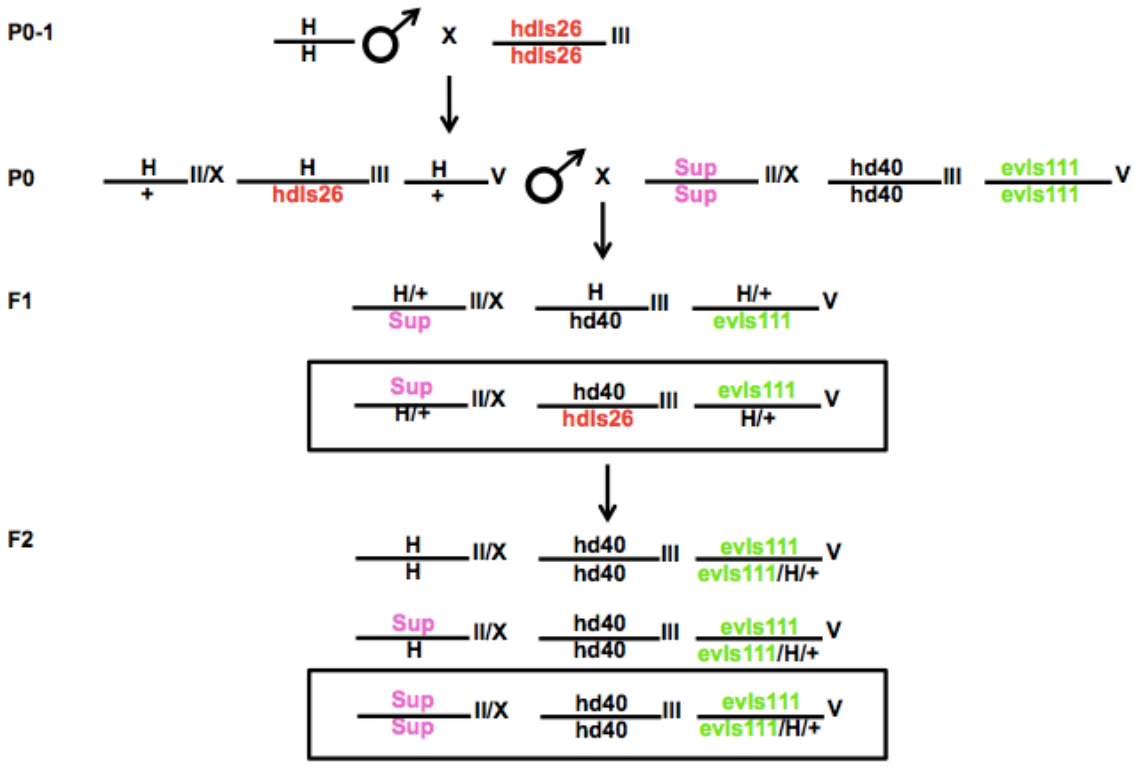

Genetic scheme 2.2 **SNP Mapping of *cdh-4(hd40)* suppressors not located on chromosome III.**

The alleles used in this genetic scheme were: *hdIs26* is a dominant red visible marker, *evIs111* is a panneuronal GFP marker, and Sup refers to the suppressor gene that could be either on chromosomes II, V, or X, H for Hawaiian. P0=Parent generation, F1=First filial generation, F2=second filial generation. At the F1 stage, hermaphrodites are selected for *hdIs26* and allowed to self-fertilize. Subcloned F1s are checked for being heterozygous H for Hawaiian. At the F2 stage, hermaphrodites from heterozygous Hawaiian F1 were selected for *evIs111* and against *hdIs26* and allowed to self-fertilize.

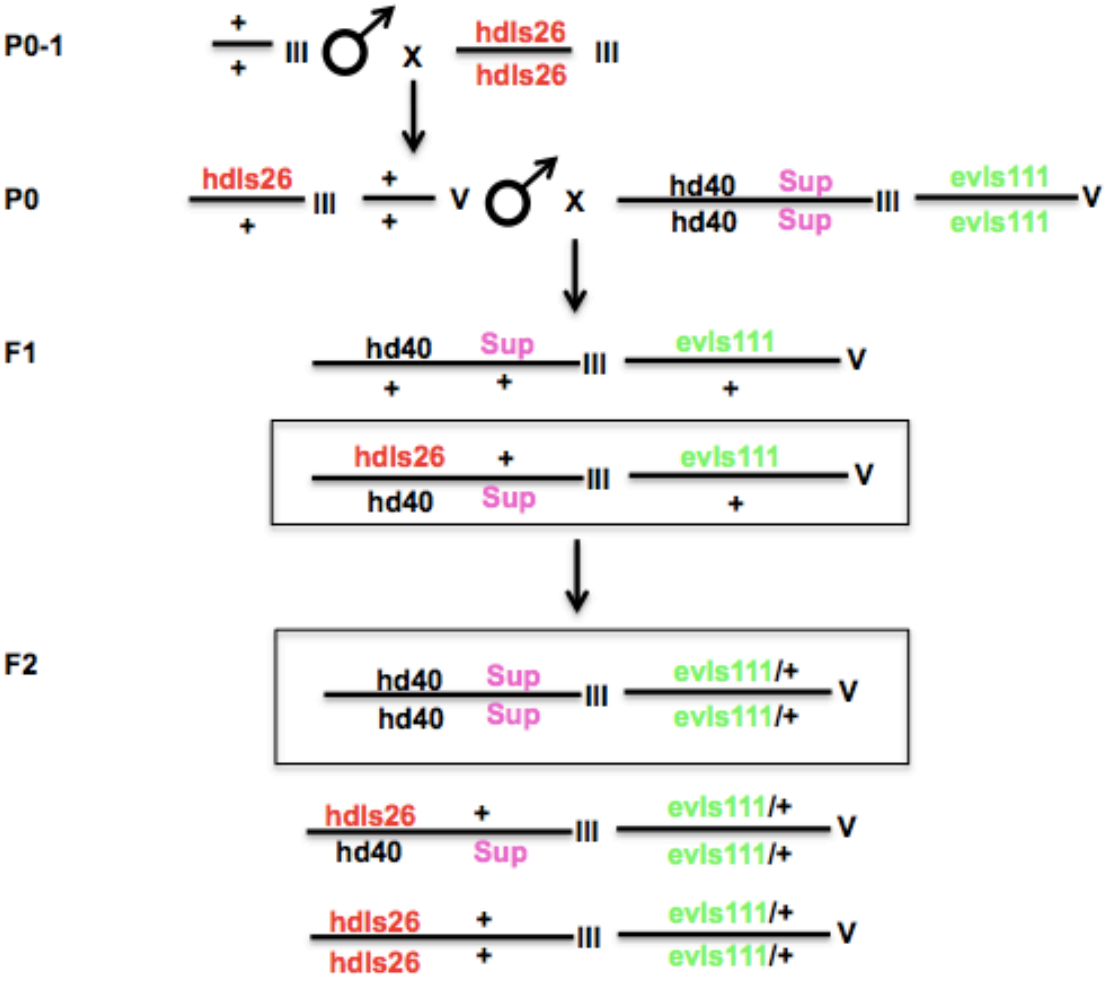

Genetic Scheme 2.3 **Testing *cdh-4(hd40)* suppressors for being on chromosome III and SNP mapping of *cdh-4(hd40)* suppressors for chromosome III via crossing with *hdIs26*.**

The alleles used in this genetic scheme were: *hdIs26* is a transgene that marks PVQ neurons with a red fluorescent protein, *hd40* is an allele of *cdh-4* located on chromosome III, *evIs111* is an allele on chromosome V that tags the nervous system with GFP, and Sup refers to the suppressor gene that would be on chromosome III. P0=Parent generation, F1=First filial generation, F2=second filial generation. At the F1 stage, hermaphrodites were selected for *hdIs26* and allowed to self-fertilize. At the F2 stage hermaphrodites were selected for *evIs111* and against *hdIs26* and allowed to self fertilize.

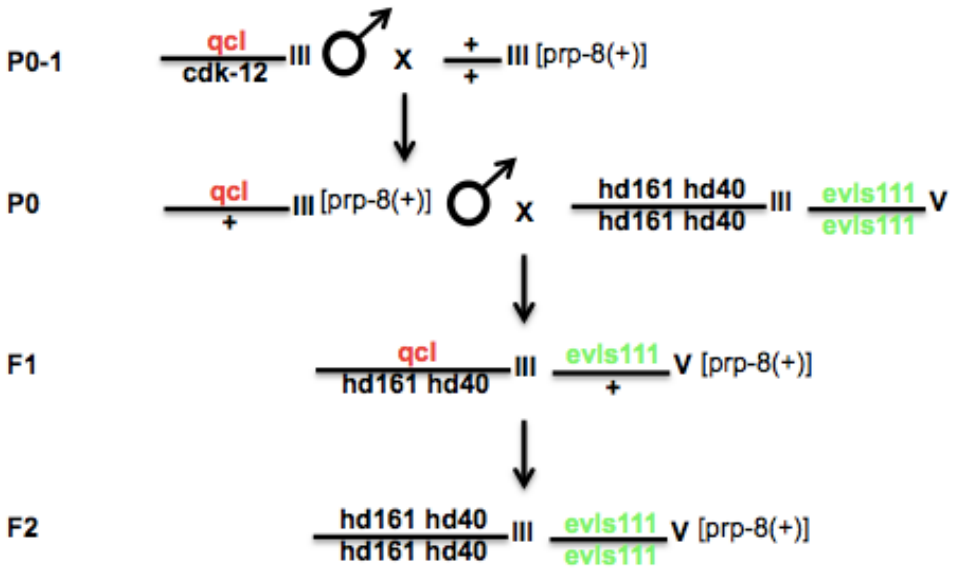

Genetic Scheme 2.4 **Crossing *prp-8(+)* transgenic lines into the *cdh-4(hd40)* suppressor *hd161*.**

The alleles used in this scheme were: *qcI* is a chromosome III balancer with a red pharyngeal marker, *hd40* is an allele of *cdh-4* located on chromosome III, *evIs111* is a transgene on chromosome V that tags the nervous system with GFP, and *hd161* is a *cdh-4(hd40)* suppressor. P0=Parent generation, F1=First filial generation, F2=second filial generation. At the P0 stage, males with *qc1* and transgene were selected to mate with *hd161* suppressor. At the F1 stage, hermaphrodites with *qc1, evIs111*, and transgene were selected and allowed to self-fertilize. At the F2 stage, hermaphrodites were selected for having the transgene, *evIs111*, and not *qc1*.

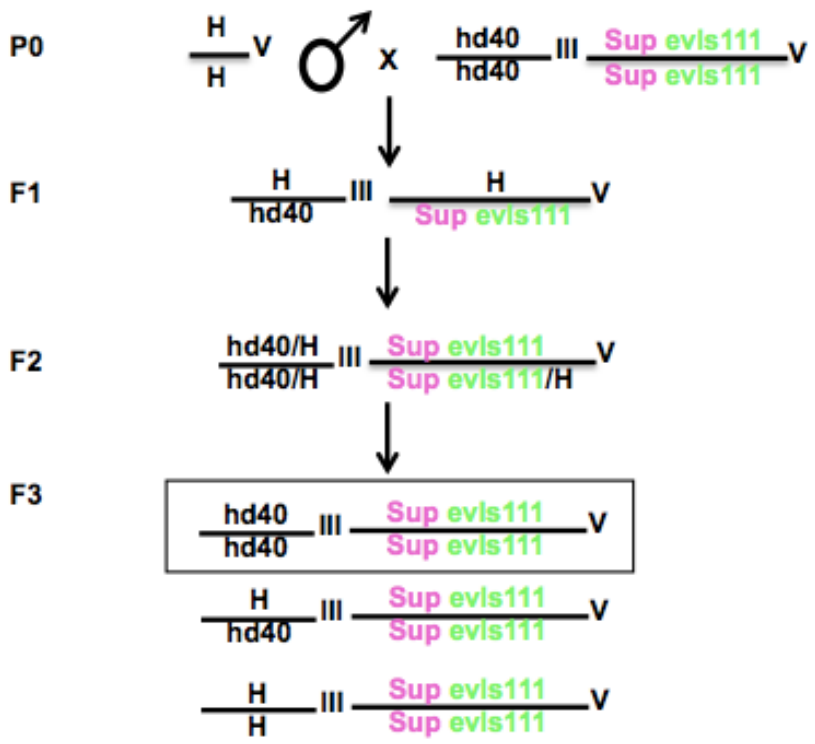

Genetic scheme 2.5 SNP Mapping chromosome V in *hd170*.

H refers to the Hawaiian genotype, *hd40* is an allele of *cdh-4* located on chromosome III, *evIs111* is a transgene on chromosome V that tags the nervous system with GFP, and Sup refers to the suppressor gene. P0=Parent generation, F1=First filial generation, F2=second filial generation. At the F1 stage, animals with *evIs111* were selected and allowed to self-fertilize. At the F2 stage, animals homozygous for *evIs111* are selected and allowed to self-fertilize. At the F3 stage, animals were checked for being homozygous for *hd40* via PCR.

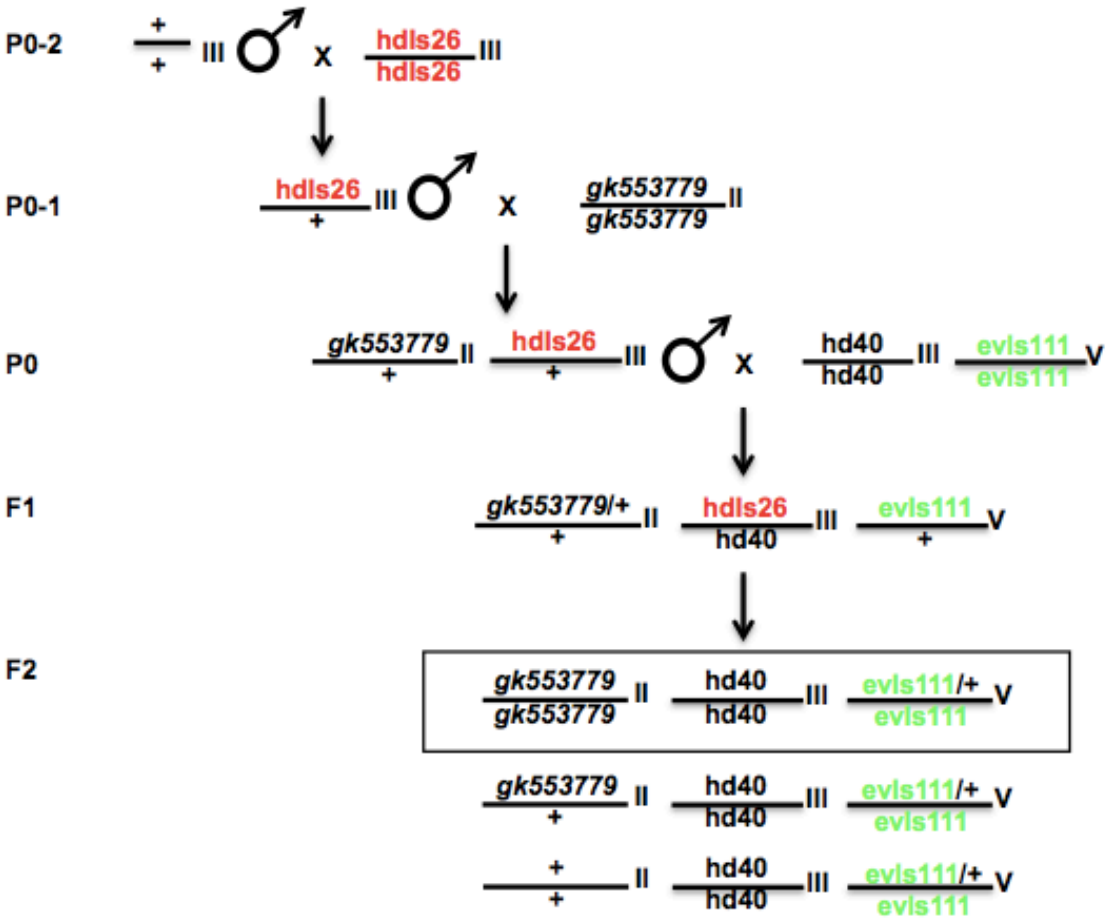

Genetic Scheme 2.6 **Crossing *math-48(gk553779)* into *cdh-4(hd40)* to test for suppression of axon guidance defects and to determine whether *math-48* is the suppressor in the *hd158* strain.**

hd40 is an allele of *cdh-4* on chromosome III, *gk553779* is an allele of *math-48* on chromosome II, *evIs111* is a transgene on chromosome V that tags the nervous system with GFP, *hdIs26* is a transgene on chromosome III that tags the PVQ neurons with a red fluorescent protein. P0=Parent generation, F1=First filial generation, F2=second filial generation. At the F1 stage, animals with *hdIs26* were selected and allowed to self-fertilize. At the F2 stage, animals were selected for *evIs111* and against *hdIs26* and allowed to self-fertilize. At the F3 stage, animals that are homozygous for *evIs111* are selected, allowed to self-fertilize, then send for sequencing to check for presence of *gk553779.*

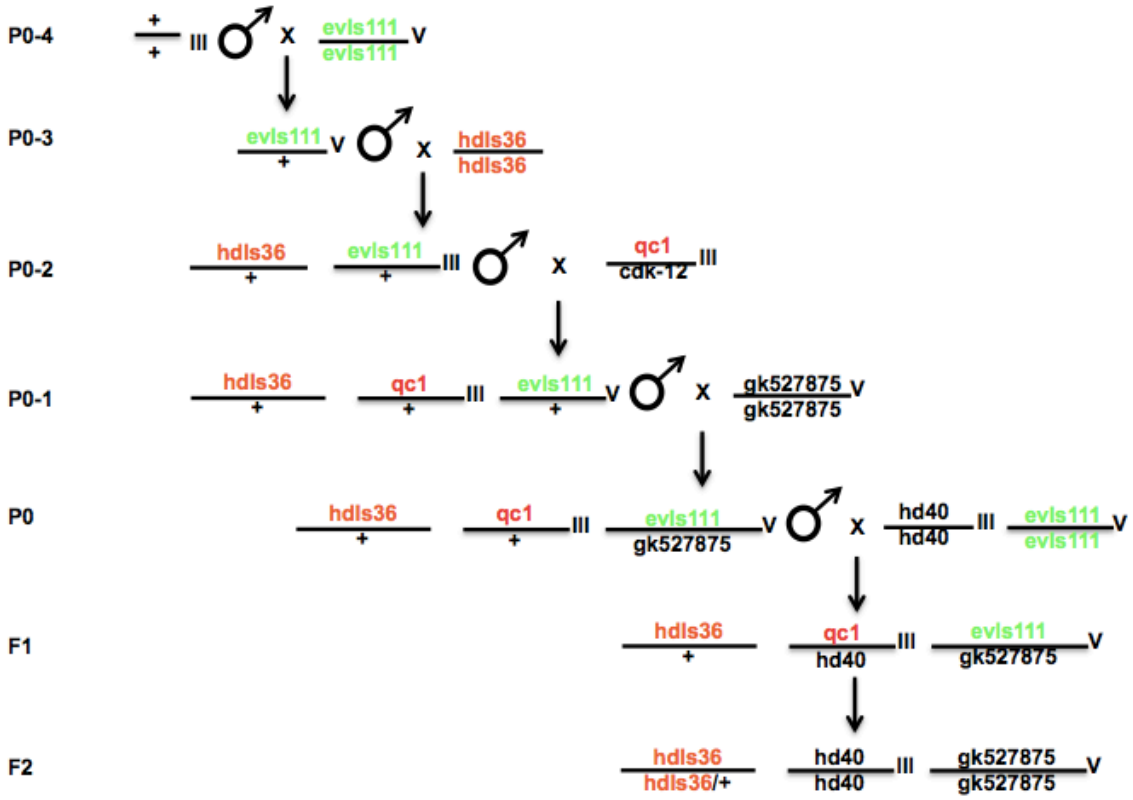

Genetic Scheme 2.7 **Crossing *prp-6*(*gk527875*) into *cdh-4(hd40)* to test for suppression of axon guidance defects and to determine whether *prp-6* is the suppressor in the *hd170* strain.**

evIs111 is a transgene on chromosome V that tags nervous system with GFP, *hdIs36* is a transgene that tags the nervous system with a red fluorescent marker, *qc1* is a chromosome III balancer with a visible red pharyngeal marker. P0=Parent generation, F1=First filial generation, F2=second filial generation. At the P0 stage, males with *hdIs36, qc1, and evIs111* are selected for mating with *hd40; evIs111*. At the F1 stage, animals that have *hdIs36* and are heterozygous for both *qc1* and *evIs111* are subcloned and allowed to self-fertilize. At the F2 stage, animals were selected for *hdIs36* and against both *qc1* and *evIs11*

2.11. Figures

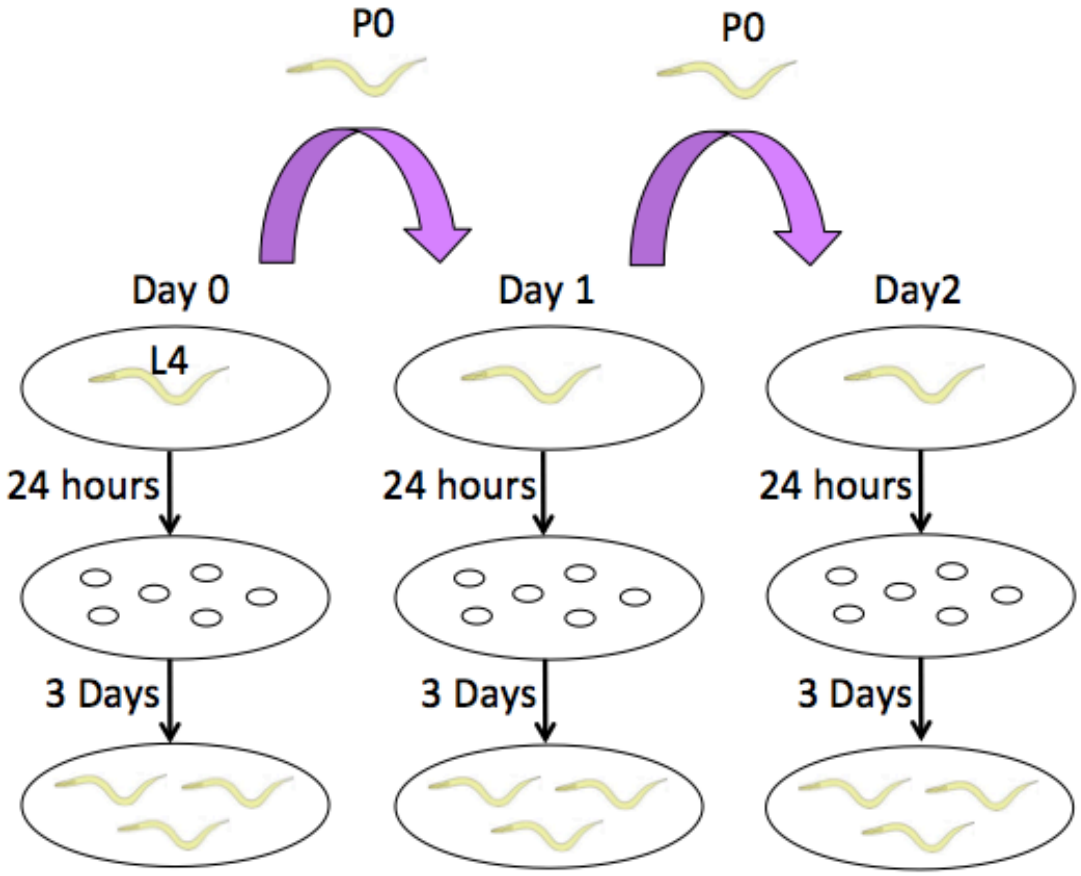

Figure 2.1 Lethality of *cdh-4(hd40)* suppressors.

Total number of eggs were counted over two days, starting with five to twelve L4-stage P0 worms on day 0. P0 worms were transferred everyday until day 3. Total number of F1 worms were counted when they reached adult stage.

2.12. References

Brenner, S., 1974 The genetics of Caenorhabditis elegans. Genetics 77: 71–94.

Davis, M. W., M. Hammarlund, T. Harrach, P. Hullett, S. Olsen *et al.*, 2005 Rapid single nucleotide polymorphism mapping in *C. elegans*. BMC Genomics 6: 118.

Mello, C.C., Kramer, J.M., Stinchcomb, D. and Ambros, V., 1991 Efficient gene transfer in C. elegans: extrachromosomal maintenance and integration of transforming sequences. The EMBO journal 10(12): 3959-3970.

Thompson, O., M. Edgley, P. Strasbourger, S. Flibotte, B. Ewing *et al.*, 2013 The million mutation project: a new approach to genetics in *Caenorhabditis elegans*. Genome Res 23: 1749–62.

Schmitz, C., I. Wacker, and H. Hutter, 2008 The Fat-like cadherin CDH-4 controls axon fasciculation, cell migration and hypodermis and pharynx development in Caenorhabditis elegans. Dev Biol 316: 249–59.

Wicks, S.R., Yeh, R.T., Gish, W.R., Waterston, R.H. and Plasterk, R.H., 2001 Rapid gene mapping in Caenorhabditis elegans using a high density polymorphism map. Nature genetics 28(2): 160.

Chapter 3.

Results

3.1. Phenotypic characterization of suppressors of *cdh-4(hd40)* mutants

Fifteen suppressors of *cdh-4(hd40)* mutants were isolated for suppression of dorsal nerve cord (DNC) defects, with a penetrance less than 50%. Thirteen of these *cdh-4(hd40)* suppressors had DNC or VNC defects less than 40% (Table 3.1) indicating partial suppression, and thus were selected for further phenotypic characterization.

3.1.1. Characterization of axon guidance defects through examination of DNC and VNC

The *cdh-4(hd40)* suppressor candidates were evaluated for axon guidance defects in dorsal nerve cord (DNC) and ventral nerve cord (DNC). *cdh-4(hd40)* mutants showed axon guidance defects in certain classes of neurons (Table 3.2). However, the DNC and VNC were selected for assessing suppression of defects because defects are more penetrant in comparison to defects in individual classes of neurons. Therefore, suppression of defects would be more apparent in the VNC and DNC.

Animals expressing a panneuronal marker were examined for DNC defasciculation and VNC crossover defects (Figure 3.1). In wild type, the axons in the DNC are tightly bundled and fasciculated (Figure 3.1A). In the VNC the right and left axon tracts are asymmetrical, with more axons in the right tract (Figure 3.1C). *cdh-4(hd40)* animals exhibit axon crossover defects from the right to the left tract (Figure 3.1D). The *cdh-4(hd40)* mutants have around 50% penetrance of defects in both the DNC and VNC. Thirteen out of fifteen suppressor candidates showed partial suppression of defects. In the DNC, the defects ranged from 18% to 39% and in the VNC from 21% to 32% (Table 3.1). No obvious correlation was found between DNC and VNC suppression for most of the strain. For example in *hd174*, the VNC defects (21%) were suppressed more than the DNC defects (39%). In the case of *hd161*, there was a stronger suppression of DNC defects, with19%, while the VNC had 30% defects. This

suggests that axonal navigation in the VNC might be separate from fasciculation in the DNC. In four suppressors (*hd169, prp-6(hd170), hd162, and hd172),* the DNC and VNC defects were suppressed to equal extents, indicating that the suppressors either function in the navigation pathways of both axon groups or that DNC and VNC axonal navigation share the same pathways. Overall, suppressors of *cdh-4(hd40)* mutants showed partial suppression of axon guidance defects.

3.1.2. Testing for suppression of *cdh-4(hd40)* lethality in the suppressors

In order to assess the suppression of overall adhesion defects, the lethality of *cdh-4(hd40)* suppressor candidates was compared to wild type and to *cdh-4(hd40)* mutants, having 76% of lethality (Table 3.3). The *cdh-4(hd40)* mutants exhibit both embryonic and larval lethality due to hypodermal and morphological defects. They have elongation defects at the 2-fold stage of embryogenesis and detachment of the pharynx from the mouth. These phenotypes imply a cell-cell adhesion function for CDH-4 in multiple tissues. Lethality was not suppressed by the majority of the suppressor candidates. Six of these tested suppressors had a higher lethality, ranging from 80% to 91%. In four suppressors lethality was partially suppressed ranging from 44% to 68%. The *cdh-4(hd40)* suppressors that had the most improved survival were *hd167*, *hd161* and *hd163,* having a total lethality of 44%, 53%, and 54%, respectively, which may indicate a partial suppression of adhesion defects. The number of eggs laid in the *cdh-4(hd40)* suppressors was increased, except for *hd161*, in comparison to the number produced by the *cdh-4(hd40)* mutants, ranging from 99 to 166 on average per parent animal in the suppressors compared to 62 in *cdh-4(hd40)* (Table 3.3). Overall, three out of the thirteen suppressors of *cdh-4(hd40)* mutants likely suppressed some of the adhesion defects. For the remaining suppressors, the improved growth compared to *cdh-4(hd40)* mutants seems to be due to a larger number of progeny rather than improved survival of the progeny.

3.1.3. Thrashing assay of suppressor candidates of *cdh-4(hd40)* mutants

The DNC and VNC contain motor neuron axons. Since the *cdh-4(hd40)* mutants had defects in both the DNC and VNC, the *cdh-4(hd40)* mutants were likely to also

exhibit movement defects. To evaluate suppression of movement defects a thrashing assay was done with five of the *cdh-4(hd40)* suppressor candidates, the strains that were initially sequenced. The suppressors were: *hd158, hd160, hd161, hd163,* and *hd170*. Assessment was based on two aspects: the speed of thrashing and the quality of thrashing. The speed of thrashing was based on counting the number of movements per 30 seconds. The quality of thrashing was based on counting how many animals are able to contract ventrally and dorsally in an alternating fashion. The *evIs111* GFP marker strain, serving as the positive control, since the *cdh-4(hd40)* mutants and its suppressors were in the *evIs111* background, had an average speed of 91 movements/30 seconds, with 100% of normal movement behavior (Figure 3.2). The *cdh-4(hd40)* mutants exhibited on average 18 movements/30 seconds with 29% of the worms having normal movement. Out of the five that were tested, two suppressors *hd158* and *hd170* had average speeds of 74 and 54 movements per 30 seconds and normal movements of 81% and 60%. Both of these suppressors show partial suppression of movement defects in both aspects of the experiment. As for the other three, the average speed ranged between 30 and 27 movements per 30 seconds. For animals with normal movement, they ranged from 40% to 35%. For these three suppressors, the thrashing speed and behavior were more similar to that of *cdh-4(hd40)* mutants rather than to the *evIs111* strain. Overall, only *hd158* and *hd170* exhibited suppression of movement defects, correlating with the suppression of the axon guidance defects. From these five suppressors, the thrashing speed and improved movement behavior appeared to be positively correlated only in *hd158* and *hd170* (Figure 3.2).

3.1.4. Q-cell migration defects in *cdh-4(hd40)* mutants suppressors

Q-neuroblasts migrate during initial stages of larval development along the anterior-posterior axis. The Q-cells and their descendants begin their migration around the vulva region and polarize either anteriorly or posteriorly depending on Q-cell type, giving rise to interneurons and sensory neurons. The right side Q-cell (QR) descendents, AVM and SDQR, migrate to the anterior region of the animal, while left side Q-cell (QL) descendents, PVM and SDQL, migrate to the posterior region of the animal. In *cdh-4(hd40)* mutants, the left Q-cells mismigrate, resulting in both the right and left Q-cells migrating anteriorly. Six *cdh-4(hd40)* suppressors were checked for suppression of migration defects: *hd158, hd160, hd161, hd162, hd163, hd170*. The *cdh-4(hd40)*

mutants showed 5% mismigration of QR, in which the Q-cells were migrating posteriorly, and 95% of QL mismigrating anteriorly. The suppressor *hd158* showed 25% migration defects of QR and 71% migration defects of QL. It appeared that *hd158* was enhancing the migration defects for the QR and partially suppressing the migration defects for the QL. For *hd162*, the QR and QL had 9% and 95% migration defects, respectively. For the other suppressers, *hd160, hd161, hd163,* and *hd170,* they all showed enhancement defects in the QR migration and no partial suppression in the QL migration (Table 3.4). In conclusion, none of these suppressors showed good suppression of Q-cell migration defects.

3.2. Suppressor gene identification

3.2.1. Whole-genome sequencing results of suppressors of *cdh-4(hd40)* mutants

The outcrossed suppressor candidate strains that were sent for whole genome sequencing (WGS) were: *hd158, hd160, hd161, hd162, hd163, and hd170*. These strains were selected for outcrossing since they have a better growth rate than the rest of the suppressor strains and that they appeared morphologically healthier than the *cdh-4(hd40)* mutants, facilitating the identification of individuals homozygous for the suppressor. WGS revealed mutations in both coding and non-coding regions in comparison to the reference wild type genome (Wormbase release 235). We primarily considered mutations within coding regions listed in Tables 5-10 as candidates. Mutations found in more than one suppressor strain were removed, as they likely are background mutations present in the parental strain. Mutations in coding regions were found on all chromosomes for *hd158* (Figure 3.3A) and *hd161* (Figure 3.3C). Cluster of mutations in coding regions were found on chromosome III for *hd158, hd160,* and *hd161*. Another cluster of mutations was found on chromosome X for *hd161* and on chromosome II for *hd158* and *hd160* (Figure 3.3B). Additionally, *hd160* had one mutation on each of chromosome V and I. For *hd162* and *hd163*, very few mutations in genes were found on chromosomes III and I (Figure 3.4E and 3.4F). For *hd170*, few mutations were found in genes on chromosomes II, V, and X (Figure 3.3D). Since several mutations were still present in the genomes of the *cdh-4(hd40)* suppressor strains, we were not able to unambiguously identify a suppressor gene from WGS. Therefore, SNP mapping was required in order to map and identify the suppressor candidate genes.

3.3. Mapping of *cdh-4(hd40)* suppressor candidates

Since each of the suppressors contained more than one unique mutation, mapping experiments were required to identify the actual suppressor mutation. Five of these suppressors had mutations on chromosome III, which was expected, because during outcrossing, the *cdh-4(hd40)* allele that is on chromosome III was maintained. Therefore, in order to rule in or rule out chromosome III for having the suppressor gene, the suppressors *hd158, hd160, hd161, hd162,* and *hd163* were crossed with *hdIs26*, bearing a red visible marker on chromosome III, and then selected for *cdh-4(hd40)* F2 lines (Genetic scheme 2.3). Theoretically, if a suppressor gene was on chromosome III, then 100% of all produced F2 lines would show suppression of axon guidance defects and therefore have the suppressor gene. If a suppressor gene was not on chromosome III, then only 25% of produced F2 lines would show suppression of *cdh-4(hd40)* phenotype. These percentage values in theory would apply if no recombination events have occurred in the germline. Recombination events would slightly change the percentage values depending on location of suppressor gene on chromosome III. For example, suppressor genes located near the ends of chromosome III are more likely to undergo recombination events, leading to loss of the suppressor gene.

Initially, a starvation assay was performed on the F2 lines to see how many animals would starve in a period similar to either starvation time of the suppressor strain or to the *cdh-4(hd40)* mutants. For *hd158*, 32% of the lines were starved in 15 days or less, while the rest of them took longer than three weeks (Table 3.11), indicating that the suppressor gene was unlikely to be on chromosome III. For *hd160* and *hd163* F2 lines, the percentage of animals that starved was 75% and 89%, respectively. For these suppressors, the gene could be on chromosome III. As for *hd161*, the percentage of starved animals was 60%, and hence the gene was more likely to be on chromosome III as well.

Afterwards, suppression of DNC defects was scored in some of the lines that starved in 15 days or less to confirm presence of the suppressor and in some lines that took over 15 days to starve to confirm the absence of the suppressor. Once suppression was confirmed, SNP mapping was used to identify the suppressor genes. For suppressors on chromosome III, unique mutations in the suppressor were used as SNPs, which were identified through sequencing. Hawaiian SNP mapping was used for

suppressors not on chromosome III as well as for *hd170*, since it did not have unique SNPs on chromosome III.

3.3.1. Mapping and identification of the *cdh-4(hd40)* mutant suppressor: *hd158*

The WGS results for *hd158* showed in coding regions clusters of mutations on chromosomes II and III, and one or two mutations for the rest of the chromosomes. (Figure 3.3A, Table 3.5). Therefore, the suppressor gene was predicted to be on either chromosome II or III. From the crossing that was done to test for chromosome III, 22 F2 lines were produced. The initial assessment that was based on a starvation assay indicated that the suppressor gene was more likely to be on chromosome II (Table 3.11). Out of these lines, eleven F2s were sent for sequencing to check for presence or absence of certain mutations in order to assess for recombination events on chromosome II. The mutations that were checked for were in genes *mcd-1, clr-1,* and *BO281.8*, at genetic locations 21.36, -1.3, and -13.83, respectively. Three types of informative recombinants were revealed (Table 3.12). A recombinant line with *mcd-1* mutation absent while the mutation in the other two genes present gave a DNC score of 25% defects, indicating suppression of axon guidance. The other two types of recombinants were a line that lacked the *B0281.8* mutation while mutations in the other two genes were present and a line with only the mutation in the *clr-1* present. Both of these different recombinants showed no suppression of axon guidance defects because the score for DNC defects were over 50% (Table 3.12). Therefore, the candidate genes left on chromosome II were *clr-1, nas-29, F59A6.3, camt-1, F18A12.3, B0281.8,* and *math-48*, excluding the rest (Table 3.5; Figure 3.4).

Mapping of chromosome II was done through Hawaiian SNP mapping (Genetic scheme 2.2), in which *hd158* that is in a Bristol background was crossed with the Hawaiian strain to produce recombinants. This Hawaiian crossing produced 100 F2 worms, which were tested for presence or absence of Hawaiian SNPs through restriction digests. The SNPs that were initially tested were at genetic locations 0.1, -6, and -14 (Figure 3.4). Three informative types of recombinants were produced. A recombinant that was Bristol for 0.1 SNP and Hawaiian for both -6 and -14 SNPs had 50% DNC defects and hence no suppression of axon guidance defects. A second recombinant line with Bristol SNP at -14 location and Hawaiian SNPs at -6 and 0.1 showed 30% DNC

defects (Table 3.13), indicating suppression of axon guidance defects. This same line was also tested for SNP at -7.6 location and the result was a Hawaiian SNP, leaving only two candidate genes in the Bristol region: *B0281.8* and *math-48* (Figure 3.4). The third informative recombinant line was Bristol for SNPs at locations 0.1 and -6, but heterozygous Hawaiian for the SNP at -14. For this recombinant, fourteen F3 worms were subcloned in order to get a line with Hawaiian SNP for -14 and a line with a Bristol SNP for -14 as well and then each would be scored for suppression of DNC defects. The F3 line with the Bristol SNP had 31% DNC defects, indicating suppression, while the F3 line with the Hawaiian SNP had 54% DNC defects (Table 3.13), indicating no suppression. Taken together, the suppressor gene was likely to be either *B0281.8* or *math-48*.

The expression data of *B0281.8* showed no expression at 400 minutes, the time when axons grow out, while *math-48* showed some expression at that same time (Figure 3.5). Therefore, *B0281.8* was less likely to be the suppressor. Later, the same mutation in *B0281.8* gene was found in the parental *cdh-4(hd40)* strain, indicating that *B0281.8* was not the suppressor gene (Table 3.14). Therefore, *math-48* was the most likely candidate.

To confirm the identity of the suppressor, an allele of *math-48* was crossed into *cdh-4(hd40)* to check for suppression of axon guidance defects (Genetic Scheme 2.6). The *math-48* allele was *gk553779*. This allele holds a mutation resulting in a similar amino acid change within the same exon and domain as in *hd158* (Figure 3.9). The *math-48* amino acid change in *hd158* was of glutamic acid (E), which is negatively charged, to lysine (K), which is positively charged (Figure 3.9B); while the change in *gk553779* was of glycine (G), a non-polar amino acid, to glutamic acid (E) (Figure 3.9A). Both amino acid changes are within the first MATH domain and they were 28 amino acids apart. To assess for suppression of axon guidance defects, dorsal nerve cord was scored for defasciculation and ventral nerve cord for crossovers. When a line of *math-48(gk553779)* in the *cdh-4(hd40)* background was created, a suppression of axon guidance defects was observed, with a score of 25% of DNC defects and 24% of VNC defects (Table 3.22). Sequencing of this line revealed the presence of the point mutation in *math-48(gk553779)* that results in the amino acid change (Table 3.23). Therefore, these results indicated that *math-48* was the suppressor in *hd158*.

3.3.2. Mapping and identification of the *cdh-4(hd40)* mutant suppressor: *hd170*

For *hd170*, mutations in coding regions were found on chromosomes II, V, and X (Figure 3.3D, Table 3.9). Hawaiian SNP mapping was done in order to map to a specific chromosome. The mutations on chromosome II were on the right arm of the chromosome. Therefore, the tested SNPs were at genetic location 22, 16, and 11 for chromosome II. For chromosome V, mutations being on the right arm as well, the tested SNPs were at 18 and 13. As for chromosome X, the SNPs were at 2, -4, and -8, being chosen in relation to the location of mutations (Figure 3.8). From the crossing of Hawaiian into *hd170*, nineteen F2 lines were produced, with three of them having informative recombinants (Table 3.20). All lines were Bristol for chromosome V SNPs. The lines that produced Hawaiian SNPs for chromosomes X and II still showed suppression of DNC defects, in which they were 19% and 25%, respectively. Therefore, since suppression of axon guidance was still apparent in lines that had Hawaiian chromosomes II and X, but Bristol for V, then the suppressor gene was likely to be on chromosome V.

The candidate genes on chromosome V were *F46B3.15* and *prp-6* (Figure 3.3D). *F46B3.15* is at genetic location 25.03 and *prp-6* is at 13.49. *hd170* was crossed again with Hawaiian to produce more recombinants. Chromosome V has the pan-neuronal GFP marker, *evIs111*, in the Bristol background. Therefore, the selection of F2 was based on picking animals that were homozygous for GFP (Genetic scheme 2.5). From this crossing, 240 F2 lines were obtained. Three of them were informative recombinants (Table 3.21). The SNPs used for testing for recombinants were at 25.1 close in genetic location to *F46B3.15,* 18 and 16.8, which were between the two candidate genes, and 13, the SNP being located on the left side of *prp-6*. One of the recombinants was Hawaiian for all of the four SNPs, indicating the loss of the mutation in the candidate genes. This line was scored for defects in the DNC and VNC, resulting in 50% and 65%, respectively, indicating the loss of suppression in axon guidance defects. Another line was Bristol at the 25.1 genetic location and heterozygous for Hawaiian for the other three SNPs. From this line, 20 F3 animals were subcloned in order to find the homozygous Hawaiian for the SNPs. Two F3 lines were heterozygous Hawaiian for the location 13 SNP. From these lines, 20 F4 worms were subcloned. I was not able to get a homozygous Hawaiian at the 13 location SNP. The F4 line that was sent for sequencing

was Hawaiian at 18 location and Bristol at 25.1 and 13 locations. For the *prp-6* gene, the missense mutation was present. Surprisingly, for the *F46B3.15* gene, the missense mutation was absent. This was unexpected because the SNP result for 25.1 genetic location indicated a Bristol region. Regardless of this surprising sequencing result, they were scored for suppression of DNC defects and the results came to 30% defects, indicating suppression of axon guidance, and hence indicating that *prp-6* would be likely the candidate suppressor gene. The mutations in *prp-6* and *F46B3.15* were tested for presence in the *cdh-4(hd40)* strain and it turned out that the same missense mutation in *F46B3.15* was found in the parental *cdh-4(hd40)* strain as well (Table 13.4). Therefore, *F46B3.15* cannot be the suppressor gene in *hd170,* leaving *prp-6* to be the only candidate gene left.

The confirmation of this gene was done similarly to the method of confirmation in *hd158*. The *prp-6* allele, *gk527875*, was crossed into *cdh-4(hd40)* to check for suppression of DNC defects (Genetic Scheme 2.7). The *prp-6(gk527875)* mutation causes the same kind of amino acid change as that in *hd170*, which was glutamic acid (E), negatively charged, to lysine (K), positively charged (Figure 3.10). The changed amino acids of *prp-6* in *hd170* and in *gk527875* were within the same domain and only seven amino acids apart. The *prp-6(gk527875)* mutation in the *cdh-4(hd40)* background had 25% defects in the DNC, indicating suppression of axon guidance defects (Table 3.24). Therefore, *prp-6* was the suppressor gene in *hd170*.

3.3.3. Mapping and identification of the *cdh-4(hd40)* mutant suppressor: *hd161*

WGS revealed mutations in coding regions in all of the chromosomes for *hd161* (Figure 3.3C, Table 3.6). Mutation clusters were prominent on chromosomes III and X. Initial mapping (Genetic scheme 2.3) suggested that *hd161* is likely on chromosome III (Table 3.11). Fifteen recombinant F2 lines were produced. To confirm that *hd161* is not on the X chromosome in seven of these lines the presence of three different mutations on chromosome X in *pssy-1, gcy-9,* and *R04D3.2* was tested by sequencing (Figure 3.7). An informative recombinant that lacked all of these mutations was found to have 16.5% DNC defects, indicating that the suppressor was present and therefore likely not on chromosome X. For chromosome III, the mutations tested were in *trp-2* and *B0464.9* genes. All tested lines showed absence of *trp-2* mutation, and two of them were scored

for DNC defects with a score of 16.5% (Table 3.16, Figure 3.8) and 26%, indicating suppression and that *trp-2* gene was not the suppressor.

Even though *hd161* was mapped to a cluster of five genes, *prp-8*, which was one of the genes in the cluster, was predicted to be the most likely candidate because *hd170* was an allele of *prp-6*, a gene similar in function to *prp-8*. Confirmation of *prp-8* was done through a rescue experiment by injecting a fosmid with a wild type version of *prp-8* gene into a Bristol wild type strain and then crossing the *prp-8(+)* transgenic F2 lines into *hd161* (Genetic Scheme 2.4). If *prp-8* was the suppressor gene, then worms with *prp-8* transgene would display a loss of suppression of axon guidance defects and a reversion back to the *cdh-4(hd40)* phenotype. Checking for suppression was done through scoring the DNC for defasciculation, with *hd161* having 18% DNC defects. Two lines were scored for DNC defects, and both animals with and without the transgene were evaluated. In both lines animals showed over 50% DNC defects when the transgene was present and less than 30% DNC defects when the transgene was absent (Table 3.25). Since the *prp-8*(+) transgene abolished the suppression effect of *hd161*, these results would indicate that *prp-8* was the suppressor gene in *hd161*.

The suppressor *hd161* was crossed with the Hawaiian strain (Genetic scheme 2.2) to produce recombinants. 20 F2 lines were produced and were SNP mapped for chromosome X using SNPs at genetic locations -8.0, -4.0, and 2.0 (Table 3.17). The recombinant line that was Hawaiian for all of these SNPs scored 18% DNC defects, indicating suppression and confirmation that suppressor gene was not on chromosome X. For chromosome III, fifteen F2 lines were sent for sequencing to test for presence/absence of mutation in *prp-8* and *B0464.9*. One informative line was produced that lacked both of the tested mutations and it scored 50% DNC defects, indicating loss of the suppressor mutation (Table 3.16). Therefore, *hd161* was mapped to a cluster of four genes: *B0464.9, ess-2, prp-8,* and *rps-14*.

3.3.4. Mapping of the *cdh-4(hd40)* mutant suppressor: *hd160*

WG sequencing results of *hd160* revealed in coding regions a cluster of mutations on the left arm and few mutations on the right arm of chromosome II, a cluster of mutations on the right arm of chromosome III, and a mutation each on chromosomes I and V (Figure 3.3B, Table 3.5). The initial mapping suggested linkage to chromosome III, as

explained above, producing 20 recombinant F2 lines (Genetic scheme 2.3, Table 3.11). These F2 lines were checked by sequencing for presence or absence of mutations in the genes *nac-2, cor-1, and ZK1010.8* on chromosome III. Two F2 lines had informative recombination events. One of them lacked the *ZK1010.8* mutation, while the other two mutations were present. This line showed suppression of DNC defects (Table 3.15). In addition, the starvation time for this F2 line was 10 days, confirming the presence of the *hd160* suppressor. In the other F2 line, all three mutations were absent. Unfortunately, I lost this line to the lack of maintenance before I could score it for DNC defects. However, the starvation time for this line was more similar to that of the *cdh-4(hd40)* mutants, suggesting that *hd160* was absent. Therefore, *hd160* was mapped to the mutations cluster that include the genes *Y47D3A.29*, *unc-49*, *cor-1, F54C8.6*, *T23G5.3*, and *nac-2*, with genetic locations that ranged from 6.45 to 0.11, (Figure 3.6). *nac-2* encodes a high affinity sodium-coupled citrate transporter that is orthologous to mammalian citrate transporter NaCT, *cor-1* encodes an ortholog of actin-binding protein coronin, and *unc-49* encodes a subunit of a heteromeric GABA receptor. *F54C8.6 and T23G5.3* are uncharacterized genes, and *Y47D3A.29* encodes a catalytic submit of DNA polymerase alpha, which seems unlikely to be the suppressor gene. The *hd160* suppressor was not mapped further due to lack of time.

3.3.5. Mapping of the *cdh-4(hd40)* mutant suppressor: *hd162*

For *hd162*, only three mutations in coding regions were present. They were all missense mutations in *Y54E5B.2* on chromosome I and in *Y75B8A.24* and *Y75B8A.25* on chromosome III (Table 3.8). SNP mapping was done by crossing the suppressor *hd162 into hdIs26* (Genetic scheme 2.3), creating eight F2 lines with *cdh-4(hd40)* in them. Two F2 lines were sent for sequencing to test for presence or absence of the mutations in the three genes. One of them had the best suppression of DNC defects among the eight F2 lines, which was 27%, and the other one had no suppression of DNC defects, which was 53% (Table 3.18). The line with suppression lacked the mutation in all of the three genes. Therefore, none of these genes were considered to be the suppressor, indicating that the suppressor might be one of the mutations in non-coding regions. Due to the time constraints, identifying the suppressor in *hd162* was not pursued any further.

3.3.6. Mapping of the *cdh-4(hd40)* mutant suppressor: *hd163*

For *hd163*, two mutations in the coding part of genes were found after WGS, one on chromosome I and the other mutation on chromosome III (Figure 3.3F, Table 3.9). The mutation on chromosome I was in *col-46*, which encodes a cuticular collagen. Because COL-46 is a structural protein of the cuticle, it was unlikely to be the suppressor for axon guidance defects. The mutation on chromosome III was in *Y22D7AR.14*, which was an uncharacterized gene. Thus, SNP mapping was done on chromosome III. From the F2 lines, six were sent for sequencing to check for recombinants that would have the mutation absent in the gene. The results revealed the absence of the mutation in all the tested lines. Two of them were score for DNC defects and one line showed 31% and the other 25% (Table 3.19), which indicated suppression, and hence *Y22D7AR.14* was not the suppressor gene. Therefore, since suppression of axon guidance still occurred in the lines when the gene was absent, no candidate genes were found in *hd163*, indicating that the suppressor mutation was likely to be within the non-coding region. Due to these results, identifying suppressor in *hd163* was not investigated any further.

3.4. Figures

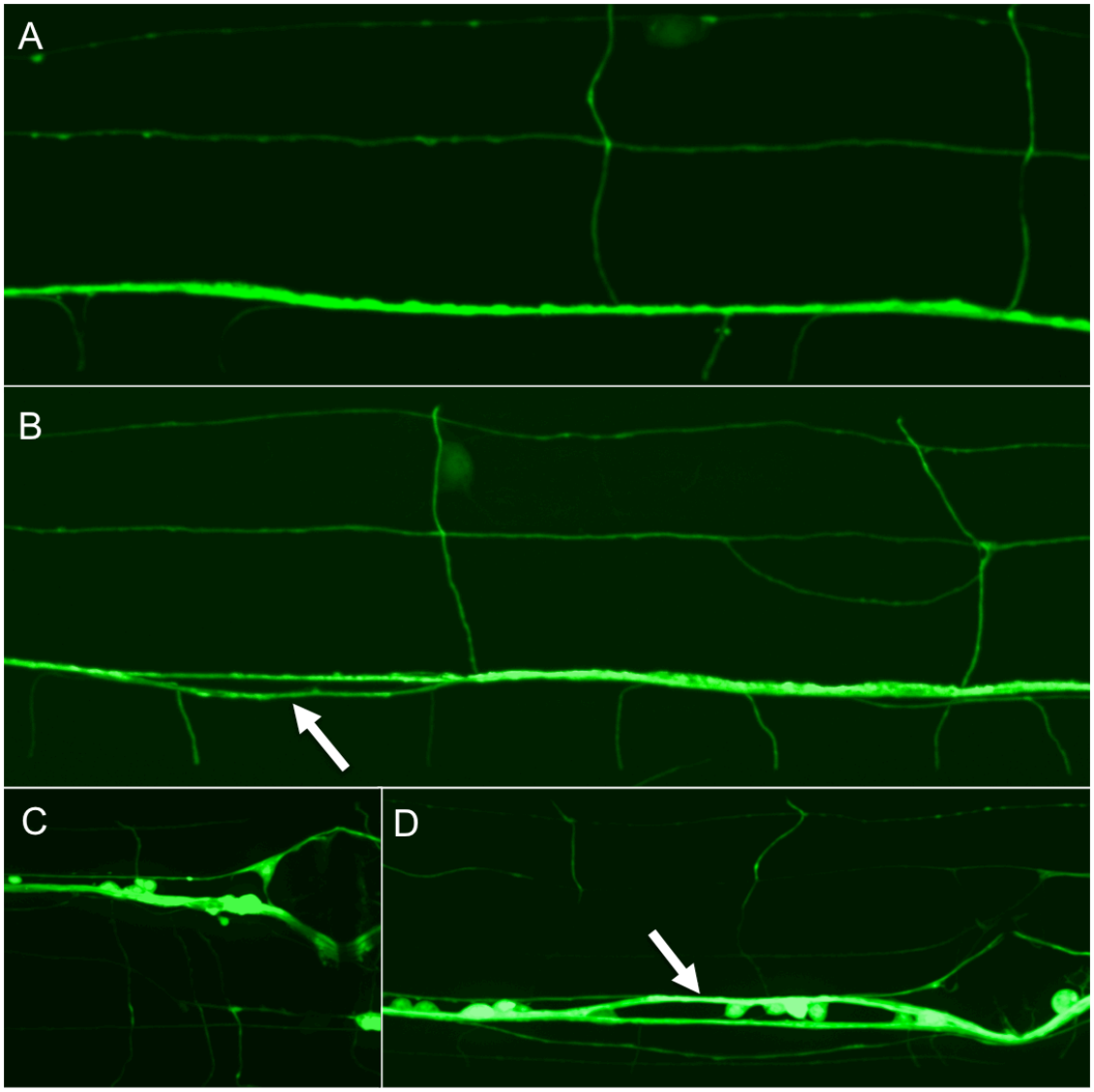

Figure 3.1 Scoring for dorsal nerve cord (DNC) defasciculation & ventral nerve cord (VNC) crossovers in adult hermaphrodite worms.

Images are oriented with anterior to the right. A) DNC in wild type. B) DNC defasciculation in *cdh-4(hd40); prp-6(hd170)* as pointed out by the white arrow. C) Wild type VNC in wild type. D) VNC crossover from right to left axon tract in *cdh-4(hd40); prp-6(hd170)* as pointed out by the white arrow.

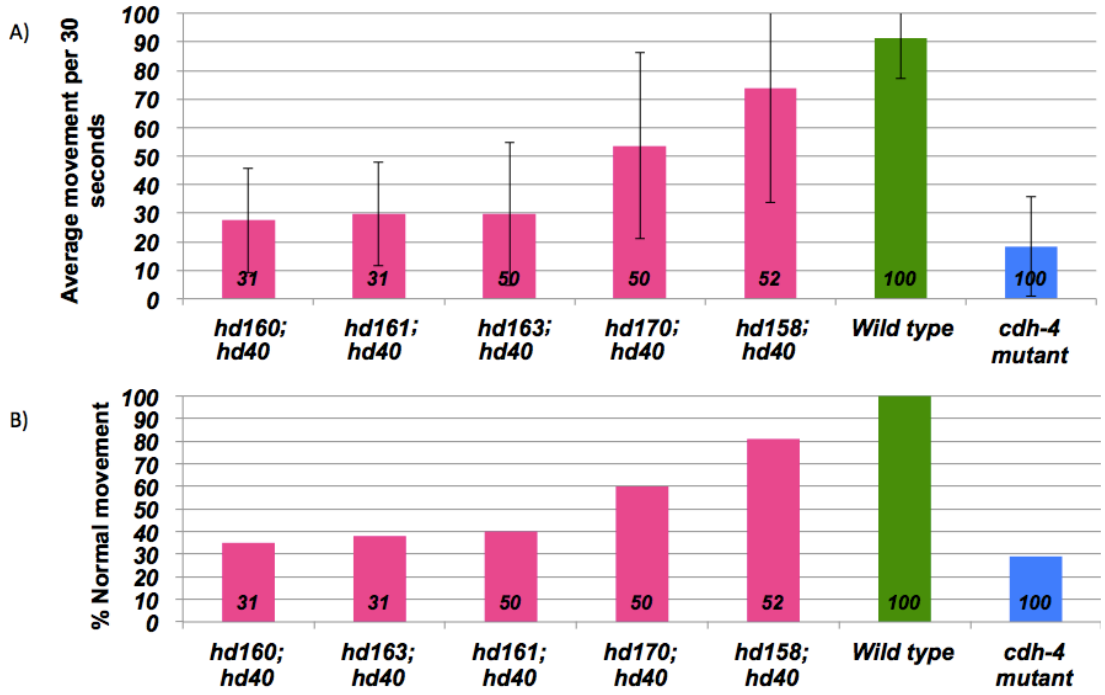

Figure 3.2 Thrashing assay of *cdh-4(hd40)* suppressors.

A) Quantitative assay that involves counting the number of contractions, that could be dorsally and/or ventrally, in 30 seconds for each animal. B) Qualitative assay that includes counting the number of animals with normal movement, which ventral and dorsal contractions in alternating manner.

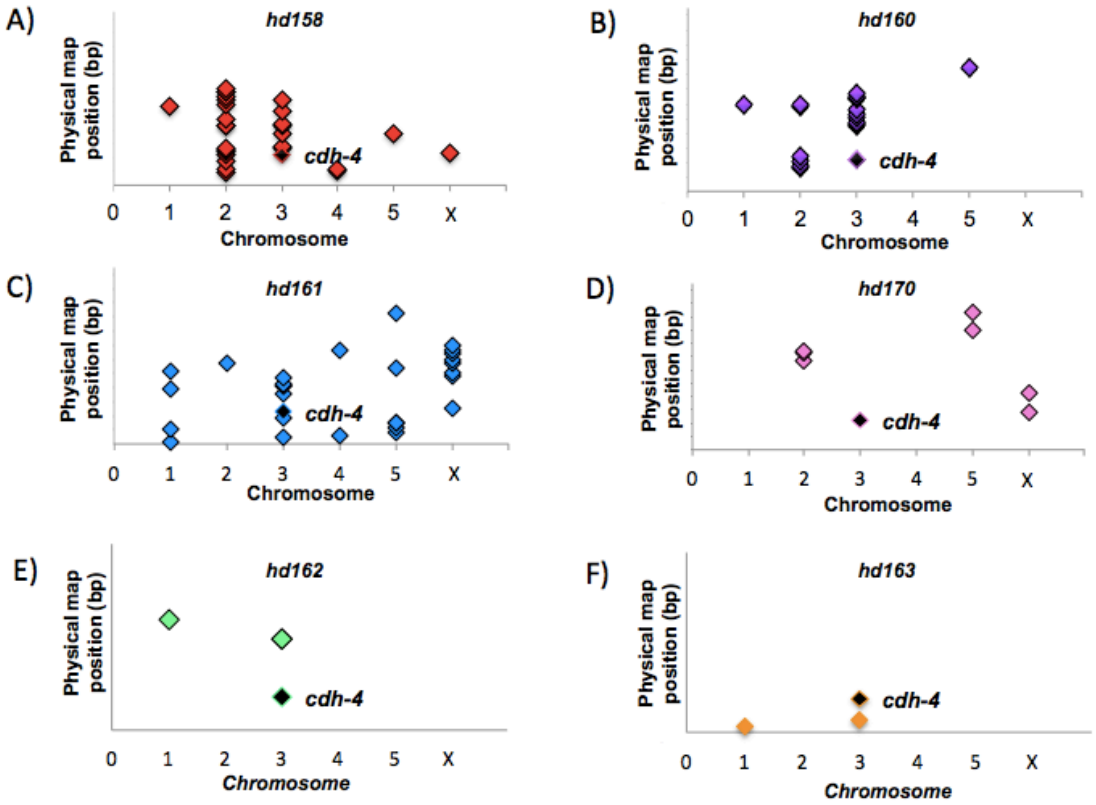

Figure 3.3 Distribution of mutations in coding regions in *cdh-4(hd40)* suppressor strains after outcrossing.

A) *hd158*. B) *hd160*. C) *hd161*. D) *hd170*. E) *hd162*. F) *hd163*.

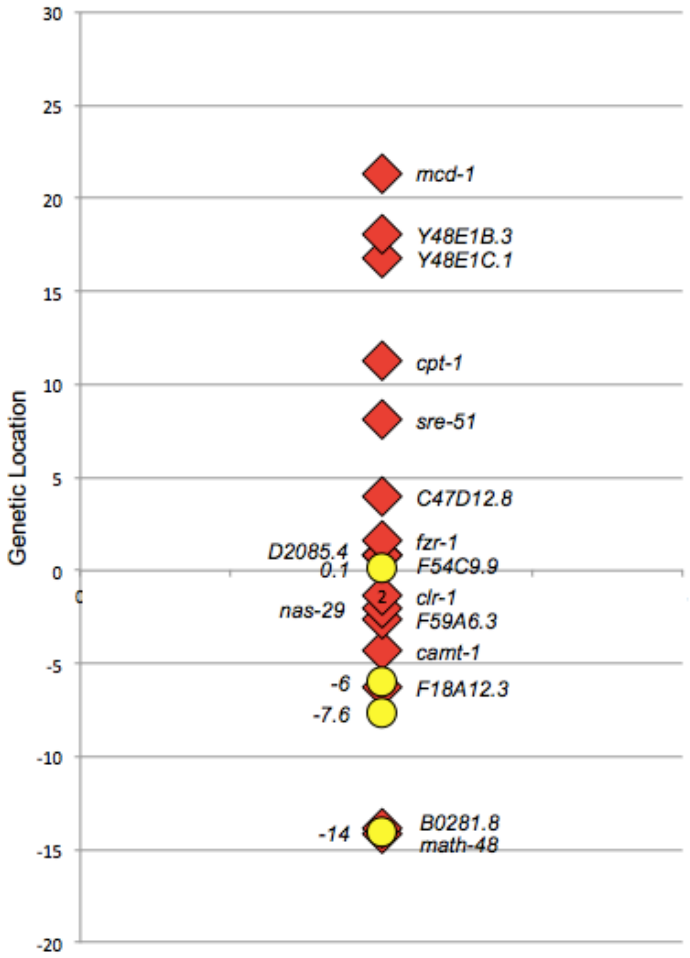

Figure 3.4 Genetic locations of the tested Hawaiian SNPs in relation to the mutations in *hd158* on chromosome II.

The yellow circle refers to the genetic location of tested SNP. The red diamonds are genetic locations of the mutations in coding regions on chromosome II in *hd158* that were revealed by WGS.

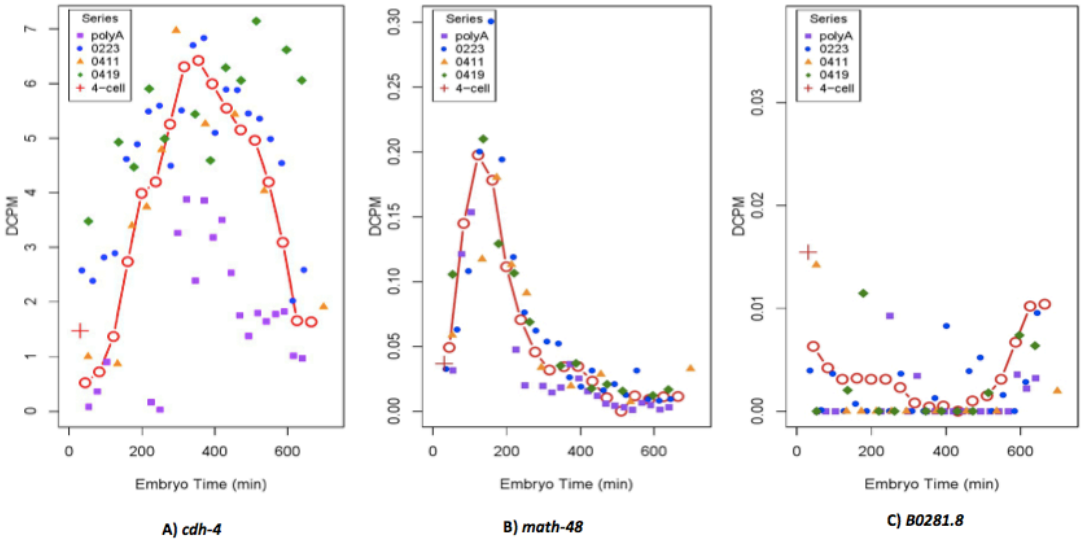

Figure 3.5 Gene expression data during embryogenesis.

A) *cdh-4,* and *hd158* suppressor candidate genes, B) *math-48* and C) *B0281.8*, obtained from Gexplore (Hutter et al. 2009) The unit used to measure expression of a gene is dcpm (depth of coverage per million reads).

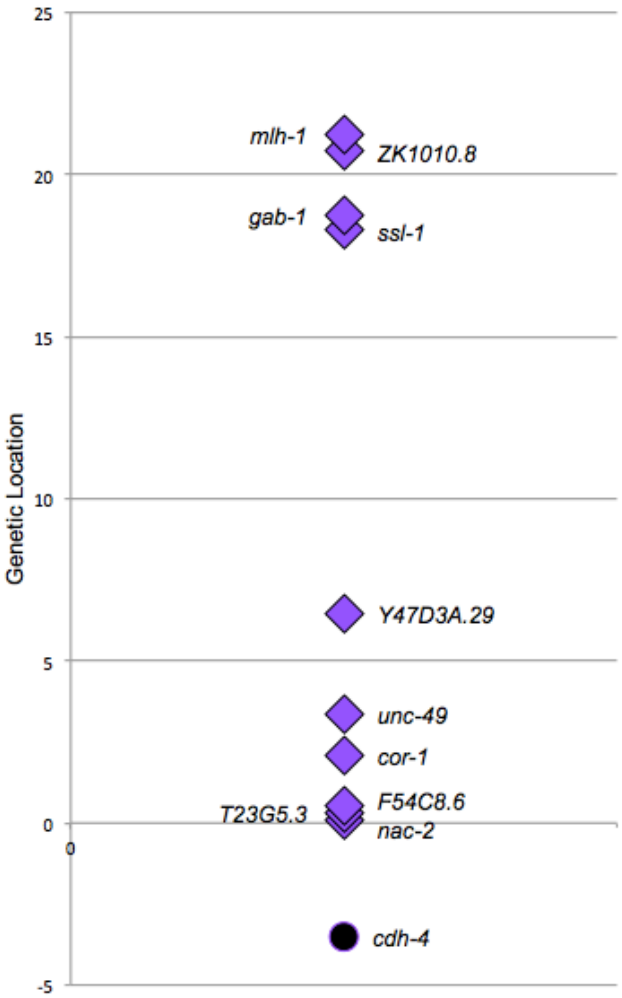

Figure 3.6 Genetic location of the genes with mutations in *hd160* revealed by WGS on chromosome III.

The purple diamonds are the genetic locations of the genes. The black circle is the genetic location for *cdh-4* gene, which was included for reference.

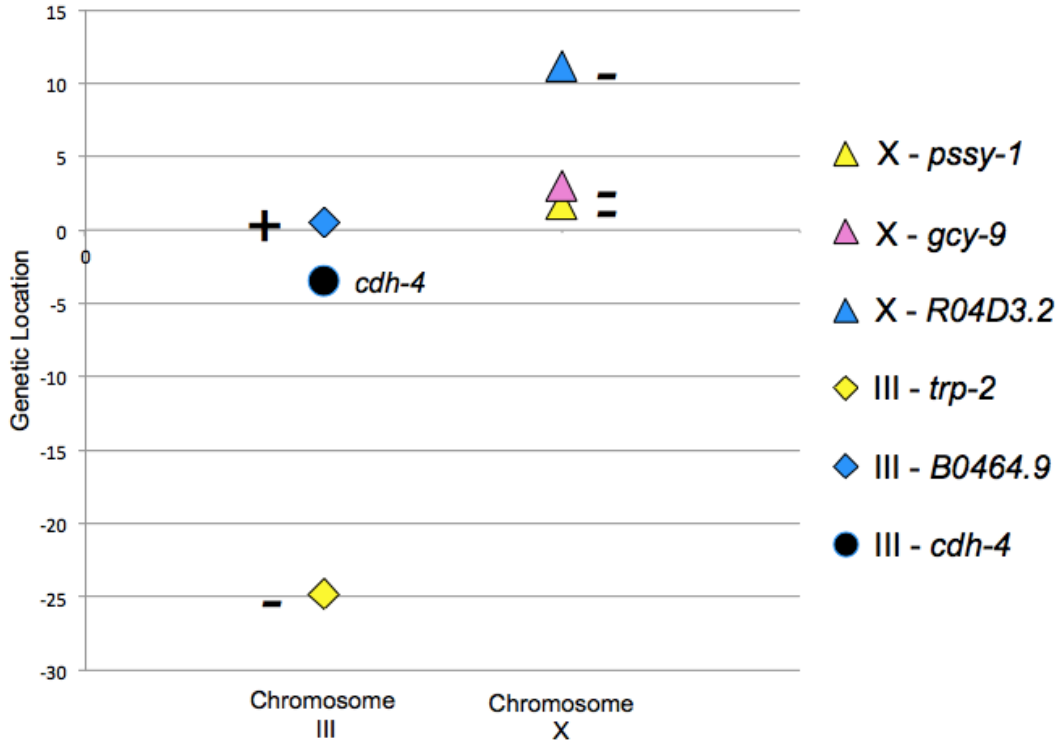

Figure 3.7 SNP mapping chromosomes III and X in an F2 informative recombinant line produced from crossing *hd161* suppressor with *hdIs26*, displaying suppression of DNC defects (16.5%).

The diamonds are genetic locations of genes on chromosome III that bear mutations in *hd161*. The order of genes on graph from most positive to most negative genetic locations is *B0464.9, trp-2*. The triangles are genetic locations of genes on chromosome X bearing mutations in *hd161*. The order of genes on X is *R04D3.2, gcy-9, pssy-1.* The circle is genetic location of *cdh-4* gene. The (+) sign refers to the presence of the mutation, while the (-) sign refers to the absence of the mutation in the recombinant.

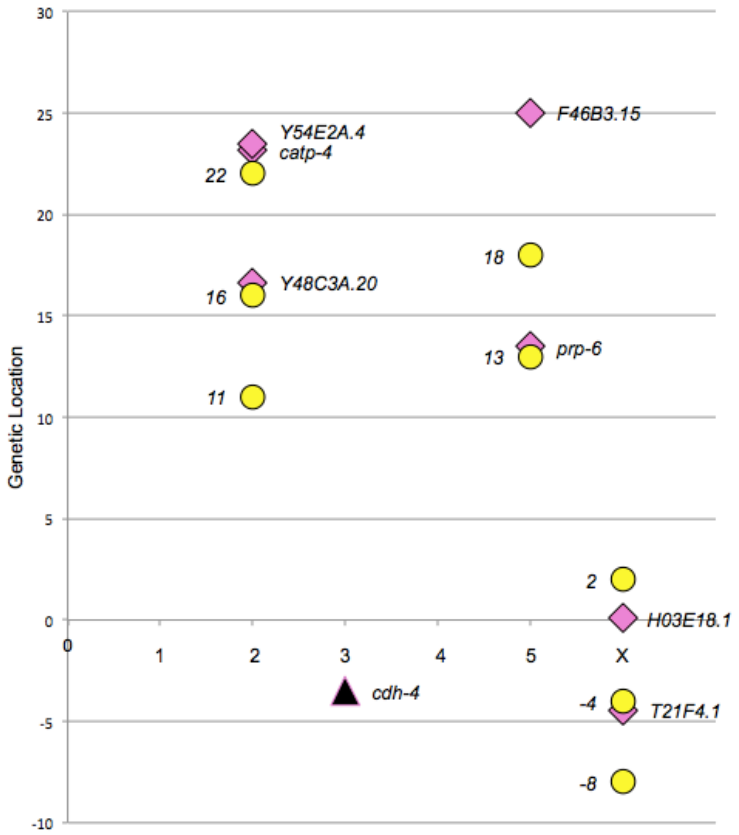

Figure 3.8 Genetic locations of the tested Hawaiian SNPs in relation to the mutations in *hd170* on chromosomes II, V, and X.

The yellow circle refers to the genetic location of tested SNP. The pink diamonds are genetic locations of the mutations in coding regions in *hd170* that were revealed by WGS. The black triangle is the genetic location of *cdh-4*.

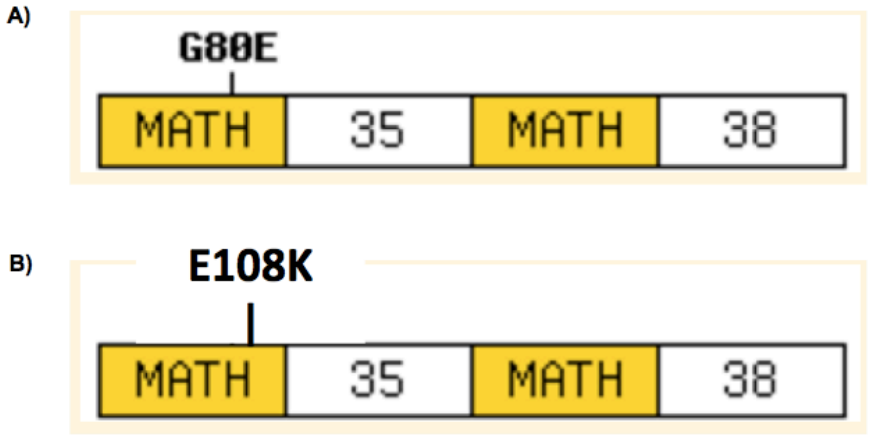

Figure 3.9 Location of missense mutation in *math-48* between *hd158* and *gk553779*.

A) The *gk553779* allele results an amino acid change from glycine to glutamic acid at the amino acid position 80 in the Math domain. B) *hd158* allele results in an amino acid change from glutamic acid to lysine at amino acid position 108 within the Math domain. Math: Math (Meprin and TRAF homology related) domain.

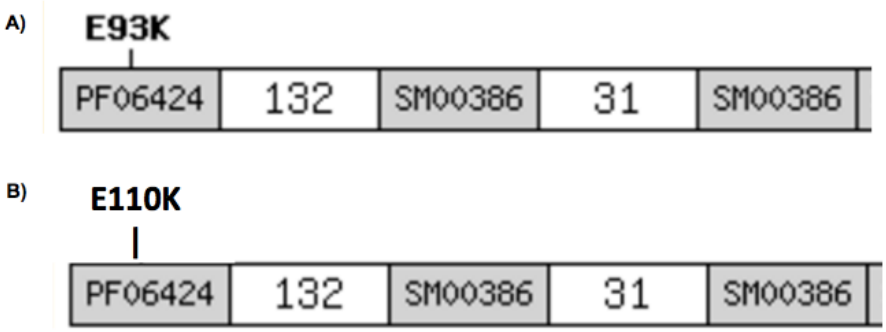

Figure 3.10 Location of missense mutation in *prp-6* in *hd170* and *gk527875*.

Both mutations result in the same amino acid change in PRP-6, that is a change from glutamic acid to lysine. A) *gk527875* affects the glutamic acid at position 93 B) *hd170* affects the glutamic acid at position 103. Only a portion of the protein from the N terminus is shown. PF06424: PRP1 splicing factor, a domain specific to N-terminus and involved in mRNA splicing. SM00386: HAT (Half-A-TPR) repeat domain is characterized by having a repetitive pattern of three aromatic residues with a conserved spacing and is commonly found in RNA-binding proteins.

3.5. Tables

Table 3.1 Axon guidance defects in DNC and VNC in suppressor candidates of *cdh-4(hd40)* mutants

Strain*	DNC Defasciculation % (n)	VNC Crossover % (n)
hd169	24 (105)	19 (106)
hd168	19 (105)	21 (109)
hd174	39 (120)	21 (113)
hd167	32 (105)	23 (128)
prp-6(hd170)	27 (109)	24 (100)
hd162	28 (120)	25 (106)
hd171	35 (114)	25 (100)
hd172	29 (103)	25 (107)
hd173	37 (124)	28 (109)
hd160	26 (135)	29 (101)
math-48(hd158)	23 (134)	29 (112)
prp-8(hd161)	18 (101)	30 (100)
hd163	25 (106)	33 (100)
cdh-4(hd40)	53 (100)	50 (100)

* All suppressor strains are in the *cdh-4(hd40)III; evIs111 V* background

Table 3.2 Axon guidance defects in the ventral cord (% animals with defects) (Schmitz et al. 2008)

Allele	Ventral cord	Dorsal cord	Interneuron Ventral cord defects	Interneuron Lateral axons	PVPR	PVQL
Wild type	4	5	3	2	11	11
cdh-4(hd40)[a]	51**	54**	39**	58**	33**	34**
cdh-4(hd13)	56**	63**	29**	41**	28**	33**
cdh-4(rh310)	37**	68**	20**	23**	75**	61**

$n \geq 100$ for all data points; markers used: *evIs111* (ventral cord/dorsal cord), *rhIs4* (Interneuron), *hdIs26* (AVG, PVP, PVQ); no significant defects were found for AVG, PVPL and PVQR axon navigation in any of the mutants.

Table 3.3 Lethality assay of *cdh-4(hd40)* suppressors

Strain*	No. of eggs/P0	% Lethality
hd167	154	44
prp-8(hd161)	57	53
hd163	119	54
hd174	105	58
hd172	81	65
prp-6(hd170)	166	67
hd162	99	68
math-48(hd158)	129	80
hd173	99	82
hd160	126	86
hd169	135	86
hd168	163	90
hd171	123	91
Wild type (N2)	315	0
cdh-4(hd40)	62	76

P0 laid eggs over 2 days, starting with L4 as day 0
N2 P0 n = 5, *hd40* & suppressors P0 n = 10-12
*All Suppressor are in the *cdh-4(hd40)* background

Table 3.4 Q-cell migration defects in *cdh-4(hd40)* suppressors

Strain**	Q-cell migration defects % (n)	
	QR	QL
*math-48(hd158)**	25 (107)	71 (100)
*hd160**	11 (101)	89 (101)
*prp-8(hd161)**	22 (102)	78 (103)
*hd162**	9 (55)	95 (58)
*hd163**	24 (100)	84 (100)
*prp-6(hd170)**	20 (100)	83 (150)
cdh-4(hd40)	5 (100)	95 (105)

*all suppressors are in the *cdh-4(hd40)* background
**all strains are in the *evIs111* background

Table 3.5 Whole genome sequencing results of mutations in coding regions for the *cdh-4(hd40)* suppressor *hd158*

Chromosome	Physical location	Base pair change		Gene name	Type of mutation	Amino acid change
I	11311907	C	T	*H25P06.1*	missense	A->T
II	1944797	C	T	*math-48*	missense	E->K
II	2312135	C	T	*B0281.8*	missense	G->E
II	3407181	GCCCC	GCCC	*F18A12.3*	frameshift	
II	4492718	C	T	*camt-1*	missense	A->T
II	5008576	G	A	*F59A6.3*	missense	R->H
II	5139876	C	T	*nas-29*	missense	E->K
II	5468952	G	A	*clr-1*	missense	E->K
II	8578110	C	A	*F54C9.9*	missense	Q->K
II	8668812	A	C	*D2085.4*	missense	T->P
II	9643718	C	T	*fzr-1*	missense	G->S
II	11696304	C	T	*C47D12.8*	missense	A->V
II	12313286	G	A	*sre-51*	splicing	
II	12791283	C	T	*cpt-1*	missense	A->T
II	13416597	G	A	*Y48E1C.1*	missense	M->I
II	13560844	C	T	*Y48E1B.3*	missense	G->E
II	13896590	C	T	*mcd-1*	missense	A->V
III	5450919	C	T	*paa-1*	missense	T->M
III	5675708	G	A	*par-3*	missense	A->T
III	7461449	C	T	*mls-1*	missense	P->L
III	8539263	A	C	*trp-1*	missense	M->L
III	8889012	G	A	*ZK637.14*	missense	S->L
III	10788105	G	A	*ptr-19*	missense	E->K
III	12431213	C	T	*Y49E10.16*	missense	P->L
IV	2087084	A	C	*mca-2*	missense	E->A
IV	2355183	G	T	*Y38F2AR.6*	missense	V->F
V	7399936	G	A	*cnc-9*	missense	P->S
X	4601988	T	C	*spat-3*	missense	R->G

Table 3.6 Whole genome sequencing results of mutations in coding regions for the *cdh-4(hd40)* suppressor *hd160*

Chromosome	Physical location	Base pair change		Gene name	Type of mutation	Amino acid change
I	11999960	C	A	Y53C10A.5	missense	L->I
II	3336311	T	C	F14D2.19	missense	I->V
II	3583360	C	T	srh-59	missense	S->F
II	4220852	T	A	F31D5.1	missense	S->T
II	5012055	A	T	F59A6.12	start_ATG	M->K
II	11696002	A	C	kel-1	readthrough	*->S
II	11909518	G	A	ZK930.1	missense	P->L
III	9040631	C	T	nac-2	missense	D->N
III	9230064	C	T	T23G5.3	splicing	
III	9449790	C	T	F54C8.6	missense	V->I
III	10252631	C	T	cor-1	missense	R->C
III	10528759	C	T	unc-49	nonsense	R->*
III	11144560	G	A	Y47D3A.29	missense	G->E
III	12727683	G	A	ssl-1	missense	A->T
III	12773731	C	T	gab-1	missense	R->H
III	13000152	C	T	ZK1010.8	missense	A->T
III	13511204	C	T	mlh-1	missense	G->D
IV	17010795	G	A	rom-4	missense	A->T

Table 3.7 Whole genome sequencing results of mutations in coding regions for the *cdh-4(hd40)* suppressor *hd161*

Chromosome	Physical location	Base pair change		Gene name	Type of mutation	Amino acid change
I	349357	C	T	*Y48G1A.1*	missense	R->W
I	2010098	C	A	*gap-3*	missense	G->C
I	7850585	G	T	*taf-5*	missense	V->F
I	10195454	G	A	*aha-1*	missense	R->C
II	11444484	C	A	*adbp-1*	missense	A->E
III	997529	G	T	*trp-2*	missense	L->F
III	3657499	C	A	*C46F11.5*	start_ATG	M->I
III	7179388	C	A	*rps-14*	missense	G->V
III	8168133	G	A	*prp-8*	missense	R->K
III	8187771	G	A	*C50C3.2*	missense	E->K
III	8489037	G	A	*ess-2*	missense	P->L
III	9466758	G	A	*B0464.9*	missense	C->Y
IV	1246225	G	A	*clec-165*	missense	S->F
IV	13247306	T	C	*JC8.7*	missense	S->P
V	1583726	G	A	*cdc-25.2*	missense	E->K
V	2208754	G	T	*Y5H2B.1*	nonsense	E->*
V	2999750	G	T	*srw-119*	missense	N->K
V	2999752	T	C	*srw-119*	missense	N->D
V	10703478	G	T	*pph-1*	nonsense	G->*
V	18620020	G	C	*nhr-70*	missense	E->Q
X	5074103	A	T	*C24H10.1*	missense	I->F
X	9721614	G	A	*him-4*	missense	G->E
X	9967023	G	A	*pssy-1*	missense	E->K
X	11337278	G	A	*gcy-9*	missense	P->L
X	11946708	T	A	*nfya-1*	missense	K->M
X	12745925	G	T	*pgp-14*	missense	A->E
X	13285301	A	G	*R04D3.2*	missense	I->T
X	13984570	G	A	*C31E10.1*	missense	A->V

Table 3.8 Whole genome sequencing results of mutations in coding regions for the *cdh-4(hd40)* suppressor *hd162*

Chromosome	Physical location	Base pair change		Gene name	Type of mutation	Amino acid change
I	14819325	C	T	Y54E5B.2	missense	G->D
III	12253611	C	T	Y75B8A.24	missense	G->E
III	12275957	C	T	Y75B8A.25	missense	P->L

Table 3.9 Whole genome sequencing results of mutations in coding regions for the *cdh-4(hd40)* suppressor *hd163*

Chromosome	Physical location	Base pair change		Gene name	Type of mutation	Amino acid change
I	743074	G	A	*col-46*	missense	P->L
III	1688193	T	C	*Y22D7AR.14*	missense	N->S

Table 3.10 Whole genome sequencing results of mutations in coding regions for the *cdh-4(hd40)* suppressor *hd170*

Chromosome	Physical location	Base pair change		Gene name	Type of mutation	Amino acid change
II	13370666	G	A	*Y48C3A.20*	missense	G->E
II	14594901	G	A	*catp-4*	missense	R->H
II	14776688	G	A	*Y54E2A.4*	missense	A->T
V	18024067	G	A	*prp-6*	missense	E->K
V	20633364	C	T	*F46B3.15*	missense	G->R
X	5630985	C	T	*T21F4.1*	missense	P->L
X	8510033	C	T	*H03E18.1*	missense	T->I

Table 3.11 Testing for presence of *cdh-4(hd40)* suppressor gene on chromosome III

Suppressor Strain*	Total no. of animals	No. of animal with suppressor [1]	% Suppressor	Chromosome
hd158	22	7	32	Not III
hd160	20	15	75	III
hd161	15	8	60	III
hd163	18	16	89	III

[1] presence of suppressor was based on results from a starvation assay
Suppressor = 15 days or less to starve a plate
No Suppressor = No starvation within 3 week
* All suppressor are in the *cdh-4(hd40)* and *evIs111* background

Table 3.12 Scoring for DNC suppression in informative recombinants for *hd158* crossed with *hdIs26*

Recombinant line	Presence/absence of mutation in gene			DNC%	Suppressor
	mcd-1	*clr-1*	*B0281.8*		
1	absent	present	present	25	present
2	present	present	absent	53	absent
3	absent	present	absent	54	absent

Table 3.13 Scoring for DNC suppression in informative Hawaiian recombinants for *hd158*

Recombinant line	Presence of hawaiian/bristol SNP at specified genetic location				DNC%	Suppressor
	0.1	-6	-7.6	-14		
1	B	H	NA	H	50	absent
2	H	H	H	B	30	present
3	B	B	NA	H	54	absent

B=Bristol SNP background
H=Hawaiian SNP background

Table 3.14 Common mutations between *cdh-4(hd40*) suppressors and *cdh-4(hd40)*

Suppressor strain*	Gene	Base pair change (wild type/variant)	Chromosome
hd158	*B0281.8*	C/T	II
hd170	*F46B3.15*	C/T	V

*Strains are in the *cdh-4(hd40)* and *evIs111* backgrounds

Table 3.15 Scoring for DNC suppression in informative recombinant for *hd160* crossed with *hdIs26*

Presence/absence of mutation in gene			DNC%	Suppressor
ZK1010.8	*cor-1*	*nac-2*		
absent	present	present	25	present

Table 3.16 Scoring for DNC suppression in informative recombinants for *hd161*

Recombinant F2 line	Presence/absence of mutation in gene			DNC%	Suppressor
	B0464.9	***prp-8***	***trp-2***		
hd161 x hawaiian	absent	absent	NA	50	absent
hd161 x hdIs26	present	NA	absent	16.5	present

NA=Not Applicable

Table 3.17 Scoring for DNC suppression in an informative Hawaiian recombinants on chromosome X for *hd161*

Presence of hawaiian/bristol SNP at specified genetic location			DNC%	Suppressor
2	**-8**	**-4**		
H	H	H	18	present

B=Bristol SNP background
H=Hawaiian SNP background

Table 3.18 Scoring for DNC suppression in informative recombinants for *hd162* crossed with *hdIs26*

Recombinant line	Presence/absence of mutation in gene (chromosome)			DNC% (n)	Suppressor
	Y54E5B.2 (I)	***Y75B8A.25 (III)***	***Y75B8A.24 (III)***		
1	absent	absent	absent	27 (111)	present
2	absent	absent	NA	53 (110)	absent

Table 3.19 Scoring for DNC suppression in informative recombinants for *hd163* crossed with *hdIs26*

Recombinant line	Presence/absence of mutation in gene (chromosome)	DNC% (n)	Suppressor
	Y22D7AR.14 (III)		
1	absent	31 (106)	present
2	absent	25 (106)	present

Table 3.20 Scoring for DNC suppression in informative hawaiian recombinants for *hd170*

Recombinant line	Presence of hawaiian/bristol SNP at specified genetic location (Chromosome)								DNC%	Suppressor
	11 (II)	16 (II)	22 (II)	13 (V)	18 (V)	-8 (X)	-4 (X)	2 (X)		
1	B	B/H	H	B	B	H	H	H	19	present
2	B	H	H	B	B	B	B	B/H	25	present
3	B/H	B/H	B/H	B	B	H	H	H	33	present

B=Bristol SNP background
H=Hawaiian SNP background

Table 3.21 Scoring for DNC suppression in informative hawaiian recombinants on chromosome V for *hd170*

Recombinant line	Presence of hawaiian/bristol SNP at specified genetic location				DNC% (n)	Suppressor
	25.1	18	16.8	13		
1*	H	H	H	H	50 (100)	absent
2**	H	H	H	B	24.5 (101)	present
3**	B	H	NA	B	30 (100)	present

B=Bristol SNP background
H=Hawaiian SNP background
*Both missense mutations in *F46B3.15* and *prp-6* were absent
**the missense mutation for *F46B3.15* was absent, while present for *prp-6*

Table 3.22 Testing for suppression of axon guidance defects in *hd40; math48 (gk553779)* via scoring DNC and VNC defects

Strain*	DNC % (n)	VNC % (n)
cdh-4(hd40); math-48 (gk553779)	25 (119)	24 (101)
cdh-4(hd40); hd158	23 (134)	29 (112)
cdh-4 (hd40)	53 (100)	50 (100)

* All strains were in the *evIs111* background

Table 3.23 Testing for presence of the missense mutation in *cdh-4(hd40); math-48(gk553779)*

Strain*	[1]Presence of *math-48(gk553779)* point mutation	[2]Presence of *hd158* point mutation
cdh-4(hd40); math-48 (gk553779)	present	absent
cdh-4(hd40); hd158	absent	present
cdh-4 (hd40)	absent	absent

* All strains were in the *evIs111* background
[1]missense mutation (wild type/variant) = C/T
[2]missense mutation (wild type/variant) = C/T

Table 3.24 Testing for suppression of axon guidance defects in *hd40; prp-6(gk527875)* via scoring DNC defects

Strain	DNC % (n)
cdh-4(hd40); prp-6 (gk527875)*	25 (107)
cdh-4(hd40)**	50 (100)
cdh-4(hd40); hd170**	27 (109)

*Strain was in the *hdIs36* (red pan-neuronal marker) background
**Strain was in the *evIs111* (green pan-neuronal marker) background

Table 3.25 Testing for rescue of axon guidance defects in *hd161* with a *prp-8(+)* transgene via scoring for DNC defects

Strain*	Presence of *prp-8* transgene	DNC % (n)
Line 1	Transgene	51 (103)
	No Transgene	27 (110)
Line 2	Transgene	56 (101)
	No Transgene	29 (112)
cdh-4(hd40)	NA	53 (100)
cdh-4(hd40); hd161	NA	26 (101)

* all strains were in the *evIs111* background

Chapter 4.

Discussions

4.1. Role of cadherins in axonal navigation

The CDH-4 protein consists of three major domains. It has a highly conserved extracellular domain containing a large number of cadherin repeats (33-34 repeats), laminin A globular and EGF-like domains, and a non-conserved intracellular domain (Schmitz *et al.* 2008). Classical cadherins are the best understood members of the cadherin superfamily of metazoans. They function in homophilic cell-cell adhesion, mediated by the cadherin domains (Patel *et al.* 2003). Linking the intracellular domain of classical cadherin to actin cytoskeleton facilitates this cell-cell interaction (Nagar *et al.* 1996; Oda and Takeichi 2011) During embryo development, these cadherins are found in apical junctions of epithelial cells of both vertebrates and invertebrates (Costa *et al.* 1998), while in *C. elegans* they are found in neurons as well (Broadbent and Pettitt 2002). In *C. elegans*, HMR-1B, an isoform of classical cadherin confined to neurons, functions in axon guidance for a subset of motor neurons in VNC and DNC by stabilizing the interactions between the growth cone and the substrate for axonal growth during embryogenesis (Broadbent and Pettitt 2002). In wild type, DNC axons are tightly bundled and VNC axons form two asymmetrical tracts with more axons on the right side. Mutants of *hmr-1b* exhibit DNC defasciculation and axonal crossover from right to left VNC tract. These axonal guidance defects are similar to *cdh-4* mutant phenotypes (Schmitz *et al.* 2008); thus, CDH-4 could be functioning as an adhesion molecule in a similar fashion. Also, around 80% of *cdh-4* mutant animals do not survive to the adult stage due to improper elongation of cells during embryogenesis, resulting in disorganized tissues, or due to detachment of pharynx from mouth, preventing the animal from feeding (Schmitz *et al.* 2008). These phenotypes are likely the result of losing the cell-cell contacts, and thus suggesting that CDH-4 is acting as an adhesion molecule, and possibly in a homophilic type of interaction in this case. Therefore, the *cdh-4* suppressors could act as adhesion molecules that partially compensate for the loss of CDH-4, activating an alternate pathway for axon guidance. This might be the

case in the *prp-8(hd161)* strain because the animals showed suppression of DNC and VNC defects and of lethality.

Fat cadherins are conserved across species from invertebrates, such as *Drosophila,* having two: Fat and Fat2, to vertebrates, having four: Fat1-3 and Fat-J (Tanoue and Takeichi 2005). In *Drosophila*, Fat has been implicated in PCP (planar cell polarity) and guiding cell migrations (Horne-Badovinac 2017). In *Drosophila* eyes, there are a group of cells in the ommatidia that are polarized along the dorsal-ventral axis in the plane of the epithelium, and in the *fat* mutants, the polarity is reversed (Yang *et al.* 2002). The *Drosophila* Fat proteins have not been studied with regards to nervous system development but they are widely expressed in neurons (Zartman *et al.* 2009). In mice, Fat1 and Fat4 have been implicated in regulating PCP during kidney development (Tanoue and Takeichi 2004; Saburi *et al.* 2008) and Fat3 in PCP for retinal development (Krol *et al.* 2016). In *C. elegans*, CDH-4 functions in polarization and migration of the Q neuroblast cells (Schmitz *et al.* 2008). The tested suppressors are unlikely to be involved in Q cell migration since none of them showed rescue of Q cell migration defects.

In mice, Fat1 regulates cell-cell adhesion at epithelial cell junctions associated with actin-filaments and regulates organization of actin-cytoskeleton at cell boundaries (Tanoue and Takeichi 2004). Fat1 controls actin cytoskeleton dynamics through the Ena/VASP proteins, which is suggested to be a downstream effector of Fat1. Similarly, Fat3 has been implicated in actin filament polarization and assembly towards cell peripheries via the Ena/VASP system in neuronal cells within the mouse retina (Krol *et al.* 2016). The Ena/VASP system is linked to Fat1 and Fat3 through a EVH1 mediated-interaction domain within their cytoplasmic domain. CDH-4 contains a EVH1 binding site within the intracellular domain, thus suggesting a role of *cdh-4* in regulating actin cytoskeleton dynamics and its association with cell-cell adhesion and cell polarity (Schmitz *et al.* 2008). Suppressors of *cdh-4* mutants could be components of ENA/VASP signaling or molecules that interact with ENA/VASP proteins to mediate organization of cytoskeleton arrangements to facilitate cell-cell adhesion, so that DNC axons remain bundled and VNC axons remain in the right axon tract. Overall, the six suppressors that have been studied in detail in this thesis (*math-48*(*hd158), hd160, prp-8(hd161), hd162, hd163,* and *prp-6(hd170)*) are likely to be involved in cell-cell adhesion through regulating actin-cytoskeleton dynamics and less likely in cell polarity.

4.2. Identification of *cdh-4* suppressor candidate gene required gene mapping in addition to WGS

A genetic suppressor screen was used in a *cdh-4* mutant background to create mutants in genes within the *cdh-4* pathway or in genes that interact with components of the pathway. Various background mutations exist in those lines as a result of the mutagenesis. The traditional approach to identifying the phenotype-causing mutation involves a time-consuming strategy known as SNP (single nucleotide polymorphism) mapping. SNP mapping narrows down the location of a mutation within the genome (Zuryn and Jarriault 2013). The strategy includes setting up a cross between the mutant strain and a strain with known identifiable SNPs; in the F2 generation, 25% of progeny would be homozygous for the mutation of interest and hence display the mutant phenotype. This is under the assumption that the mutation is not dominant or a maternal-effect gene. The modern approach to identifying causal mutation generated from forward mutagenesis screening employs simultaneous mapping and then whole genome sequencing (WGS). This methodology includes outcrossing with a wild type strain in order to create recombinants with wild type alleles, and thus eliminating mutations unrelated to the phenotype (Zuryn and Jarriault 2013). According to studies in *C. elegans*, outcrossing at least three to four times with wild type strain and perform WGS afterwards should be sufficient enough to reveal the identity of the mutation causing phenotype in the mutant strain (Zuryn and Jarriault 2013; Hu 2014). Surprisingly, that was not the case when attempting to identify the suppressor in the *cdh-4* mutants. Five of the suppressors sent for WGS were outcrossed four times (*math-48(hd158), hd160, prp-8(hd161), hd163*, and *prp-6(hd170)*), and *hd162* was outcrossed three times. The WGS data did not pinpoint the suppressor gene in any of these suppressor strains, since background mutations were still apparent on every chromosome, and thus the traditional SNP mapping approach was mandated.

4.3. Relation between *cdh-4* mutants and the *cdh-4* mutant suppressors

4.3.1. Suppression of Axon guidance and Q-neuroblasts migration defects

In the *cdh-4(hd40)* mutants, the VNC crossovers, and DNC defasciculation defects had each around 50% penetrance. Thirteen suppressors were scored for suppression of both DNC and VNC defects. Suppression of VNC defects ranged from 19% to 33%, while suppression of DNC defects ranged from 18% to 37%. *hd169* was the most and *hd163* was the least effective suppressor of VNC defects. *hd161* showed the best suppression of DNC defects, and *hd173* the least. It does not appear that there is an obvious correlation between the VNC and DNC suppression in most of the strains. This may suggest that the suppressor functions differently for axons in the VNC and DNC. The lack of correlation may imply that separate pathways control guidance of axons in VNC and DNC, and that CDH-4 activates multiple pathways. In *hd174* for example, the VNC defects (21%) are more suppressed than the DNC defects (39%), suggesting that the suppressor gene is likely to be more involved in navigation of VNC axons, preventing VNC crossovers, and less involved in DNC fasciculation. However, in strains like *hd168*, *prp-6(hd170)*, *hd162*, *hd172*, and *hd160*, the difference between the VNC and DNC scoring ranges from 2-4%, suggesting that in these the suppressor gene is likely to be involved in DNC and VNC axon navigation.

Q neuroblasts and their descendants are cells that migrate to defined positions along the anterior-posterior axis of the animal, with right side Q-cells (QR) migrating anteriorly and left side Q-cells (QL) posteriorly, differentiating into interneurons and sensory neurons (Sulston and Horvitz 1977). The mechanism to establish the polarization of these Q cells is fairly complex as it involves multiple signaling pathways such as components of canonical Wnt/B-catenin and the *cdh-4* pathway, and separate mechanisms between migration of QL and QR cells. *cdh-4* mutants exhibit Q-cell polarity defects (Schmitz *et al.* 2008), causing the QL cells to mismigrate anteriorly, suggesting that CDH-4 is mainly involved in polarization of the QL cells. Four of the six suppressor strains that were checked for suppression (*math-48(hd158), prp-8(hd161), hd163,* and *prp-6(hd170)*) had Q-cell polarity defects in right and left Q cells, while the Q cell migration defects in *hd160* and *hd162* were similar to those in *cdh-4*. Surprisingly, the

suppressor strains, except for *hd160* and *hd162*, exhibited enhanced migration defects of QR cells when compared to that in *cdh-4* mutant. It is likely that this enhancement could be due to other mutation(s) in genes involved in anterior migration or in initial steps of Q cells polarization. Overall, in these strains the suppressor may not have a direct role in neuronal cell polarization. Unlike *cdh-4* having multiple diverse functions within neurons and non-neuronal cells, these suppressors appear to have less diverse and more specific roles towards axon navigation.

4.3.2. Suppression of lethality and relation to axon guidance

The *cdh-4* mutants show 24% survival, producing an average of 62 eggs per animal, while 100% survival and an average of 315 eggs per animal is typical in wild type. Initially, suppressors of *cdh-4* were screened for growing better than the *cdh-4* mutants. This screening was based on the time in which a worm and its progeny depleted the food on a plate. One of the causes of lethality in the *cdh-4* mutants is due to elongation defects at the two fold-stage of the embryo. The embryo fails to elongate properly likely due to the absence of the CDH-4 adhesion molecules that would be required to hold the tissues together. At the larval stage, some worms show detachment of the pharynx from the mouth, preventing the worm from feeding. This tissue detachment phenotype is likely due an adhesion defect. Morphological defects, such as bulges, are observed at both embryonic and larval stages of the worm, leading to lethality. To assess for suppression of these defects, the *cdh-4* mutant suppressors were phenotyped for suppression of lethality. From the characterized suppressors, *prp-8(hd161)* showed partial suppression of lethality and produced a number of eggs similar to what is produced by the *cdh-4* mutants. Therefore, survival of the worm was improved in this strain. Partial loss-of-function of *prp-8* causes up-regulation of several genes and one of these genes is *cdh-5* (Rubio-Peña *et al.* 2015), a gene encoding a cadherin. An overexpression of *cdh-5* may compensate for the loss of *cdh-4* function and thus suppress adhesion defects causing the lethality. *hd167* and *hd163* also exhibit partial suppression of lethality with increased number of eggs produced in comparison to the *cdh-4* mutants; however, the suppressor has not been identified yet. Mild suppression of lethality was seen in *hd174*, *hd172*, and *prp-6(hd170)*, and no suppression of lethality in the rest of the suppressors. The number of eggs produced by these suppressors, ranging from 81 to 166 per worm, was higher than that produced by the *cdh-4* mutants.

The suppressor in these strains does not appear to be improving the adhesion defects and hence survival, but rather improving the number of egg laying to produce more progeny and thus increasing the number of animals surviving until adult stage.

4.3.3. Suppression of movement defects and relation to axon guidance

cdh-4 mutants exhibit movement defects apparent by their slow movement on a culture plate and the lack of coordinated movement in a swimming assay. Since *cdh-4* mutant animals have defects in motor neuron axons in the DNC and VNC, the animals would be expected to experience movement defects as well. Five suppressors, in which the axon guidance defects in the VNC and DNC were partially suppressed, were assessed for swimming movement qualitatively and quantitatively. Three out of the five suppressors (*hd160*, *prp-8(hd161)* and *hd163*) did not exhibit suppression of movement defects, failing to show correlation between axon guidance defects in the motor neurons to defects in movement. The suppressors that showed suppression of movement defects were *math-48(hd158)* and *prp-6(hd170).*

To produce coordinated movement, neuromuscular junctions (NJMs) are formed between body wall muscles and both cholinergic (excitatory) and GABAergic (inhibitory) motor neurons (White *et al.* 1986; Hall and Russell 1991). *cdh-4* has been shown to be within the same genetic pathway as *fmi-1*, a Flamingo-like cadherin that functions cell non-automatously in patterning of GABAergic NJMs (Najarro *et al.* 2012). *cdh-4* is implicated in synapse development of GABAergic motor neurons as both *fmi-1* and *cdh-4* single mutants had similar synaptic defects and no defect enhancement in the *fmi-1; cdh-4* double mutants (Najarro *et al.* 2012). *cdh-4*, unlike *fmi-1*, is expressed in GABAergic motor neurons, suggesting that CDH-4 is likely the candidate receptor for FMI-1 for regulating synapse formation in GABAergic neuron development (Ackley Brian D. 2013). Therefore, it is possible for *math-48(hd158)* and genes affected by *prp-6(hd170)* to be functioning downstream of the *fmi-1* and *cdh-4* genetic pathway in synapse development, in addition to axon guidance. As for the suppressors in *hd160, prp-8(hd161),* and *hd163* strains, they are likely to be involved in the axon navigation process but not synapse formation. Hence, the lack of suppression of movement defects in these strains is likely due to failing to recognize and properly synapse with the muscle cells that produce muscle contraction in the dorsal and ventral directions. Since the VNC

and DNC defects were suppressed in these strains, the suppressors would then have to be involved in either the *cdh-4* pathway or in parallel pathway that is also involved in controlling the actin-filament dynamics of axons. Taken together, there is no strong correlation between suppression of axon guidance defects and suppression of movement defects, indicating the pathway for axon guidance is not likely to be the same as for development of synapses.

4.4. What is known about *math-48*

One of the identified suppressors was *math-48*. In *C. elegans*, there are approximately 110 genes with a MATH domain (Thomas 2006). The genes are named *math* after the MATH domain they all contain. Five of the MATH proteins have other domains in addition to the MATH domains, such as a ubiquitin domain, F-box domain, and a transmembrane domain. *math-48* specifically does not contain any additional domains other than the MATH domain (Hutter *et al.* 2009; Harris *et al.* 2010). *math-48* expression in the embryo peaks during early embryogenesis, but *math-48* is still expressed at the time when axons grow out. MATH-48 is functionally uncharacterized.

MATH stands for meprin-associated Traf (Thomas 2006) homology domain containing. Meprin is a metalloprotease that has roles in inflammation, induction of extracellular matrix assembly and fibrosis, and also involved pathologically in cancer progression (Prox *et al.* 2015). *meprin* encodes alpha and/or beta subunits. Meprin alpha subunit is the secreted form of the protein, while the meprin beta subunit is associated with the plasma membrane. Traf stands for TNF (Tumor Necrosis Factor: cytokine receptors) receptor associated factor and these intracellular proteins are involved in apoptosis and regulation of inflammation.

The MATH domain is a protein-protein interacting domain (Thomas 2006; Xie and Roy 2012). The MATH domain of TRAF holds the protein-binding cleft. It was suggested that in *C. elegans* the large number of proteins with MATH domains was due to their ability to bind to a variety of different protein-binding partners (Thomas 2006). *math-48* could be an inhibitor downstream of *cdh-4* pathway. The mutation in *math-48* may cause a partial loss of function that leads to partial activation of the *cdh-4* pathway. The other possibility is that the mutation causes a gain of function. In this case, *math-48* could be a downstream activator of *cdh-4* pathway or activating a parallel pathway that

bypasses a requirement for CDH-4. Further studies on *math-48* will be required to differentiate between these hypotheses.

4.5. PRP-6 and PRP-8 proteins are components of the active form of the spliceosome

Two of the identified suppressors, PRP-6 and PRP-8*,* are components of the spliceosome machinery (Maita *et al.* 2005; Liu *et al.* 2006). *prp-6* and *prp-8* are evolutionary conserved among metazoans and yeast (Fabrizio *et al.* 2009). The spliceosome removes introns from pre-processed mRNA. The core of the spliceosome consists of proteins and uridine-rich small nuclear RNAs complexes, thus forming small nuclear ribonucleoproteins (snRNPs). These snRNPs complexes are named U1, U2, U4, U5, and U6 (Maita *et al.* 2005; Liu *et al.* 2006). The spliceosome exists in two forms, the active and the inactive form (pre-spliceosome). In order to perform the splicing reaction, the spliceosome components have to be remodeled to convert a pre-spliceosome to an active spliceosome. The process of splicing involves the pre-spliceosome components U1 and U2 flanking an intron on each end close to the exons. The tri-snRNP complex (U4, U6, and U5) reassembles the spliceosome, thus eliminating U1 and U4 from the spliceosome complex. The maintained snRNAs components are U2, U5, and U6, creating the active spliceosome. Once the spliceosome is activated, the intron is removed and the two exons that were flanking the intron are joined together (Rubio-Peña *et al.* 2015). A dysfunctional spliceosome causes inefficiencies in splicing and transcriptional activities, as the two processes are coordinated (Das *et al.* 2007).

PRP-6 and PRP-8 are part of the U5 component, which is part of the active core of the spliceosome (Maita *et al.* 2005; Liu *et al.* 2006). The mutation in *prp-6(hd170)* is a missense mutation that causes an amino acid change from glutamic acid, which is negatively charged, to lysine, which is positively charged. *prp-8(hd161)* is also a missense mutation, causing an amino acid change from arginine (R) to lysine (K). Since complete loss-of function mutations in these genes are lethal (Rubio-Peña *et al.* 2015), the missense mutations in the suppressors most likely cause a partial loss-of-function that leads to splicing retention and/or transcriptional inefficiency. Alternatively, a dysfunctional spliceosome may lead to a shift in the prevalence of different splice variants of genes that have more than one splice variant. PRP8 and PRP6 have been implicated in affecting alternative splicing site choices when PRP8 is defective in cell

lines or depleted in mammalian cells (Tanackovic *et al.* 2011)n and when PRP6 is depleted in human cells (Moore *et al.* 2010).

Partial loss-of-function of *prp-6* and *prp-8* also leads to changes in the expression levels of 475 genes, 407 of which are up-regulated and the rest are down-regulated (Rubio-Peña *et al.* 2015). In the context of axon guidance, *prp-6* and *prp-8* mutations may cause either an increase in expression of a gene acting as an activator or a decrease in expression of an inhibitor downstream of the *cdh-4* pathway. Another possibility is the increase in expression of gene that activates an alternate pathway that holds the same function as the *cdh-4* pathway with respect to axon navigation. Bioinformatics analysis of the transcriptome of *prp-6(RNAi)* and *prp-8(RNAi)* animals revealed a list of misregulated genes (Rubio-Peña *et al.* 2015). Genes from the list that could affect *cdh-4* phenotypes are the overexpressed genes: *cdh-5, zig-4, grd-2, grl-5, grl-7, grl-15, grl-16* and *grl-22*.

Interestingly, both *prp-8(hd161)* and *prp-6(hd170)*, except for the partial suppression of axon guidance defects in *cdh-4* mutants, show distinct phenotypes: *prp-8(hd161)* demonstrated partial suppression of lethality, while *prp-6(hd170)* displayed partial suppression of movement defects. The list of up-regulated genes mentioned earlier showed differential overexpression of genes between *prp-6(RNAi)* and *prp-8(RNAi)* animals. For example, *cdh-5* showed higher overexpression in *prp-6* depleted than in *prp-8* depleted animals. These results may explain the discrepancy in phenotypes between *prp-6(hd170)* and *prp-8(hd161).* This would indicate that PRP-8 and PRP-6 hold different roles with regards to splicing machinery. PRP-6 has been implicated in stabilization of the spliceosome tri-snRNP complex (U4, U6, and U5) and PRP-8 in participation in the catalysis reaction and in recognition of the 5’ splice site (Will and Lührmann 2011).

cdh-5 encodes a cadherin and is functionally uncharacterized. The domain structure of CDH-5 is similar to that of CDH-4. Both CDH-5 and CDH-4 consist of a signal peptide, extracellular cadherin repeats, a transmembrane domain, and a cytoplasmic domain. The major difference between them is the length, with CDH-4 being almost three times larger than CDH-5. The protein length for CDH-5 is 1507 amino acids while CDH-4 is 4307 (Hill *et al.* 2001). Overexpression of *cdh-5* and hence increasing its levels could compensate for the loss of *cdh-4* and function either as an adhesion

molecule for DNC fasciculation or as a receptor for guiding axons in VNC. Partial suppression of movement defects was observed in the *prp-6* allele, *hd170*; therefore, since *cdh-5* is up-regulated in *prp-6(RNAi)* animals, *cdh-5* could be working together with *fmi-1* to regulate synapse development of motor neurons. This theory is under the assumption that *cdh-5* compensates for *cdh-4*. In order to test this hypothesis, transgenic strains overexpressing *cdh-5* could be generated. Enhancing levels of *cdh-5* should result in suppression of axon guidance defects of *cdh-4(hd40).*

zig-4 encodes a secreted immunoglobulin (Ig) domain protein that is involved in VNC maintenance and architecture; more specifically in axon positioning of PVQ and AVK neurons (Aurelio *et al.* 2002). ZIG-4 is secreted from PVT neurons but can function in a cell non-autonomous action. Knockout of *zig-4* results in VNC axon flip-over across the midline (Hobert and Bulow 2003), indicating that *zig-4* functions in fasciculating VNC axons (Bénard *et al.* 2009) to prevent midline crossing. It is not clear how ZIG-4 functions. However, due to the presence of Ig domains and its adhesive properties, ZIG-4 could be interacting with other Ig-domain containing proteins such as IgCAMs, which are cell surface adhesion molecules that are implicated in axon guidance, especially in the VNC (Schwarz *et al.* 2009). Therefore, an increase in *zig-4* levels could lead to inhibiting axonal crossovers in the VNC. To show whether *zig-4* is the gene causing the partial rescue in VNC axons, overexpression of *zig-4* in *cdh-4* mutants should result in suppression of *cdh-4* mutant defects or the loss of suppression of *prp-6(hd170)* and/or *prp-8(hd161)* in a *zig-4* mutant background.

grl (ground-like) genes and *grd-2* (Ground) are functionally uncharacterized. *grd* and *grl* genes encode secreted proteins containing a ground domain with conserved cysteine residues that are believed to from disulfide bonds. Both members share a common ancestral gene with each other and with the hedgehog gene in mice and *Drosophila* (Aspock *et al.* 1999). Sonic Hedgehog (S*hh*) acts as a chemoattractant guidance cue of distinct class of axons, known as commissural neuronal axons, towards ventral midline in mouse (Charron *et al.* 2003). Therefore, the *grd* and *grl* genes may function in a similar pathway as the *Hh* pathway. From the list of up-regulated genes (Rubio-Peña *et al.* 2015), there was one ground gene (*grd-2*), and five ground-like genes (*grl-5, grl-7, grl-15, grl-16* and *grl-22*). *grl-22* has been implicated in axon guidance, since depletion of *grl-22* resulted in commissural defects and in midline crossing defects within VNC (Schmitz *et al.* 2007). GRL-22 could be functioning as an attractive guidance cue,

under the assumption that GRL-22 has a conserved function with hedgehog, to guide VNC axons towards the correct VNC tract. Therefore, an overexpression of *grl-22* should rescue the VNC crossover defects in *cdh-4* mutants.

In order to check which of these genes is the suppressor(s), transgenic *cdh-4* mutants should be created with each of the genes mentioned above to check for overexpression rescuing effects of the *cdh-4* mutant phenotypes. These genes are up-regulated in both *prp-6* and *prp-8* depleted strains (Rubio-Peña *et al.* 2015). However, the *prp-6*(*hd170)* and *prp-8*(*hd161)* alleles do not share exact phenotypes, except for the partial suppression of axon guidance defects. *prp-6*(*hd170)* showed partial suppression of movement defects while *prp-8*(*hd161)* showed partial suppression of lethality. This indicates that the effects of the modified amino acids that are different in each of the PRP proteins cause differential up-regulation levels of genes between *prp-6* and *prp-8*. Therefore, it is possible that some of the genes leading to the suppression of various aspects of the *cdh-4* phenotype in *prp-8(hd161)* and *prp-6(hd170)* are different.

4.6. Conclusions

CDH-4 is involved in fasciculation of motor neurons of DNC and guidance of axons in the VNC, Q neuroblasts polarity and migration, and proper cell elongation during embryogenesis. A suppressor screen was carried on *cdh-4* mutants, identifying fifteen suppressors of *cdh-4* axon navigation defects. Thirteen of these suppresses were characterized for suppression of axon guidance defects, specifically the DNC defasciculation and VNC crossover defects, and suppression of lethality. Six of them (*hd158, hd160, prp-8(hd161), hd162, hd163,* and *prp-6(hd170)*) were evaluated for suppression of Q-cell migration and, except for *hd162*, for movement defects.

All thirteen suppressors demonstrated partial suppression of DNC and VNC defects, with *prp-8(hd161)* and *hd168* being best suppressed for DNC defasciculation, and *hd169* for suppression of VNC crossover defects. *prp-8(hd161)* and *hd163* showed suppression of lethality that may suggest suppression of adhesion defects, while the remaining suppressors showed no survival improvement but rather an increase in number of progeny. There was no suppression of Q-cell migration defects in any of the tested strains, indicating that the suppressor genes are not involved in polarity and migration of Q neuroblasts. The movement defects were partially rescued in *math-48(hd158)* and *prp-6(hd170)* strains. The remaining tested suppressors that showed no suppression of movement defects indicates that there is not an obvious correlation between movement and axon guidance. Three suppressors were identified: the functionally uncharacterized gene, *math-48*, which could be acting downstream of *cdh-4* pathway, and *prp-6* and *prp-8*, genes encoding components of the spliceosome machinery, more specially the active form of the complex. These *prp* genes, when depleted, affect expression of several genes, with the majority of them being up-regulated. An overexpression of genes may lead to activating gene(s) downstream of *cdh-4* or activating gene(s) that compensate for the loss of *cdh-4* and thus an alternate pathway.

The molecular mechanism of how *cdh-4* regulates axon guidance is currently unknown. The complexity of the mammalian nervous system makes it difficult to dissect and understand the development of neuronal circuits. The *cdh-4* gene is highly conserved across phyla. Therefore, identifying the suppressor genes of *cdh-4* and the signaling pathways will give insights into the functions of their homologs in vertebrate.

The molecular mechanisms for axon navigation is evolutionary conserved, thus the molecular basis of axon guidance is better investigated in the simple model organism, *C. elegans*, to give insights into the mechanisms of axon guidance in vertebrates.

4.7. References

Ackley Brian D., 2013 Wnt-signaling and planar cell polarity genes regulate axon guidance along the anteroposterior axis in C. elegans. Dev. Neurobiol. 74: 781–796.

Aspock, G., H. Kagoshima, G. Niklaus, and T. R. Burglin, 1999 Caenorhabditis elegans has scores of hedgehog-related genes: sequence and expression analysis. Genome Res 9: 909–23.

Aurelio, O., D. H. Hall, and O. Hobert, 2002 Immunoglobulin-domain proteins required for maintenance of ventral nerve cord organization. Science 295: 686–90.

Broadbent, I. D., and J. Pettitt, 2002 The C. elegans hmr-1 gene can encode a neuronal classic cadherin involved in the regulation of axon fasciculation. Curr Biol 12: 59–63.

Charron, F., E. Stein, J. Jeong, A. P. McMahon, and M. Tessier-Lavigne, 2003 The Morphogen Sonic Hedgehog Is an Axonal Chemoattractant that Collaborates with Netrin-1 in Midline Axon Guidance. Cell 113: 11–23.

Costa, M., W. Raich, C. Agbunag, B. Leung, J. Hardin *et al.*, 1998 A putative catenin-cadherin system mediates morphogenesis of the Caenorhabditis elegans embryo. J Cell Biol 141: 297–308.

Das, R., J. Yu, Z. Zhang, M. P. Gygi, A. R. Krainer *et al.*, 2007 SR proteins function in coupling RNAP II transcription to pre-mRNA splicing. Mol. Cell 26: 867–881.

Fabrizio, P., J. Dannenberg, P. Dube, B. Kastner, H. Stark *et al.*, 2009 The evolutionarily conserved core design of the catalytic activation step of the yeast spliceosome. Mol. Cell 36: 593–608.

Hall, D. H., and R. L. Russell, 1991 The posterior nervous system of the nematode Caenorhabditis elegans: serial reconstruction of identified neurons and complete pattern of synaptic interactions. J Neurosci 11: 1–22.

Harris, T. W., I. Antoshechkin, T. Bieri, D. Blasiar, J. Chan *et al.*, 2010 WormBase: a comprehensive resource for nematode research. Nucleic Acids Res 38: D463-7.

Hill, E., I. D. Broadbent, C. Chothia, and J. Pettitt, 2001 Cadherin superfamily proteins in Caenorhabditis elegans and Drosophila melanogaster. J Mol Biol 305: 1011–24.

Hobert, O., and H. Bulow, 2003 Development and maintenance of neuronal architecture at the ventral midline of C. elegans. Curr Opin Neurobiol 13: 70–8.

Horne-Badovinac, S., 2017 Fat-like cadherins in cell migration—leading from both the front and the back. Curr. Opin. Cell Biol. 48: 26–32.

Hu, P. J., 2014 Whole genome sequencing and the transformation of C. elegans forward genetics. Methods San Diego Calif 68: 437–440.

Hutter, H., M. P. Ng, and N. Chen, 2009 GExplore: a web server for integrated queries of protein domains, gene expression and mutant phenotypes. BMC Genomics 10: 529.

Krol, A., S. J. Henle, and L. V. Goodrich, 2016 Fat3 and Ena/VASP proteins influence the emergence of asymmetric cell morphology in the developing retina. Development 143: 2172–2182.

Liu, S., R. Rauhut, H.-P. Vornlocher, and R. Lührmann, 2006 The network of protein-protein interactions within the human U4/U6.U5 tri-snRNP. RNA N. Y. N 12: 1418–1430.

Maita, H., H. Kitaura, H. Ariga, and S. M. M. Iguchi-Ariga, 2005 Association of PAP-1 and Prp3p, the products of causative genes of dominant retinitis pigmentosa, in the tri-snRNP complex. Exp. Cell Res. 302: 61–68.

Moore, M. J., Q. Wang, C. J. Kennedy, and P. A. Silver, 2010 An alternative splicing network links cell-cycle control to apoptosis. Cell 142: 625–636.

Nagar, B., M. Overduin, M. Ikura, and J. M. Rini, 1996 Structural basis of calcium-induced E-cadherin rigidification and dimerization. Acta Crystallogr. A 52: 174–174.

Najarro, E. H., L. Wong, M. Zhen, E. P. Carpio, A. Goncharov *et al.*, 2012 Caenorhabditis elegans flamingo cadherin fmi-1 regulates GABAergic neuronal development. J Neurosci 32: 4196–211.

Oda, H., and M. Takeichi, 2011 Evolution: structural and functional diversity of cadherin at the adherens junction. J. Cell Biol. 193: 1137–1146.

Patel, S. D., C. P. Chen, F. Bahna, B. Honig, and L. Shapiro, 2003 Cadherin-mediated cell-cell adhesion: sticking together as a family. Curr Opin Struct Biol 13: 690–8.

Prox, J., P. Arnold, and C. Becker-Pauly, 2015 Meprin α and meprin β: Procollagen proteinases in health and disease. Matrix Biol. J. Int. Soc. Matrix Biol. 44–46: 7–13.

Rubio-Peña, K., L. Fontrodona, D. Aristizábal-Corrales, S. Torres, E. Cornes *et al.*, 2015 Modeling of autosomal-dominant retinitis pigmentosa in Caenorhabditis elegans uncovers a nexus between global impaired functioning of certain splicing factors and cell type-specific apoptosis. RNA N. Y. N 21: 2119–2131.

Saburi, S., I. Hester, E. Fischer, M. Pontoglio, V. Eremina *et al.*, 2008 Loss of Fat4 disrupts PCP signaling and oriented cell division and leads to cystic kidney disease. Nat. Genet. 40: 1010–1015.

Schmitz, C., P. Kinge, and H. Hutter, 2007 Axon guidance genes identified in a large-scale RNAi screen using the RNAi-hypersensitive Caenorhabditis elegans strain nre-1(hd20) lin-15b(hd126). Proc Natl Acad Sci U A 104: 834–9.

Schmitz, C., I. Wacker, and H. Hutter, 2008 The Fat-like cadherin CDH-4 controls axon fasciculation, cell migration and hypodermis and pharynx development in Caenorhabditis elegans. Dev Biol 316: 249–59.

Schwarz, V., J. Pan, S. Voltmer-Irsch, and H. Hutter, 2009 IgCAMs redundantly control axon navigation in Caenorhabditis elegans. Neural Dev 4: 13.

Sulston, J. E., and H. R. Horvitz, 1977 Post-embryonic cell lineages of the nematode, Caenorhabditis elegans. Dev Biol 56: 110–56.

Tanackovic, G., A. Ransijn, P. Thibault, S. Abou Elela, R. Klinck *et al.*, 2011 PRPF mutations are associated with generalized defects in spliceosome formation and pre-mRNA splicing in patients with retinitis pigmentosa. Hum. Mol. Genet. 20: 2116–2130.

Tanoue, T., and M. Takeichi, 2004 Mammalian Fat1 cadherin regulates actin dynamics and cell-cell contact. J Cell Biol 165: 517–28.

Tanoue, T., and M. Takeichi, 2005 New insights into Fat cadherins. J Cell Sci 118: 2347–53.

Thomas, J. H., 2006 Adaptive evolution in two large families of ubiquitin-ligase adapters in nematodes and plants. Genome Res. 16: 1017–1030.

White, J. G., E. Southgate, J. N. Thomson, and S. Brenner, 1986 The structure of the nervous system of the nematode Caenorhabditis elegans. Phil Trans R. Soc Lond. B 314: 1–340.

Will, C. L., and R. Lührmann, 2011 Spliceosome Structure and Function. Cold Spring Harb. Perspect. Biol. 3:.

Xie, M., and R. Roy, 2012 Increased Levels of Hydrogen Peroxide Induce a HIF-1-dependent Modification of Lipid Metabolism in AMPK Compromised C. elegans Dauer Larvae. Cell Metab. 16: 322–335.

Yang, C. H., J. D. Axelrod, and M. A. Simon, 2002 Regulation of Frizzled by fat-like cadherins during planar polarity signaling in the Drosophila compound eye. Cell 108: 675–88.

Zartman, J. J., J. S. Kanodia, N. Yakoby, X. Schafer, C. Watson *et al.*, 2009 Expression patterns of cadherin genes in Drosophila oogenesis. Gene Expr. Patterns 9: 31–36.

Zuryn, S., and S. Jarriault, 2013 Deep sequencing strategies for mapping and identifying mutations from genetic screens. Worm 2:.